



The Design of a Containership Propulsion System

Noufal Paravilayil Najeeb

Master Thesis

presented in partial fulfillment
of the requirements for the double degree:
"Advanced Master in Naval Architecture" conferred by University of Liege
"Master of Sciences in Applied Mechanics, specialization in Hydrodynamics, Energetics
and Propulsion" conferred by Ecole Centrale de Nantes

developed at "Dunarea de Jos" University of Galati
in the framework of the

"EMSHIP"
Erasmus Mundus Master Course
in "Integrated Advanced Ship Design"

Ref. 159652-1-2009-1-BE-ERA MUNDUS-EMMC

Supervisor: Prof: Mihaela Amoraritei University of Galati

Reviewer: Prof: Lionel Gentaz , Ecole Centrale de Nantes

Galati, February 2016



ABSTRACT

The main objective of a Naval Architect is to design most efficient ship with optimized hull to meet the challenges of a globalized market. So the final design has to achieve maximum speed, increase of cargo capacity, minimum fuel consumption and maximizing maneuverability, etc. Maritime industry is driven by such optimization process or researches for improved design to minimize the operational cost, fuel consumption and to maximize hydrodynamic performances at its service speed.

Whereas optimization of propulsion systems means to develop a propeller design for choosing engine power which gives the maximum propulsive efficiency without any noise and vibration problems. The transmission system connecting engine with propeller can be obtained once an optimized propeller design is realized for a suitable marine engine.

The objective of this master thesis is to design a container ship propulsion system with the selection of optimized propeller, main engine and other fundamental components. The type of propeller selected is a fixed pitch propeller as it is the most suitable one for the container ship since the service speed for the operational route is fixed. Engine will be selected by its power (MCR) to overcome ship resistance (including sea margin) accounting for other losses and shaft line will be design using classification society for its dimensioning and for the type of propeller.

The most important parameter required to begin propeller design is Resistance of ship at her design velocity which can be described as hydrodynamic force exerted by the fluid opposing its motion at that velocity. The final outcome of propeller design is to develop a propelling device capable of generating thrust sufficient enough to overcome this resistance.

Design of a propeller will be divided in three stages: preliminary design, detailed design and hydrodynamic analysis of the final propeller. On the first stage, main characteristics of propeller such as diameter, rotation rate, blade area ratio will be obtained using B Wageningen series data. Secondly, detailed design will be performed via lifting line theory. The objective of this stage is to find the propeller geometry for a radially varying distribution of the loading. While in final stage using CFD methods, propeller will be investigated in steady conditions in uniform flow (open water test) and unsteady condition in radially varying inlet velocity considering ship wake (self propulsion test).

TABLE OF CONTENTS

ABSTRACT.....	3
LIST OF FIGURES.....	7
LIST OF TABLES	10
LIST OF SYMBOLS.....	11
1. INTRODUCTION	15
1.1. General.....	15
1.2. Objectives	16
1.3. Methods and Procedures.....	17
2. LITERATURE STUDY	18
3. CASE STUDY	19
4. SHIP RESISTANCE.....	20
4.1. Holtrop & Mennen – 1984 Method	20
4.2. Experimental Data from Towing Tank Test.....	21
4.3. Resistance Calculated Using Maxsurf Software.....	23
4.4. Results and Comparison of Total Resistance	24
5. PROPULSIVE POWER ESTIMATION AND ENGINE SELECTION.....	25
5.1. General.....	25
5.2. Propeller Characteristics	26
5.3. Initial Propeller Data.....	28
5.3.1. <i>Statistical Analysis</i>	28
5.3.2. <i>Propeller – Hull interaction</i>	28
5.3.3. <i>Procedure</i>	31
5.3.4. <i>Selection of number of blades</i>	34
5.3.5. <i>Selection of Main Engine</i>	36
6. PROPELLER DESIGN.....	37
6.1. General considerations.....	37
6.2. Propeller Preliminary Design	37

6.3.	Optimal propeller diameter	39
6.4.	Ship Speed Estimation with Preliminary Propeller Design	41
6.5.	Experimental result	45
6.6.	Cavitation Checking	46
7.	DETAIL DESIGN	48
7.1.	Propeller Detail Design stage	48
7.2.	Lifting Line Theory	49
7.3.	Lifting Line Theory in Propeller Design	50
7.4.	Lifting Line Theory computation	53
7.4.1.	<i>Mean circumferential wake</i>	54
7.4.2.	<i>Velocities at blade sections</i>	55
8.	PROPELLER GEOMETRY	57
8.1.	NACA 66(mod-0.8) Profile	57
8.2.	Geometry Generation.....	59
9.	CFD ANALYSIS	60
9.1.	Numerical Analysis using SHIPFLOW software	60
9.2.	Numerical Solvers of SHIPFLOW software	60
9.2.1.	<i>XPAN module – Potential Flow solver</i>	60
9.2.2.	<i>XCHAP module – RANSE solver</i>	60
9.2.3.	<i>Theory behind ShipFlow computation for propeller analysis[4]</i>	61
9.2.4.	<i>Computation resources</i>	62
9.3.	Resistance Calculation.....	63
9.3.1.	<i>Pre-processing</i>	63
9.3.2.	<i>Grid Convergence Study</i>	63
9.3.3.	<i>Post Processing</i>	64
9.4.	Open Water Test	67
9.4.1.	<i>Pre-Processing</i>	67

9.4.2. Computation	69
9.4.3. Post Processing	70
9.5. Self-Propulsion	72
9.5.1. Pre-Processing	72
9.5.2. Computation	75
9.5.3. Post-Processing.....	75
10. PROPELLER STRENGTH CALCULATION	77
11. SHAFTLINE SYSTEM	78
11.1. Introduction.....	78
11.2. Purpose of Shaft line.....	78
11.3. Material Selection	78
11.4. Components of Shaft line system	78
11.5. Installation	79
12. CONCLUSION	80
ACKNOWLEDGEMENT.....	82
REFERENCES	83
APPENDIX	84

LIST OF FIGURES

Fig 1: Flowchart showing objective of this thesis	16
Fig 2 : Input and Output of Holtrop & Mennen	21
Fig 3: The surface of the vessel created in Rhino (2).....	23
Fig 4: Comparison of total resistance against velocity in knots.....	24
Fig 5 :Position of different power definitions and efficiencies[.....	25
Fig 6: An example of K_T , K_Q and efficiency Chart.....	33
Fig 7: Input Data and Output Result of propeller design ($Z=3$).....	34
Fig 8:Input Data and Output Result of propeller design ($Z=4$).....	35
Fig 9:Input Data and Output Result of propeller design ($Z=5$).....	35
Fig 10: Representative engine curves with corresponding propeller design point.....	38
Fig 11: Input Data and Output Result for finding optimum diameter for selected main engine	40
Fig 12: Propeller clearances for single screw ships (DNV)	40
Fig 13: Input and output data for ‘Ship_speed’ software	42
Fig 14: Ship velocity estimation according to delivered power to the propeller	43
Fig 15: Burrill's Diagram for Cavitation % checking	47
Fig 16:Lift generation on a cylinder due to circulation.....	48
Fig 17:Streamlines around the Blade section	49
Fig 18: Free Vortices Shedding Varied in radial direction	49
Fig 19: Schematic representation of lifting line theory.....	50
Fig 20:Velocity diagram for a blade section	51
Fig 21:Circumferencial wake distribution along blade sections at different radii	54
Fig 22:Typical NACA profile	57
Fig 23:Representation of two dimensional point on NACA profile	58
Fig 24: Propeller blade sections generated using Rhino software.....	59
Fig 25: Values of C_w plotted for different panelization mode.....	64
Fig 26: The mesh of the hull below waterline and free surface obtained from CAESES.....	64
Fig 27: Showing different set of wave system generated due to motion of ship.	64
Fig 28: Wave height along the hull from free surface.....	65
Fig 29: Comparison of resistance for range of velocity obtained from different methods	66
Fig 30: Grid generated for BOX with stretching at center enclosing Propeller Disk	68

Fig 31: Cylindrical grid generated for Propeller Disk.....	68
Fig 32: Boundary conditions for Open Water Computation	69
Fig 33: Comparison between KT , KQ , ηO obtained from different methods for Wageningen B propeller.....	70
Fig 34: KT , KQ , ηO plotted against advance coefficient J for NACA 66 propeller	71
Fig 35: The entire grid setup for fluid domain for XCHAP	73
Fig 36: Refinement at stern region	74
Fig 37: Overlapping grid structure	74
Fig 38: The pressure coefficient distribution around hull using Global approach	75
Fig 39: The effective wake distribution along the propeller plane.....	75

LIST OF TABLES

Table 1: Principal Particulars of the Vessel.....	19
Table 2: Results obtained from Holtrop & Mennen – 1984 Method.....	20
Table 3: Data of ship model for Towing Tank test.....	22
Table 4: Experiment Results of the model from towing tank test	22
Table 5: Results of the ship resistance calculated by ITTC 1978.....	23
Table 6: Optimal B-Wageningen standard series propeller for the ship.....	41
Table 7: Prediction of performance characteristics of propeller at different speeds	42
Table 8: Main geometrical and hydrodynamic characteristics of optimal propeller	43
Table 9: Geometrical Characteristics of Wageningen propeller.....	44
Table 10 : KT, KQ & ηO values for pitch ratio = 0.9 for different values of advance coefficient(Statistical).....	44
Table 11: KT, KQ & ηO values for different values of J at 20 Knots from open water test(experimental)	45
Table 12: Result of self propulsion test(experimental)	45
Table 13: Cavitation Checking with Burrill's Diagram	46
Table 14: Digitized Burrill Chart	47
Table 15: Data input for lifting line method.....	53
Table 16: Mean wake value at different radii from experimental test.....	54
Table 17: Axial, Tangential and resultant velocities along the propeller sections at each radii.....	55
Table 18: Geometry of blade sections at each radii.....	55
Table 19: Propeller characteristics based on detail design	56
Table 20: Wave resistance coefficient for different automatic mesh modes	63
Table 21: Total Resistance of the ship obtained from Ship Flow.....	65
Table 22: Dimension of the box tunnel for Propeller	67
Table 23: KT, KQ & ηO (Numerical & Statistical) values for pitch ratio = 0.9 for different values of J	70
Table 24: $KT, KQ, \eta O$ obtained for various advance ratio for final propeller (NACA 66).....	71
Table 25: Comparison of various propeller characteristics and propeller-hull interaction factors obtained from numerical analysis and experimental	76

LIST OF SYMBOLS

- L_{OA} - Length overall (m)
 L_{BP} - Length between perpendiculars (m)
 L_{WL} - Length at waterline (m)
 B_{WL} - Breadth at waterline (m)
 T_A - Draft Aft(m)
 T_F - Draft Fwd(m)
 D - Depth of ship (m)
 V - Velocity of ship (m/s)
 A_{WL} - Area of waterplane (m²)
 A_m - Midship section area (m²)
 C_b - Block coefficient
 C_P - Prismatic coefficient
 C_{wL} - Waterplane area coefficient
 C_M - Midship coefficient
 lcb - Longitudinal center of buoyancy (m)
 Δ - Mass displacement (tonnes)
 ∇ - Volume displacement (m³)
 S - Wetted surface area (m²)
 TEU - Twenty-foot equivalent unit
 R_T - Total resistance (KN)
 R_F - Frictional resistance according to the ITTC 1957 friction formula (KN)
 R_{app} - Appendage resistance (KN)
 R_w - Wave-making and wave-breaking resistance (KN)
 R_a - Air resistance (KN)
 R_{aa} - Model-ship correlation resistance (KN)
 $1 + k$ - Form factor describing the viscous resistance of the hull form in relation to
 C_{TM} - Total resistance coefficient of the model
 C_{FM} - Friction resistance coefficient of the model
 C_{RM} - Residual resistance coefficient of the model
 C_{TS} - Total resistance coefficient of the full scale ship
 C_{FS} - Friction resistance coefficient of the full scale ship
 C_{RS} - Residual resistance coefficient of the full scale ship

- P_E - Effective power to tow the vessel (KW)
- P_T - Thrust power transferred to water by propeller (KW)
- P_D - Delivered power (KW)
- P_B - Brake power (KW)
- V_A - Velocity of Advance (m/s)
- T - Thrust force developed by propeller (KN)
- w - Wake fraction coefficient
- t - Thrust deduction coefficient
- Q - Torque force transmitted to propeller (KNm)
- D - Diameter of propeller (m)
- Z - Number of propeller blades
- J - Advance coefficient
- n - Number of rotation of propeller per second
- K_T - Thrust coefficient
- K_Q - Torque coefficient
- EAR - Blade area ratio
- η_H - Hull efficiency
- η_O - Open water efficiency
- η_R - Relative rotative efficiency
- η_B - Behind hull efficiency
- η_D - Quasi Propulsive efficiency
- η_S - Shaft efficiency
- H - Height of the shaft center line from the baseline of ship
- U_{TH} - Tangential inflow velocity at leading edge (m/s)
- U_A - Axial propeller induced velocity (m/s)
- U_T - Tangential propeller induced velocity (m/s)
- Γ - Strength of Circulation
- C_L - Lift coefficient
- C_{L0} - Ideal Lift coefficient
- α - Angle of Attack
- c_f - Camber correction due to lifting surface effect.
- R - Radius of propeller disk (m)
- r_h - Radius of propeller hub (m)
- r_0 - Radius of propeller from shaft centreline (m)

DECLARATION OF AUTHORSHIP

I declare that this thesis and the work presented in it are my own and have been generated by me as the result of my own original research.

Where I have consulted the published work of others, this is always clearly attributed.

Where I have quoted from the work of others, the source is always given. With the exception of such quotations, this thesis is entirely my own work.

I have acknowledged all main sources of help.

Where the thesis is based on work done by myself jointly with others, I have made clear exactly what was done by others and what I have contributed myself.

This thesis contains no material that has been submitted previously, in whole or in part, for the award of any other academic degree or diploma.

I cede copyright of the thesis in favor of the University of Galati.

Date: 15th January, 2016.

Signature: Noufal Paravilayil Najeeb

1. INTRODUCTION

1.1. General

At present maritime industry plays a very vital role in day to day life of billions of people around the world. Around 90% of transport of commodities happens or are directly linked to shipping. As the demand for transport of commodity is steadily increasing proportional to global population, the engineers who design these vessels have to come up with ideas or solutions to build larger, efficient, faster and safer vessels.

Large vessels require greater power to propel at higher speed carrying more cargo, which means large fuel consumption. So the design has to be more energy efficient leading to minimize required engine power installation and to reduce fuel oil consumption not only to save operational cost but as well as to reduce environmental pollution which has become more stringent under IMO regulations setting emission standards. Most of ongoing research in marine industry is to make future vessels more energy efficient either by hull optimization, installing energy saving devices, propeller optimization etc.

Here the objective at hand is to design propulsion system with an efficient propeller for a 1200 TEU container ship. In order to begin the propeller design and determine propulsive power which depends upon the resistance and the design speed for which one has to understand the hull form and characteristics of containership.

Container ships are classified as a special type of conventional vessels which transport cargoes in containers. Some of main features of container ships includes they are faster compared to other conventional vessels like Bulk Carriers or Tankers and has better streamline characteristics (fullness of the form) i.e low block coefficient.

These characteristics of container ship pose various propeller design problems for example streamlined stern section constrain space requirements for engine room in aft resulting in a semi-aft location of engine with longer shaft line which in turn increases power transmission losses. And also because of higher service speed, the engine brake power and RPM which makes engine propeller matching difficult and may result in installation of Gear.

1.2. Objectives

The main objective in design of a optimized propulsion system is to find propulsive power, suitable engine, propeller characteristics and to verify that it is the best available solution. Step by step procedure carried out for this thesis is depicted in below flowchart.

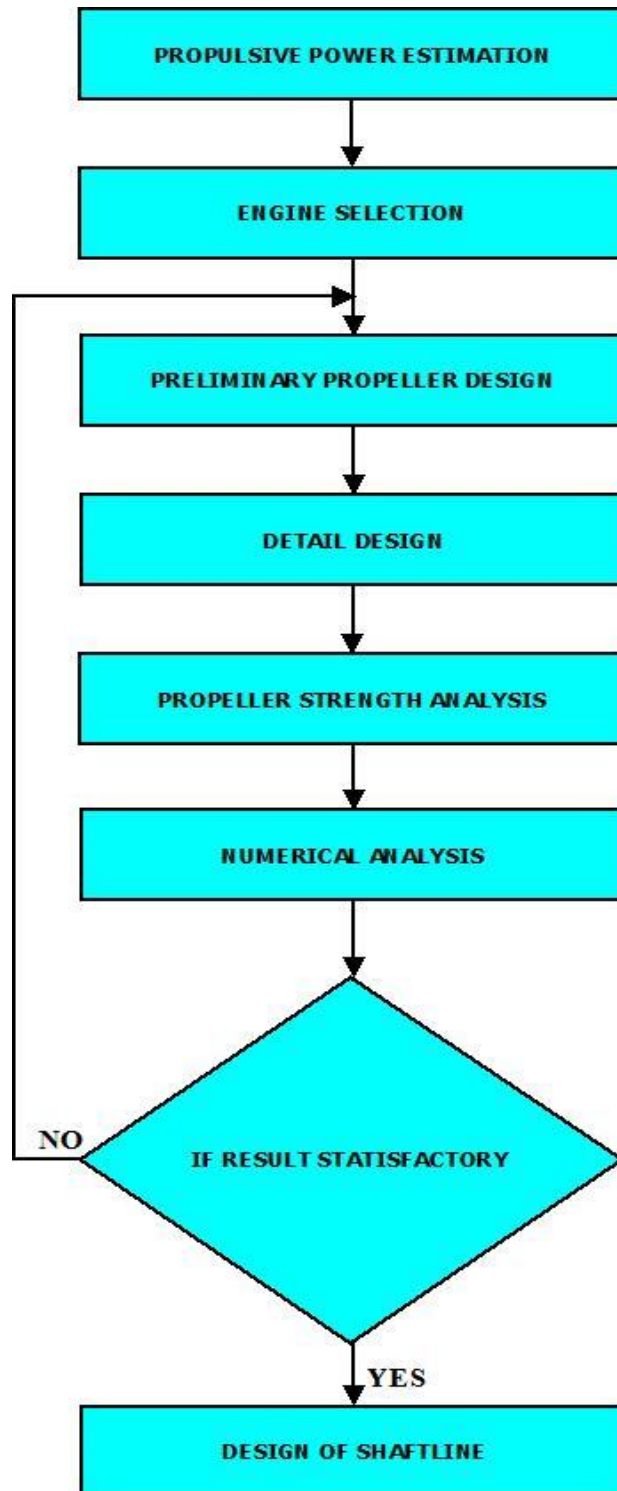


Fig 1: Flowchart showing objective of this thesis

1.3. Methods and Procedures

In this thesis, the design of a container ship propeller will be performed in three stages: preliminary design stage, detailed design stage and hydrodynamic analysis of the final propeller with CFD solver (SHIPFLOW- Global Approach using RANSE Solver).

Before starting the design of a propeller, the resistance of the container ship will be analysed by empirical formulae (Holtrop) and experimental data. The comparison of these two methods will be done and the resistance of the vessel at its design speed will be finalized for the propeller design.

During the preliminary design stage, a propeller design will be realized with maximum efficiency in desired operating condition by fixing the main characteristics of propeller such as diameter, number of rotation, pitch ratio, blade area ratio etc..and using B Wageningen series data. Here propeller optimization process is carried out in such a way to generate maximum efficiency with minimum cavitation.

Secondly, detailed design will be performed via Prindtl's lifting line theory. The main idea of this stage is to find the propeller geometry for a radially varying distribution of the loading. The first step in producing the open water diagram is to use lifting line theory to characterize the propeller blades. The bound circulation on the lifting line is a function of the blade geometry along with the blade velocity (both rotational and axial).

Using CFD codes is possible to identify problems early in the design stage, and to evaluate changes rapidly which will be our final stage. After propeller detailed design is finished, propeller performances are investigated numerically in steady and unsteady flow. Steady analysis consist of calculation of open water characteristics and calculation of the pressure distribution on propeller blades operating in uniform flow or in a radially varied circumferential mean flow. Unsteady analysis comprises of calculation of the propeller characteristics, propeller-hull interaction characteristics and finally, prediction of propeller rotation speed and required delivered power.

Once the propeller characteristics are satisfactory then the blade sections will be investigated for the strength critetia as per the classification society rules.

Upon the selection of and main engine and the design of the final propellor is completed, the design of the shafting system will be performed according to the classification rules.

2. LITERATURE STUDY

This thesis is concerned with resistance estimation, engine selection, propeller design and its shafting system of a container ship. There are some papers and books available for the study of optimization of a propeller, estimation of resistance and ship hydrodynamic performance.

Volker Bertram, 2000 [1] explained various approaches for ship resistance and propulsion system in “Practical Ship Hydrodynamics” which are as follows:

- Empirical/statistical approaches
- Experimental
- Numerical approaches using computational fluid dynamics (CFD)

J. Holtrop and J. Mennen, 1982 [2] wrote the paper named “An Approximate Power Prediction Method”. That paper explained the resistance and power prediction methods focused on high- block ships with low L/B ratios. It presented the empirical formula for prediction of the form factor based on prismatic coefficient for resistance prediction, prediction of propulsion factors such as wake fraction, thrust deduction factor and relative rotative efficiency and prediction of propulsive efficiency.

As per the ITTC - Recommended Procedures[3] ”1978 ITTC Performance Prediction Method for Single Screw Ships ” which predicts rate of revolution and delivered power of a ship from model results. The residuary resistance coefficient can be obtained from model test runs which can be extrapolated to full scale using froude similitude while the viscous coefficient from ITTC formula considering the form factor determined using Prohaska’s method. Where as the delivered power and rate of revolution prediction are result of model test of propeller carried out to study characteristics and considering thrust or torque identity to extrapolate to full scale

For numerical analysis using CFD software Shipflow will be used in this thesis. It uses a finite volume method that solves the Reynolds Average Navier Stokes Equation[6]. Also it relies on potential methods to solve specific problems. It uses the approach of actuator disk with a lifting line model to simulate the propeller action. Interactive coupling between the RANS solver and lifting line method is achieved through body forces accelerating the flow[4]. Results depend on blade geometry such as: camber ratio, pitch ratio, blade thickness and chord length [8]. Main computations include performing open water and self propulsion test to study propeller characteristics in steady and unsteady flow respectively.

3. CASE STUDY

The vessel is a conventional container ship with bulbous bow, transom stern, single rudder and single screw propeller. The propulsion machinery with main engine located at the aft part of the ship. The principal dimension of the vessel has been finalized after study of various hull forms to obtain as per the owners specification as given in table 1.

Table 1: Principal Particulars of the Vessel

Parameters	Units	Values
L_{PP}	[m]	145.9
L_{WL}	[m]	150.51
L_{OA}	[m]	153.6
B_{WL}	[m]	23.25
T_F	[m]	7.3
T_A	[m]	7.3
TEU	[-]	1200
Design Speed	[Knots]	20
∇	[m ³]	16109.79
Δ	[tonnes]	16512.53
S	[m ²]	4167.37
lcb	[m]	71.609
C_B	[-]	0.65
C_W	[-]	0.98
C_P	[-]	0.6582

The service speed of the design container vessel as owner's requirement is one of most important design parameter since the movement of containers between the ports has to be faster and carried out as scheduled to meet charterer requirements.

The designed propulsion system for this container ship should be capable of generating sufficient thrust to propel the vessel at 20 knots speed carrying 1200 containers of 20 foot at a design draft of 7.3m. And the main proposal through this work is to realise the above requirement and to obtain an optimized propulsion system which will be confirmed to be the best available solution.

4. SHIP RESISTANCE

The resistance of a ship at a given speed can be defined as the hydrodynamic fluid force exerted on the ship opposing its motion. Total resistance of a ship can be divided into two main sections namely Frictional Resistance and Residuary Resistance.

The frictional resistance is due to viscosity of the fluid and can be obtained by integrating the tangential stresses over the wetted surface of the ship in the direction of motion. Residuary resistance in case of a container ship mainly comprise of wave making resistance which is the energy transferred from ship in generating gravity waves radiating out .

Resistance of a hull form can be calculated experimentally by tank testing of the model or by empirical methods like Holtrop-Mennen1984 method or by computational fluid dynamics. The resistance calculations are performed for a range of speeds ranging from 16 knots to 22 knots including the service speed (20 knots).

4.1. Holtrop & Mennen – 1984 Method

The total resistance R_T of the ship can be obtained using Holtrop and Mennen method which is empirical approach where the resistance coefficients are estimated using with empirical formula based on systematic series or statistical regressions to experimental data.

$$R_T = R_F(1 + k) + R_{app} + R_w + R_a + R_{aa} \quad (1)$$

The resistance prediction using Holtrop & Mennen -1984 method is done with the help of C++ code named Holtrop & Mennen as shown in figure 2 (Attached to Annexure).

Table 2: Results obtained from Holtrop & Mennen – 1984 Method

No	Speed Vs (Kn)	Frictional Resistance (kN)	Wave Resistance (kN)	Bulb Resistance (kN)	Correlation Resistance (kN)	Air Resistance (kN)	Total Resistance (kN)
1	16	383.982	64.532	15.523	61.912	14.817	398.9
2	17	381.112	98.097	20.524	69.893	16.727	472.2
3	18	378.435	138.577	26.284	78.357	18.753	556.2
4	19	375.928	189.260	32.794	87.306	20.894	654.7
5	20	373.574	264.835	40.038	96.737	23.152	778.9
6	21	371.354	370.552	47.999	106.653	25.525	927.4
7	22	369.256	484.690	56.653	117.052	28.014	1079.1

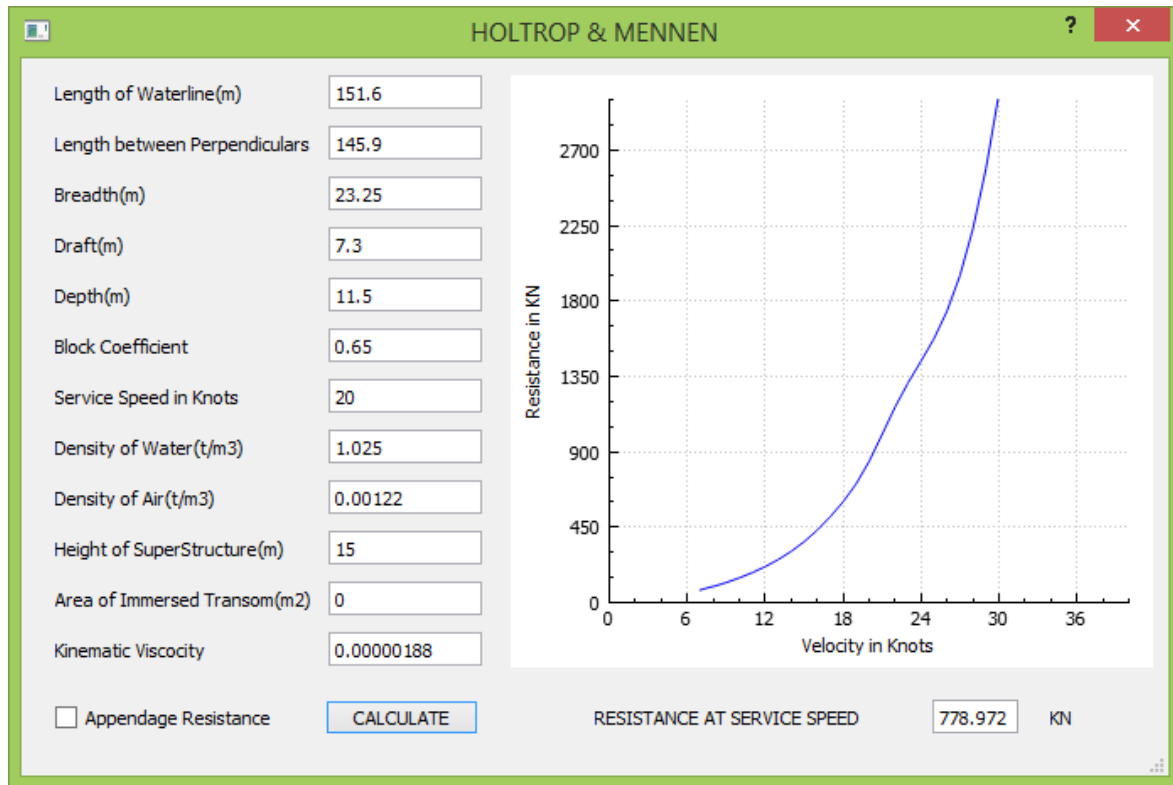


Fig 2 : Input and Output of Holtrop & Mennen

4.2. Experimental Data from Towing Tank Test

Testing of a small scale model of actual Ship (geometrically similar) in towing tank at various speeds to measure its total resistance which can be extrapolated to compute full scale resistance. As for the experimental approach by ITTC recommended procedure, the total resistance of the model (R_{Tm}) is expressed in the non-dimensional form.

$$C_{Tm} = \frac{R_{Tm}}{0.5 \times \rho m \times S_m \times V_m^2} \quad (2)$$

$$C_{Fm} = \frac{0.075}{\text{Log}(Re_m - 2)^2} \quad (3)$$

$$C_{Rm} = C_{Tm} - (1 + k)C_{Fm} \quad (4)$$

Considering froude number similitude, the residual resistance coefficients of the model and full scale are the same. With the same procedure as the model scale, the total resistance coefficient of the full scale ship (C_{TS}) and total resistance of the ship can be achieved.

$$C_{RS} = C_{Rm} \quad (5)$$

$$C_{FS} = \frac{0.075}{\text{Log}(Re_s - 2)^2} \quad (6)$$

$$C_{TS} = C_{RS} + (1 + k)C_{FS} \quad (7)$$

A model test for the subject vessel at a scale factor of 29.428 was conducted at ICEPRONAV test basin .The results are given in Tables 4 & 5.

Table 3: Data of ship model for Towing Tank test

PARAMETERS	SHIP	MODEL
Length between perpendiculars L_{pp} (m)	145.9	4.958
Length at waterline L_{WL} (m)	150.51	5.115
Breadth at waterline B_{WL} (m)	23.25	0.79
Draught at FP T_F (m)	7.3	0.248
Draught at AP T_A (m)	7.3	0.248
Displacement volume ∇ (m ³)	16109.79	0.632
Displacement mass Δ (tonnes)	16512.53	0.632
Wetted surface (bare hull) S (m2)	4167.37	4.812
Longitudinal centre of buoyancy LCB (m)	71.609	2.433
C_B	0.65	
C_P	0.6585	
Material of model hull	wood	
Friction coefficient according to	ITTC '57	
Model-ship correlation coefficient , DCF	0.4088 x 10-3	
Air resistance coefficient , C_{AA}	0.0618 x 10-3	
Temperature of the tank water	11.5 ° C	
Form factor k	0.22	

Table 4: Experiment Results of the model from towing tank test

F_n	V_M (m/s)	R_{TM} (N)	$1000 \cdot C_W$	$1000 \cdot C_{FM}$	$1000 \cdot C_{TM}$
0.214	1.517	22.298	0.003	3.2667	3.9884
0.228	1.612	25.182	0.0475	3.2311	3.9895
0.241	1.707	29.038	0.2014	3.1981	4.1031
0.254	1.802	33.982	0.4454	3.1673	4.3095
0.268	1.897	40.898	0.852	3.1385	4.6809
0.281	1.991	50.924	1.4909	3.1114	5.2868
0.295	2.086	62.794	2.175	3.086	5.9399

Table 5: Results of the ship resistance calculated by ITTC 1978

F_n	V_s	$1000 \cdot C_R$	$1000 \cdot C_{FS}$	$1000 \cdot C_{TS}$	$R_{TS}(kN)$	Effective Power
0.214	16	0.7217	1.5231	2.358	344.98	2839.6
0.228	17	0.7583	1.5117	2.3884	394.48	3450
0.241	18	0.905	1.5011	2.5293	468.34	4336.8
0.254	19	1.1422	1.4912	2.761	569.63	5567.8
0.268	20	1.5424	1.4819	3.1561	721.48	7423.2
0.281	21	2.1754	1.4731	3.7841	953.71	10303.3
0.295	22	2.8539	1.4648	4.458	1233.11	13956

4.3. Resistance Calculated Using Maxsurf Software

Surface of the vessel has been created using Aveva software from the offset as shown below and imported to Maxsurf resistance module to find resistance.

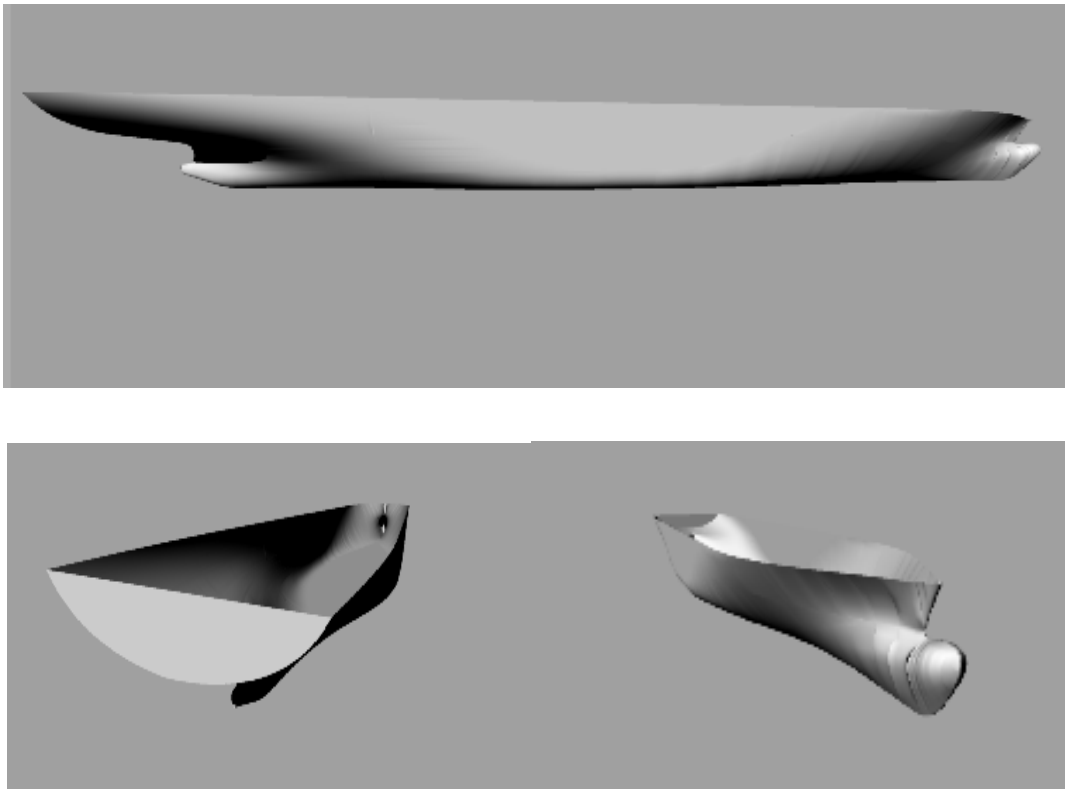


Fig 3: The surface of the vessel created in Maxsurf

Resistance calculation results has been provided as software output result(Attached as annexure). The resistance obtained by software for 20 knots speed is 735.6 kN.

4.4. Results and Comparison of Total Resistance

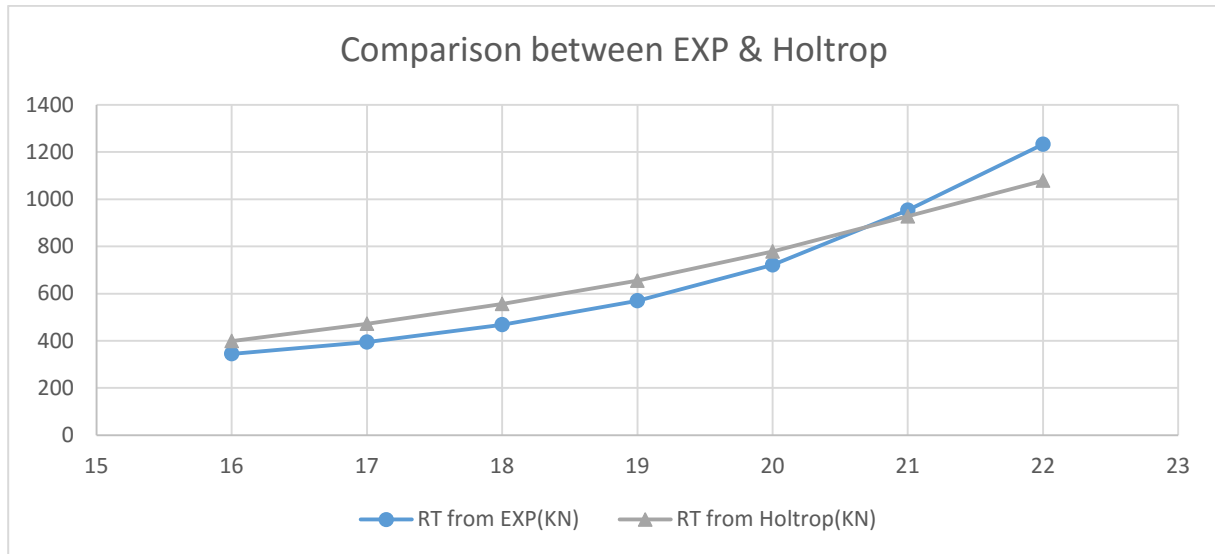


Fig 4: Comparison of total resistance against velocity in knots

From Figure 4, it can be observed that the total resistance obtained from the Holtrop method (empirical method) is higher than the results obtained from towing tank test. This is due to reason that empirical methods like Holtrop & Mennen gives approximate values of resistance for given hull form from available statistical data.

From the above the methods, resistance predicted by Experimental data is considered to be most accurate. Total resistance of the vessel at design speed of 20 knots is selected as 722 kN obtained from the towing tank test to start propeller design.

5. PROPULSIVE POWER ESTIMATION AND ENGINE SELECTION

5.1. General

The propeller is the main component of the propulsion system of a ship which rotates fluid around it resulting in generation of opposing hydrodynamic forces from fluid transferring to hull and propelling it forward.

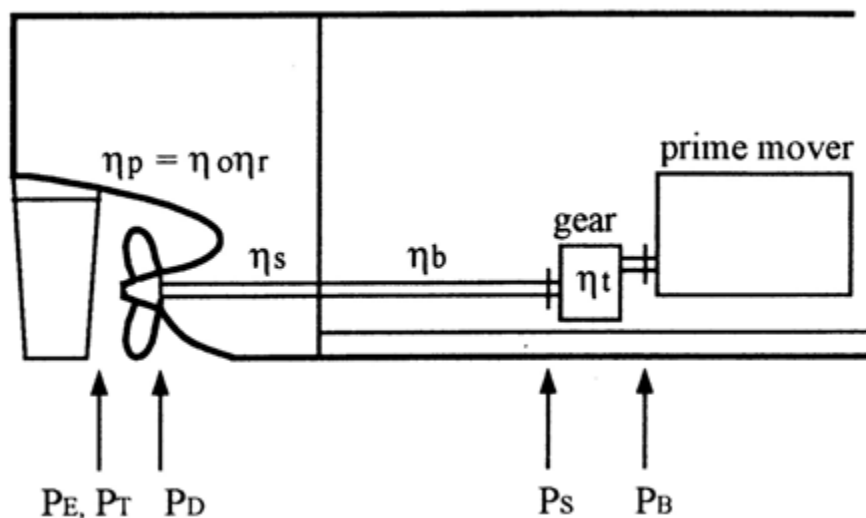


Fig 5 :Position of different power definitions and efficiencies

Propellers are typically optimized to provide the maximum thrust for the minimum torque at a specific number of revolutions per minute (RPM) at a particular ship speed. This process works very well for container ships that travel across the ocean at a relatively constant speed. There is a certain RPM at which the main engine operates most efficiently. If the propeller can produce the thrust to achieve the desired speed while turning at the proper rate, then the ship will arrive at its destination using the minimal amount of fuel.

For the present work, the container ship has one design speed, fixed route and maneuverability is not critical in comparison to offshore and tugs market. Fixed pitch propeller present a reliable solution due to simple operation and they deliver maximum efficiency at one operating point (ship speed) if designed correctly. And also this system is much simple, and consequently less initial investment, operational and maintenance cost.

Because of above reasons, a fixed pitch propeller will be used for the design of the propeller which will be directly coupled to low speed diesel engine.

5.2. Propeller Characteristics

The propellers are commonly characterised by its diameter, blade area ratio, number of blades, skew, pitch diameter ratio etc... Among these factors except skew all others have direct influence on the efficiency and performance of propeller.

Diameter (D)

Propeller diameter can be defined as the diameter of the disk containing the propeller. It has a significant role in determining propulsive efficiency. The bigger possible propeller diameter, the higher propulsive efficiency is approachable. However, there are some limitations which effect on the size of propeller diameter. For example, shape of the aft part of the ship hull is really important where the clearance between the propeller tip and hull should be considered. Obviously, some clearances must exist between the hull and the propeller tips to control noise and vibration. The extent of this clearance depends upon the application, but is usually ten to twenty percent of the diameter.

Blade Area (BAR)

The amount of blade area does not greatly affect theoretical performance, but the trend is that less blade area increases efficiency. Its primary function is to provide enough area to distribute the generated pressures so that the lift in any particular spot stays below a certain cavitation - inducing level. So the idea is to use as little blade area as possible while retaining enough to distribute the pressures. In addition to the cavitation limits, there are other upper and lower limits to maintain. If a blade area is too low, structural concerns will require that the thickness of the blades be increased resulting in a reduction in efficiency.

Number of blades (Z)

Considering conditions that are supposed to be fulfilled, propellers are usually designed with 3, 4, 5 and even 6 blades. The selection of number of blades plays a very important role in propeller design as it directly affects the propulsive efficiency and plays important role in vibrational characteristics of propulsion system. The normal trends is the optimum diameter and the open-water efficiency decrease with increase in the number of blade. The choosing of the number of blades, which have a common factor with the number of cylinders of the Diesel engine, could lead to vibrations problems and should be avoided. Propeller strength and

loading factor is another important criteria for selection of number of blades as lower number of blades results in high propeller thrust loading which affects its performance.

Pitch Diameter Ratio (P/D)

The pitch diameter ratio P/D , expresses the ratio between the propeller's pitch P and its diameter D . To achieve the best propulsive efficiency for a given propeller diameter, an optimum pitch/diameter ratio is to be found, which again corresponds to a particular design rate of revolution. If a lower design rate of revolution is desired, the pitch/diameter ratio has to be increased.

Skew

Propeller with skew decrease the susceptibility to cavitation and to the level of unsteady forces acting on the propeller. Difficulty in manufacturing skew propeller is the only drawback. The swept back blade of a skewed propeller helps to minimize these effects by causing each blade to pass through the area of still water behind an appendage a little at a time. Where a non-skewed propeller blade would encounter this area all at once, a skewed propeller will proceed into it from root to tip, reducing the large periodic pressure changes on each blade passes.

Rake

Rake of a propeller can be defined as inclination of blades with respect to the perpendicular to the propeller hub or the distance from the propeller plane to the generator line in the direction of the shaft axis as per ITTC. Rake is considered to be positive if the blade is tilted away from the hull towards the aft side while it is negative in opposite side. Rake can affect the flow of water through the propeller, and improve the hull-propeller interaction and its performance. Rake increases the blade diameter (since the blade is tilted the distance from root to tip increase within the available stern clearances) which provides more area for thrust loading.

5.3. Initial Propeller Data

For estimating the propulsive power for engine selection first an investigation on the propeller characteristics is carried out using existing statistical charts sufficient enough to generate thrust required to overcome the resistance at the design speed.

5.3.1. Statistical Analysis

Wageningen B series [12] was selected for the design of propeller. This series was developed from the open-water analysis of 120 Troost (air-foil) form, open-wheel propellers in the Netherlands Ship Model Basin (NSMB) at Wageningen. Given below are the ranges of parameters of propellers in this series.

Configuration	:	Open-water
Number of blades	:	2 to 7
Blade area ratio	:	0.3 to 1.05
Pitch-Diameter ratio	:	0.5 to 1.4
Advance coefficient	:	0.1 to 1.5

This series is based on K_t, K_q , Efficiency charts obtained using polynomial regression of data obtained from model testing. The derived curves or polynomials express thrust and torque coefficients in terms of the number of blades (Z), the blade area ratios (BAR), the pitch diameter ratio (P/D) and the advance coefficients (J).

5.3.2. Propeller – Hull interaction

The propeller works behind the Ship where the flow are considerably modified due to interaction between Hull and Propeller. So while studying the propeller characteristics we have to take into considerations factors like wake, thrust deduction.

Wake

Due to motion of Ship, the water around the stern will acquire a forward motion as it is dragged along the hull and this forward motion of water is called wake. The effective wake behind hull around propeller is calculated using the thrust identity method in open water tests.

Wake Fraction (w)

Due to wake the propeller is no longer advancing relatively to the water at the same speed as the Ship, but at a lower speed which is called velocity of advance (V_a).

$$w = (V - V_a)/V \quad (8)$$

Wake estimation using empirical relations:

$$w = 0.5 * C_B - 0.05 \quad (\text{Taylor's formula})$$

$$= 0.275$$

$$w = 0.7 * C_P - 0.18 \quad (\text{Hecksher formula})$$

$$= 0.281$$

$$w = 0.535 * C_B - 0.07 \quad (\text{BSRA formula})$$

$$= 0.278$$

$$w = 0.275 \quad (\text{selected})$$

Thrust Deduction Factor (t)

The propeller when developing thrust accelerates the water ahead of it. This increases the fluid velocity as well as lowers pressure around the stern. This reduction of fluid pressure can be considered as increase in total resistance of ship (resistance of self propelled ship is higher compared to resistance of towed ship) or increase in total thrust required to propel the ship.

$$t = (1 - R_T)/T \quad (9)$$

Thrust Deduction Factor estimation using empirical relations:

$$t = 0.5 * C_P - 0.12 \quad (\text{Hecksher formula})$$

$$= 0.209$$

$$t = K * W \quad (\text{Schoencher formula})$$

$$= 0.165, \text{ where } K = 0.5 - 0.6 \text{ for single screw.}$$

$$t = 0.23 * C_B + 0.05 \quad (\text{Taylor's formula})$$

$$= 0.1995 \text{ (selected)}$$

Hull efficiency

The work done in moving a ship at a speed V against a resistance R_T is proportional to the product $R_T \times V$ or the work done by the propeller in delivering a thrust T at a speed of Advance V_A is proportional to the product $T \times V_A$.

$$\begin{aligned}\eta_H &= (1 - t)/(1 - w) \\ &= (1 - 0.1995) / (1 - 0.275) \\ &= 1.104\end{aligned}$$

Relative Rotative efficiency

$$\begin{aligned}\eta_R &= 0.9922 - 0.05908 * BAR + 0.07424 * C_p - 0.0225 * lcb \\ \eta_R &= 0.9922 - 0.05908 * 0.8 + 0.07424 * 0.656 - 0.0225 * 69.7 \\ &= 1.02\end{aligned}$$

Required thrust

$$\begin{aligned}T &= R_T / (1 - t) \\ &= 722 / (1 - 0.1995) \\ &= 901.3 \text{ KN}\end{aligned}$$

Velocity of advance

$$\begin{aligned}V_A &= V * (1 - w) \\ &= 20 \times 0.5144 \times (1 - 0.275) \\ &= 7.4588 \text{ m/s}^2\end{aligned}$$

Propeller diameter

$$D = 0.74 * T = 5.402 \text{ m}$$

(For Container ship Propeller Dia $< 0.74 \times T$ as per Man-Basic Principle of Ship Propulsion)

Assuming the initial value of diameter to be 5.4 m, the choice of propeller RPM, number of blades, brake power calculation was done and the main engine was selected for the design vessel speed of 20 knots.

Other Efficiencies

Shaft Efficiency , $\eta_s = 0.98$

Sea margin = 15% (Owners's requirement)

Engine margin = 10% (Owners's requirement)

Gear box Efficiency, $\eta_b = 1$ (No gear used for propeller engine matching)

5.3.3. Procedure

Propeller design begins with initial approximation of the diameter of the propeller, wake and thrust deduction factor using empirical relations[7]. Using the wake and thrust deduction fraction, velocity of advance and required thrust can be estimated from ship design velocity and resistance.

Advance Coefficient:

$$J = \frac{V_A}{n \times D} \quad (10)$$

Thrust Coefficient:

$$K_T = \frac{T}{\rho \times n^2 \times D^4} \quad (11)$$

Step 1 - Since thrust coefficient and advance coefficient are fixed by empirical formula, an equation for K_T by can be determined eliminating unknown quantities by calculation.

$$K_T = \frac{T}{\rho \times V_A^2 \times D^2} \times J^2 \quad (12)$$

Step 2 - The final equation for K_T is obtained without 'n'. Using this equation, we will find the values for a range of advance coefficient.

Step 3 - Considering Wageningen B propeller series K_T and K_Q values for range of J and P/D values for a particular BAR (A_e/A_o) and number of blade (Z) has been calculated using the equation developed by Oosterveld and Oossanen. Open water efficiency η_0 has been calculated by using for a range of J and P/D values.

Step 4 - These values for K_T , K_Q and η_0 for a range of P/D (usually from 0.5 to 1.4 at an increment of 0.1) and J (usually from 0 to 1.5 at an increment of 0.1) were plotted for each Blade Area Ratio (A_e/A_o) – BAR chart for particular number of blade (Z).

Step 5 - η_0 is plotted against range of J for one BAR chart. For each P/D values, J and η_0 at each intersection point of K_T curve and is obtained.

Step 6 - Using these values a graph of η_0 is plotted against P/D . From this graph maximum η_0 value is determined for that specific BAR chart which is maximum η_0 that can be obtained for a propeller with ‘ Z ’ number of blade for that specific A_e/A_o ratio. Number of propeller revolution per second (n) is obtained from the value of J corresponding to maximum η_0 .

Before starting the propeller design calculations, the minimum blade area ratio has to be fixed by Aufer Keller formula in order to avoid cavitation[7].

$$\frac{A_E}{A_o} (\min) = K + \frac{(1.3+0.3Z) \times T}{(P_{atm} + \rho gh - P_v) \times D^2} \quad (13)$$

Where $K = 0.2$ for single screw propellers
 $Z =$ number of blades
 $h =$ height of LWL above shaft central line in meters

$(A_E/A_o) \min$ is calculated for three, four and five bladed propellers and other propeller characteristics are calculated using EXCEL generated by Author.

$P_{atm} = 101.366 \text{ kN/m}^2$ (Atmospheric Pressure)
 $P_v = 1.704 \text{ kN/m}^2$ (Vapour Pressure of water)
 $h = 2.8 \text{ m}$
 $D = 5.4 \text{ m}$
 $K = 0.2$ for single screw propellers
 $\rho = 1.025 \text{ t/m}^3$
 $g =$ acceleration due to gravity (9.81 m/s^2)

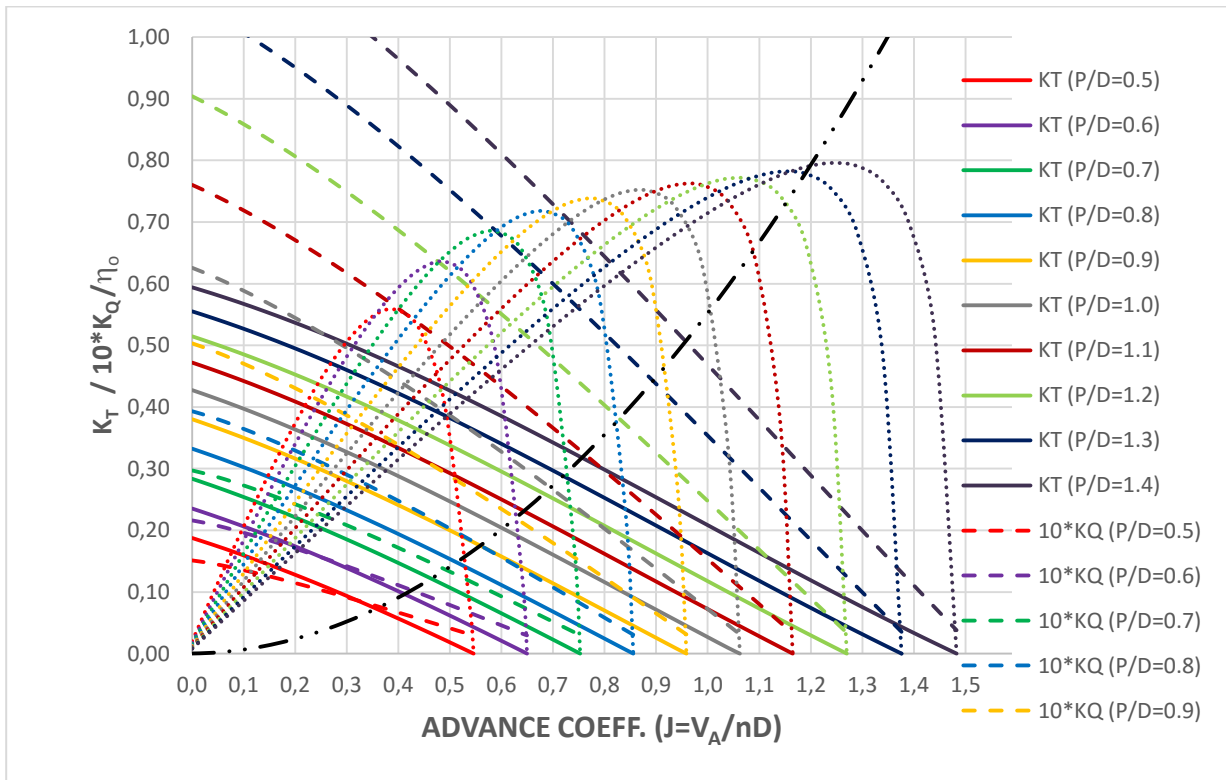


Fig 6: An example of K_T , K_Q and efficiency Chart

For **Z** = **3**

$(A_E/A_O)_{min}$ = 0.599 [Using Aufen Keller formula]

Selected (A_E/A_O) = 0.6

For **Z** = **4**

$(A_E/A_O)_{min}$ = 0.6535 [Using Aufen Keller formula]

Selected (A_E/A_O) = 0.7

For **Z** = **5**

$(A_E/A_O)_{min}$ = 0.7624 [Using Aufen Keller formula]

Selected (A_E/A_O) = 0.8

5.3.4 Selection of number of blades

Number of blades is selected based on the open water efficiencies of three ,four and five bladed propellers. Author has developed a software in C++ programming language (code is attached as Annexure) to compute propeller open water characteristics for any Blade Area Ratio, any number of blades and for all pitch ratios. This application relies on two polynomials for K_t and K_q derived with multiple regression analysis by Oosterveld[12] as follows:

$$K_T = \sum_{s,t,u,v} C_{s,t,u,v}^T (J)^5 \left(\frac{P}{D}\right)^t \left(\frac{Ae}{A_0}\right)^u (Z)^v \quad (14)$$

$$K_Q = \sum_{s,t,u,v} C_{s,t,u,v}^Q (J)^5 \left(\frac{P}{D}\right)^t \left(\frac{Ae}{A_0}\right)^u (Z)^v \quad (15)$$

Terms to control in equations above are the advance ratio, and number of blades. Results of combination of propeller curves and ship curve are shown in figure below.

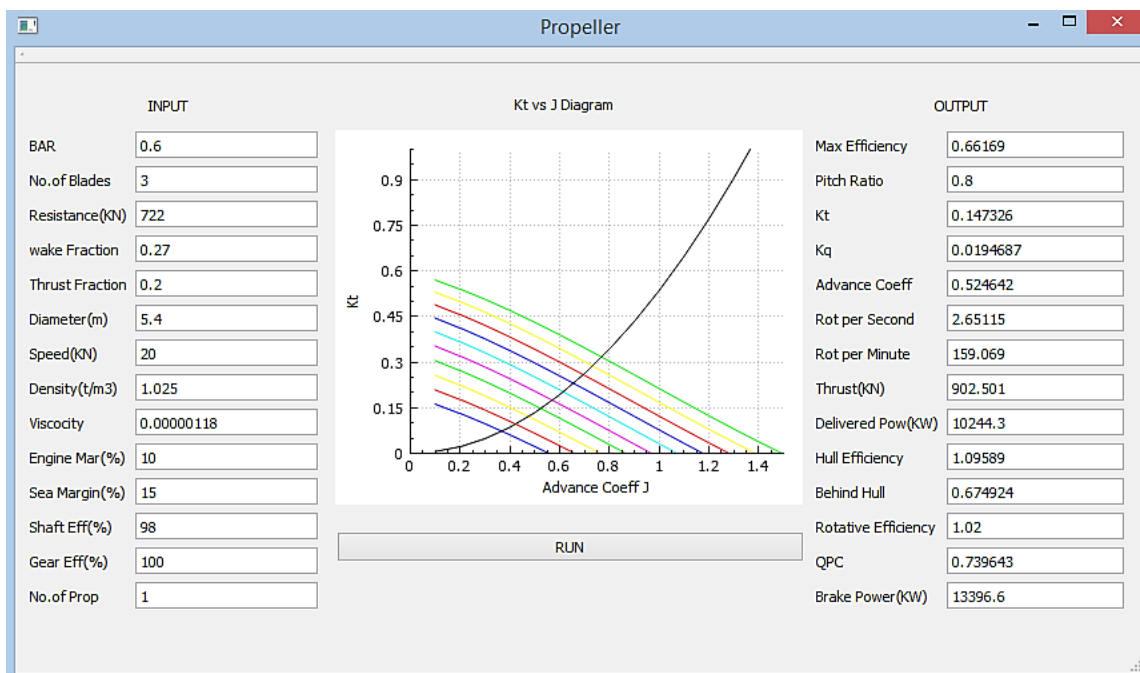


Fig 7: Input Data and Output Result of propeller design (Z=3)

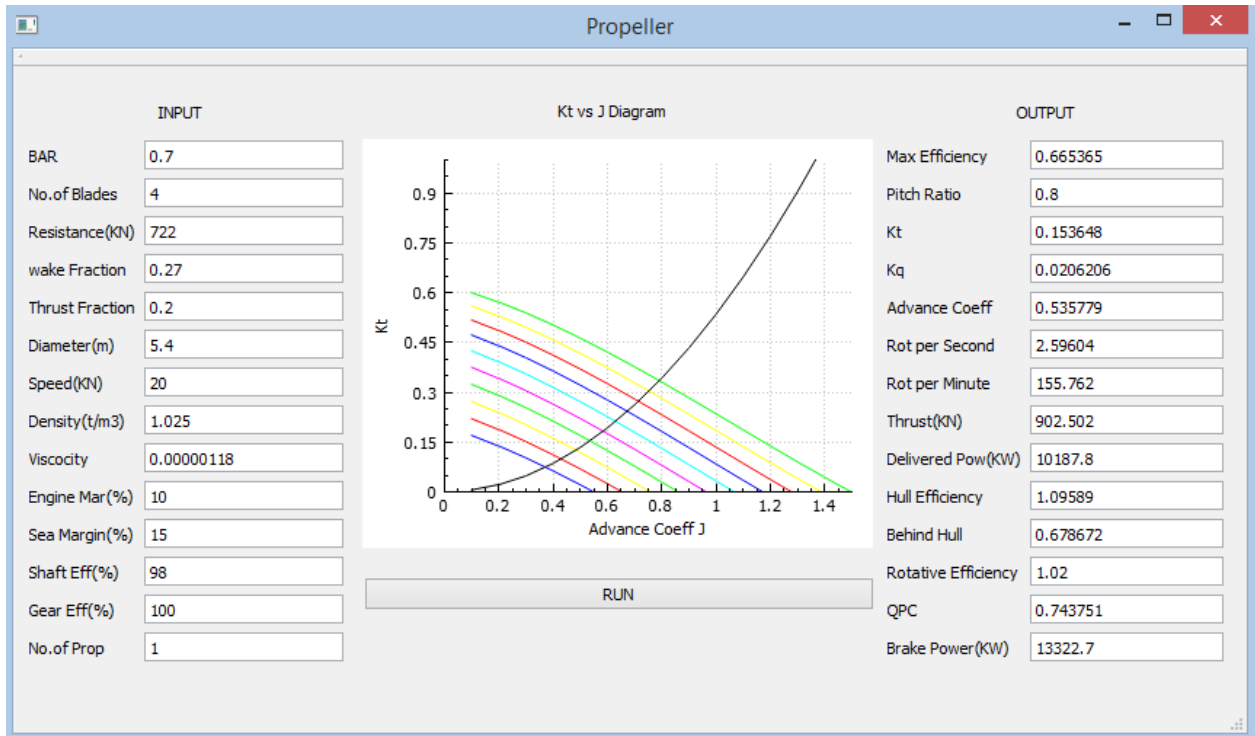


Fig 8: Input Data and Output Result of propeller design ($Z=4$)

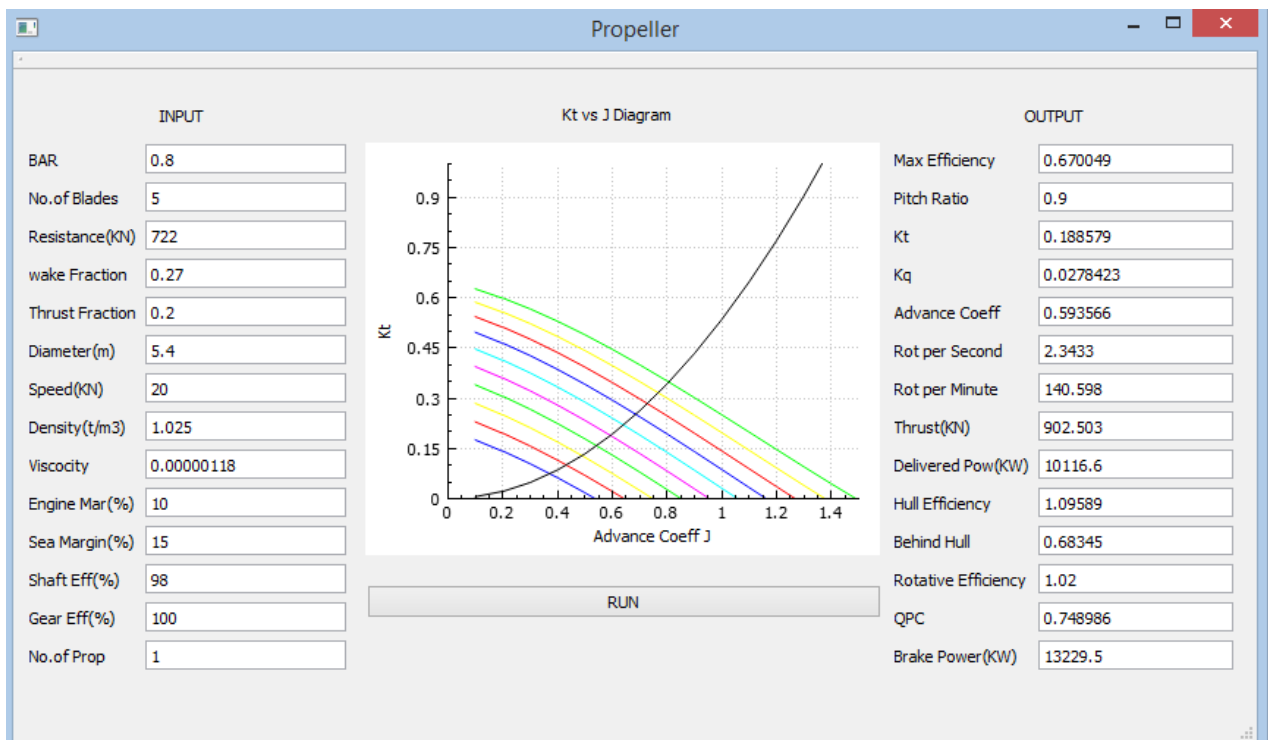


Fig 9: Input Data and Output Result of propeller design ($Z=5$)

Comparing open water efficiencies (η_o) of the three propellers the five blade propeller has more efficiency than three and four bladed propellers.

$$P_B = \frac{P_E}{\eta_h \eta_o \eta_R \eta_s \times (1 - \text{sea margin}) \times (1 - \text{engine margin})} \quad (16)$$

$$\begin{aligned} \text{Engine brake power} = P_B &= 722 \times 20 \times 0.5144 / (1.096 \times 0.67 \times 1.02 \times 0.98 \times 0.85 \times 0.9) \\ &= 13229 \text{ kW} \\ \text{N(required)} &= 141 \text{ rpm} \end{aligned}$$

5.3.5. Selection of Main Engine

According to the advantages that are relatively inexpensive fuel, low sensitivity to fuel quality and low maintenance, the diesel engine will be selected as the main engine of the container ship. They are available in a variety of velocity of rotations, from low (< 250 rpm) to high speed (>1000 rpm).

Maximizing propeller efficiency is often associated with large diameters with low rotation rate. Taking this as a starting point, we will select a low speed diesel engine to avoid the necessity of a reduction gear. From available catalogues on internet from principal manufactures and based on brake power and RPM, the main engine is selected.

Engine Manufacturer	-	MAN
Model	-	K60MC-S
No of Cylinders	-	7
Brake Power	-	13860 kW
RPM	-	150 rpm

6. PROPELLER DESIGN

6.1. General considerations

Propeller design can be divided in three stages: preliminary design, detailed design and analysis.

On the first stage, preliminary design, we use methodical series data based on open water test for model propellers to obtain characteristics for optimal efficiency. Among them, we find: diameter, number of blades, average pitch ratio and blade area ratio. At this stage, propeller is designed to attain average flow conditions behind the ship.

Subsequently, the second stage deals with the determination of necessary blade geometry to generate desired thrust or to consume a defined delivered power. Analytical methods are used to fulfil the task.

Finally, after the geometry of the propeller is completely defined, the propeller is analyzed in all operating conditions, steady and unsteady. The objective is to find the pressure distribution on propeller blades, evaluate the hydrodynamics performances of propeller in off design conditions and determine how the ship's wake influences the propeller performances and to predict the required propeller RPM and delivered power in self propelled condition of the vessel at design speed.

6.2. Propeller Preliminary Design

Propeller must be designed to consume totality of engine delivered power at a given rotation rate. Power delivered to the propeller is calculated as follows:

$$P_D = P_B (\text{ main engine}) \times (1-EM) \times (1-SM) \times \eta_s$$

$$P_D = 13860 \text{ kW} \times 0.9 \times 0.85 \times 0.98$$

$$P_D = 10390 \text{ kW}$$

In above equation, 0.9 values corresponds to 0.10 engine margin (EM) because is not recommended to use the engine at the maximum continuous power MCR, and 0.85 corresponds to sea margin (SM), given by the difference between the power required in real

6.3. Optimal propeller diameter

A new diameter that satisfies new engine rotation rate must be computed to obtain maximum efficiency, for this purpose a procedure is shown below:

Torque coefficient:

$$K_Q = \frac{Q}{\rho \times n^2 \times D^5}$$

Brake power:

$$P_B = 2\pi \times n \times Q$$

Delivered power:

$$P_D = P_B (\text{main engine}) \times (1 - \text{EM}) \times (1 - \text{SM}) \times \eta_s$$

Combining the above equations to eliminate the unknown diameter, we obtain

$$K_Q = \frac{P_D \times n^2 \times J^5}{2\pi \times \rho \times V_A^5}$$

Varying the value of advance coefficients, J in steps of 0.05 a curve is obtained. Intersection of this curve with K_q curves from B-Wageningnen diagrams for a five bladed propeller with EAR 0.8 will give the corresponding advance coefficients for each pitch ratio. Soon after, thrust coefficient is obtained for these values of J.

Author has developed a software named ‘Propeller-Diameter’ in C++ programming language (code is attached as Annexure) to compute optimum diameter while using selected main engine with the brake power of 13860 kW at 150 rpm. As the input of the program, the engine margin and sea margin are considered as 10% and 15% respectively.

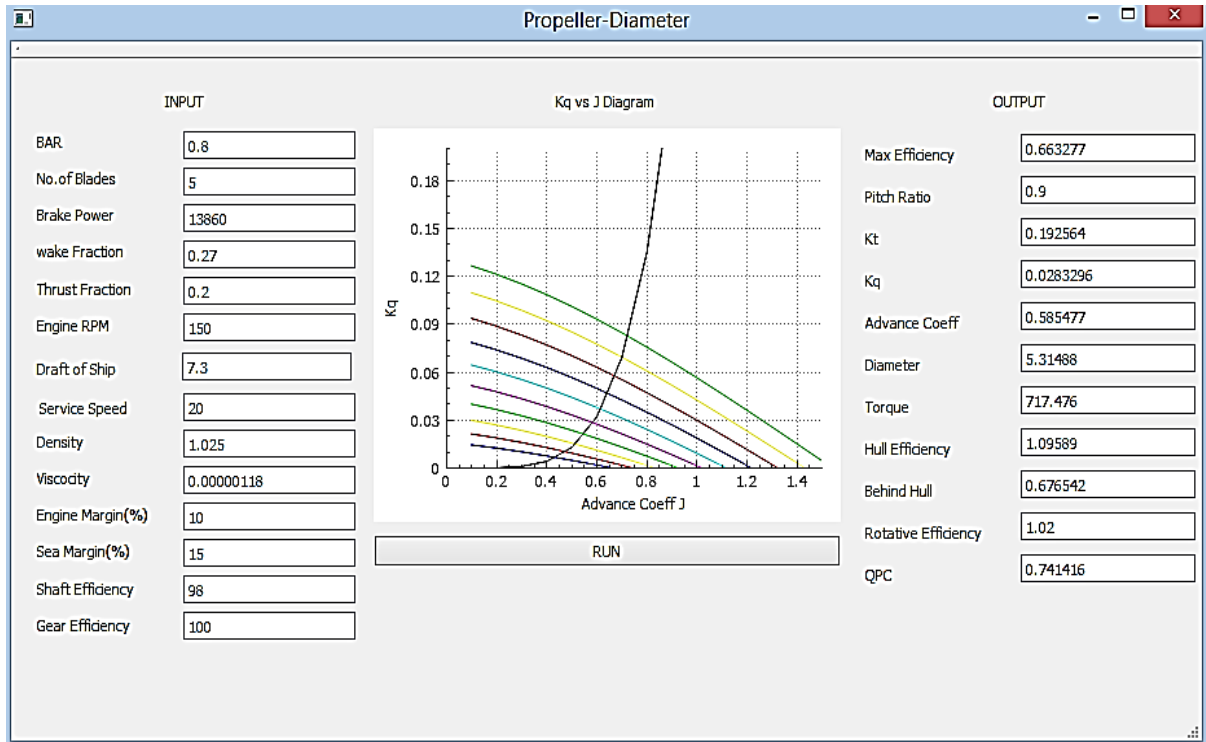


Fig 11: Input Data and Output Result for finding optimum diameter for selected main engine

After selection of the final optimal diameter, the space available for fitting the propeller is checked. Required propeller clearance to avoid and/or minimize vibrations problems at the stern of the ship has to be checked. In this matter, DNV present basic rules for minimal distance of propeller regarding ship hull [1].

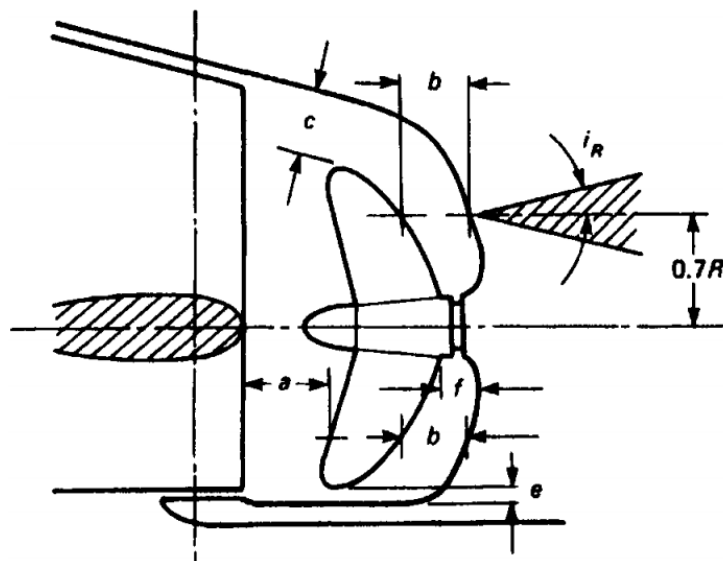


Fig 12: Propeller clearances for single screw ships (DNV)
Taken from Volker Bertram Ship design for efficiency and economy.

For optimal diameter $D = 5.31$ m, the propeller tip clearance should be greater than $0.2D = 1.062$ m as per Figure 13.

In the design container vessel,

Height of ship hull from base line = 6.5 m

Height of shaft line from baseline = 2.8 m

Actual tip clearance = $6.5\text{m} - 2.75\text{m} - (5.31\text{m} / 2) = 1.1$ m

Since the actual tip clearance is greater than the recommended clearance value and an increase value of the clearance reduces noise on the ship due to propeller, $D = 5.31$ m can be finalized as the final optimal diameter. The following table shows the information of the Optimal B-Wageningen standard series propeller.

Table 6: Optimal B-Wageningen standard series propeller for the ship

Optimum Diameter	D [m]	5.31
Maximum open water efficiency	η_o [-]	0.6633
Thrust Coefficient	K_T [-]	0.193
Torque Coefficient	K_Q [-]	0.028
Blade Area Ratio	EAR	0.8
Number of Blades	Z	5
Pitch Ratio	P/D	0.9

6.4. Ship Speed Estimation with Preliminary Propeller Design

One of owners' requirements is that the vessel is able to achieve a certain speed under power service less than maximum continuous power MCR of the engine. Checking that the service speed complies with the design speed of the vessel is crucial in the design. Estimated velocity must be $\pm 2\%$ of design speed.

Author has developed a software named 'Ship_speed' in C++ programming language (code is attached as Annexure) to compute the delivered power, RPM and Pitch ratio, etc. for different speeds and the results are shown in Table 7.

The screenshot shows a software window titled 'Ship_speed'. It is divided into two main sections: 'Input' and 'Output'. Each section contains a list of parameters with corresponding input or output fields. A 'RUN' button is located at the bottom left of the input section.

Input		Output	
BAR	0.8	Pitch Ratio	0.901538
No. of Blades	5	Efficiency	0.662841
Resistance(KN)	722	Kq	0.0284604
Brake Power(KW)	13860	Kt	0.193149
wake fraction	0.27	Advance Coefficient	0.586016
Thrust Deduction	0.2	Thrust(KN)	916.999
RPM	150	Hull Efficiency	1.09589
Diameter(m)	5.31	Behind Hull Efficiency	0.676098
Ship Service Speed(Kn)	20	Relative Rotative	1.02
Density(t/m ³)	1.025	QPC	0.740929
Viscosity	0.00000118	Delivered Power	10026
Engine Margin(%)	10		
Sea Margin(%)	15		
Shaft Efficiency(%)	98		
Gear box Efficiency(%)	100		

Fig 13: Input and output data for 'Ship_speed' software

Table 7: Prediction of performance characteristics of propeller at different speeds

Vs	[knots]	18	20	22
Vs	[m/s]	9.2592	10.288	11.31
Va	[m/s]	6.759216	7.51024	8.26
R _T	[kN]	468.34	722	1233.1
J	[-]	0.527414	0.586016	0.644
Kq	[-]	0.028	0.028	0.028
P/D	[-]	0.865	0.901	0.936
η ₀	[-]	0.62	0.66	0.69
Kt	[-]	0.201	0.193	0.183
T	[kN]	956.2	917	870.5
QPC	[-]	0.69	0.74	0.77
P _E	[kW]	4336.4	7427.9	13956
P _D	[kW]	6236.7	10026	18038

Construction of a graph considering propeller delivered power vs. ship speed will determine: V is vessel speed achieved by propeller while using the selected main engine, and for required propeller pitch ratio

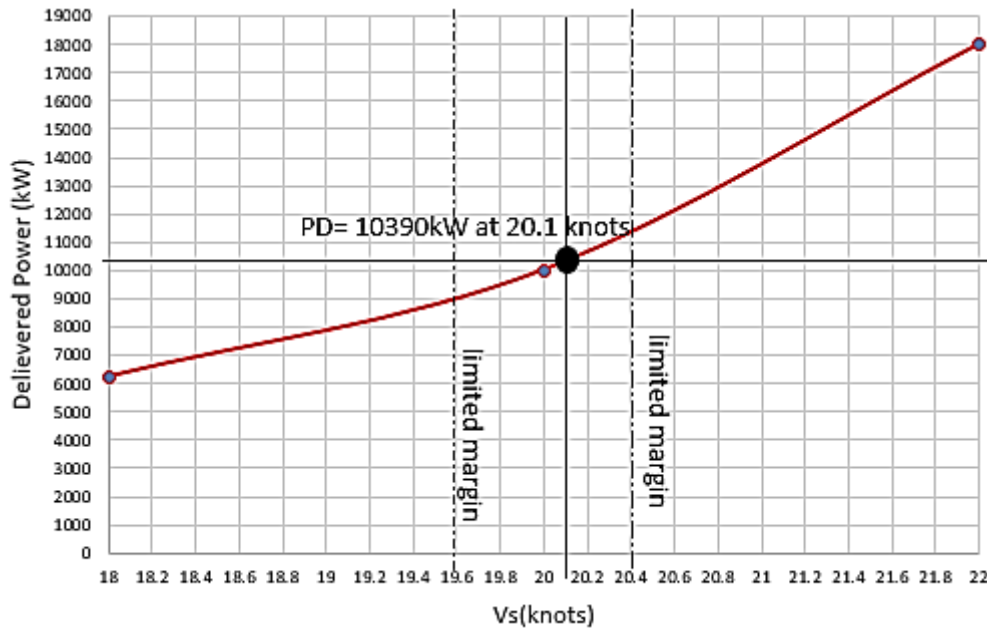


Fig 14: Ship velocity estimation according to delivered power to the propeller

From the above figure,

Main engine brake power = P_B = 13860 kW

Delivered Power = P_D = 10390 kW

Actual ship speed = V_s = 20.1 knots

Required Pitch Ratio = P/D = 0.903

Main geometrical parameters and hydrodynamic characteristics of the optimal B-Wageningen propeller are presented in table below:

Table 8: Main geometrical and hydrodynamic characteristics of optimal propeller

Propeller Type	Fixed pitch B5-Wageningen series	
Optimum Diameter	D [m]	5.31
Maximum open water efficiency	η_0 [-]	0.663
Thrust Coefficient	K_T [-]	0.193
Torque Coefficient	K_Q [-]	0.028
Blade Area Ratio	EAR	0.8
Number of Blades	Z	5
Pitch Ratio	P/D	0.9

Table 9: Geometrical Characteristics of Wageningen propeller

r/R	Chord Length(mm)	Thickness(mm)	Camber	Pitch Ratio(mm)
0.2	1409.3	172.8	0	4778
0.3	1595.9	153.2	0	4778
0.4	1738.4	133.6	0	4778
0.5	1824.9	113.9	0	4778
0.6	1854.5	94.3	0	4778
0.7	1818.1	74.7	0	4778
0.8	1670.5	55.1	0	4778
0.9	1341.5	35.5	0	4778
1.0	0	15.9	0	4778

Table 10 : K_T, K_Q & η_o values for pitch ratio = 0.9 for different values of advance coefficient (Statistical)

J	K_T	$10*K_Q$	η_o
0.1	0.394	0.514	0.122
0.2	0.360	0.476	0.241
0.3	0.321	0.433	0.354
0.4	0.278	0.385	0.460
0.5	0.233	0.332	0.559
0.6	0.1845	0.274	0.643
0.7	0.133	0.213	0.696
0.8	0.081	0.14	0.59
0.9	0	0.04	0

6.5. Experimental result

Experimental test including open water and self propulsion test were carried out at basin in ICEPRONAV Engineering SRL, Galati to study the propeller characteristics. The test results are the intellectual property of ICEPRONAV and has been produced with regards to academic purpose.

Table 11: K_T, K_Q & η_o values for different values of J at 20 Knots from open water test (experimental)

J	K_T	$10*K_Q$	η_o
0.1	0.3736	0.467	0.1273
0.2	0.3373	0.4314	0.2489
0.3	0.2987	0.3919	0.3639
0.4	0.2577	0.3485	0.4708
0.5	0.2144	0.3014	0.5661
0.6	0.1688	0.2504	0.6437
0.7	0.1208	0.1956	0.6878
0.8	0.0705	0.1371	0.6547
0.9	0	0.07	0

Table 12: Result of self propulsion test (experimental)

V(Knots)	K_T	$10*K_Q$	t	wake	η_H	η_R
16	0.156	0.2359	0.1759	0.2778	1.1411	1.0182
17	0.1591	0.2393	0.1848	0.2836	1.1379	1.0183
18	0.1635	0.2443	0.1857	0.2835	1.1365	1.0207
19	0.169	0.2506	0.1811	0.28	1.1373	1.0229
20	0.1774	0.26	0.1766	0.273	1.1326	1.0225
21	0.1866	0.2704	0.1623	0.2571	1.1276	1.0228
22	0.1968	0.2818	0.156	0.2491	1.1241	1.0226

V(Knots)	F_n	Thrust(KN)	η_o	η_D	P_D	RPM
16	0.214	418.61	0.661	0.768	3734.2	106.26
17	0.228	483.9	0.6573	0.7617	4574.5	113.15
18	0.241	575.14	0.6517	0.7559	5794.5	121.68
19	0.254	695.58	0.6442	0.7494	7503.5	131.61
20	0.268	876.25	0.632	0.7319	10243.7	144.19
21	0.281	1138.51	0.6173	0.712	14615.8	160.24
22	0.295	1460.93	0.5998	0.6894	20446.1	176.74

Data in both tables 11 and 12 will be used to compare with the numerical analysis which has been demonstrated at later stage of this work.

6.6. Cavitation Checking

Cavitation is the phenomenon that occurs when the local pressure is lower than vaporization pressure of water at a certain temperature, forming bubbles of air that collapse rapidly when the pressure increases again. Regarding propellers, because they deal with high speeds, according to Bernoulli's equation, the pressure decreases and it may sometimes induce cavitation on propellers blades.

Negative effects can arise on a cavitating propeller, such as vibration, noise, material erosion on propeller surface, and thrust reduction. Avoidance of cavitation and erosion is an important aspect in the design of any propeller. At preliminary stage, the use of Burrill's diagrams provides a lower limit of blade area ratio to reduce the danger of cavitation appearance.

Since the optimum propeller design for the preliminary design stage is finished, the percentage of cavitation will be checked as the following. A digitalized form of Burrill's diagram [7] has been developed as shown in figure.15.

Table 13: Cavitation Checking with Burrill's Diagram

Burrill's Cavitation Check		
$P_{atm} + \rho gh =$	149.57	kN/m^2
$P_v =$	1.7	kN/m^2
density =	1.025	t/m^3
$g =$	9.81	m/s^2
$h =$	4.8	m
$P_{atm} + \rho gh - P_v$	147.87	kN/m^2
$V_{0.7R}^2 =$	1005.1	
$1/2\rho V_{0.7R}^2 =$	515.1	
$A_e/A_o = EAR =$	0.8	
$A_e = EAR * \pi/4 * D^2$	17.716	m^2
$A_p = A_e * (1.067 - 0.229 P/D)$	15.252	m^2
$T = R_T / (1-t)$	902.5	kN
$\sigma_c = [P_{atm} + \rho gh - P_v] / [1/2\rho V_{0.7R}^2]$	0.2871	
$\tau_c = T / (A_p * 1/2\rho V_{0.7R}^2)$	0.1148	

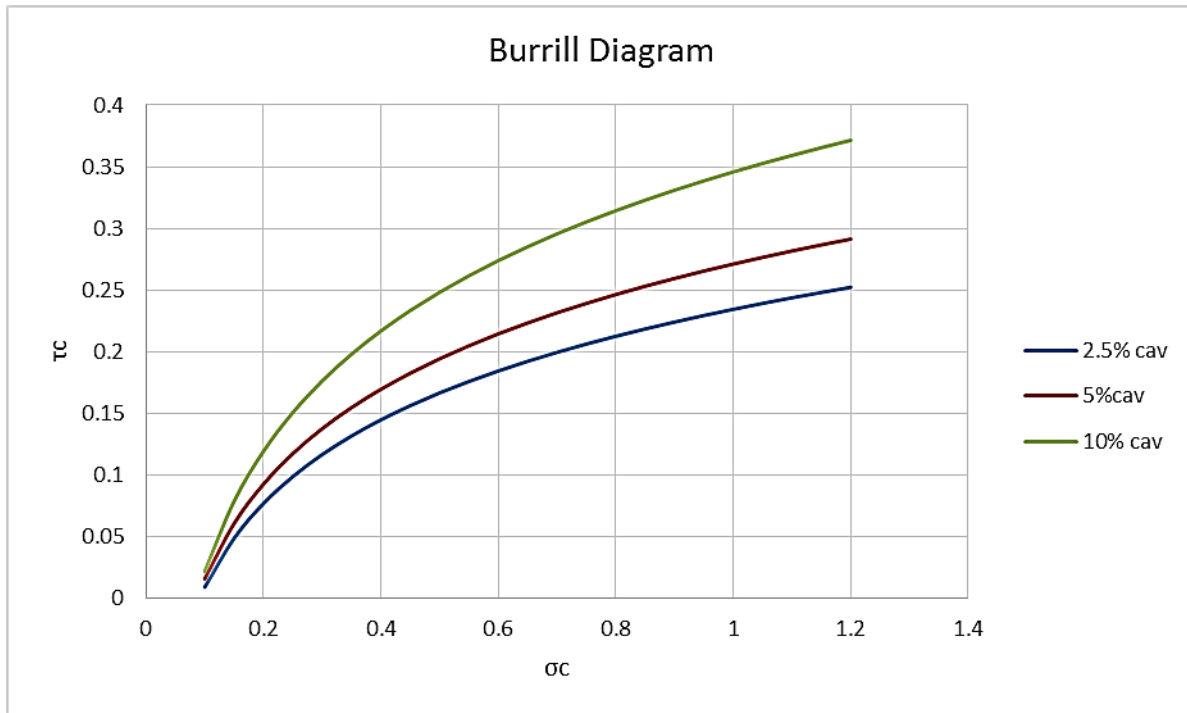


Fig 15: Digitalized Burrill's Diagram for Cavitation % checking

Table 14: Digitized Burrill Chart

Digitized Burrill Chart	
$\tau_c = 0.09798 \ln(\sigma_c) + 0.23426$	2.5% cavitation
$\tau_c = 0.11104 \ln(\sigma_c) + 0.27104$	5% cavitation
$\tau_c = 0.14093 \ln(\sigma_c) + 0.34580$	10% cavitation

From the above equations in Table 14, the cavitation percentage has been calculated as 2.85% which is acceptable for the high speed container vessel.

7. DETAIL DESIGN

7.1. Propeller Detail Design stage

At this stage the data available are nominal wake obtained by wake measurement test, propeller characteristics and the delivered power from preliminary analysis using Wageningen B propellers as explained before.

The main objective of detail design is to perform analyzed the wake adapted propeller using analytical methods like circulation or lifting line theory with surface correction. The inflow coming onto the propeller is assumed to vary radially to determine exact blade geometry for a specified radial distribution of the loading.

Lift generation on an aero foil section can be explained using Bernoulli's Principle which states that within a steady flow of constant energy, when the fluid flows through a region of lower pressure it speeds up and vice versa. When a flow passes over an unsymmetrical section the flow velocity over the upper surface increases resulting in decrease of pressure while flow velocity decreases on lower surface increasing the pressure. This difference in pressure distribution on upper and lower surface of section is estimated as Lift.

Whereas the lift generated by each propeller blade can be explained by circulation or vortex theory in terms of circulation around it in a manner similar to lift generation on an aero foil.

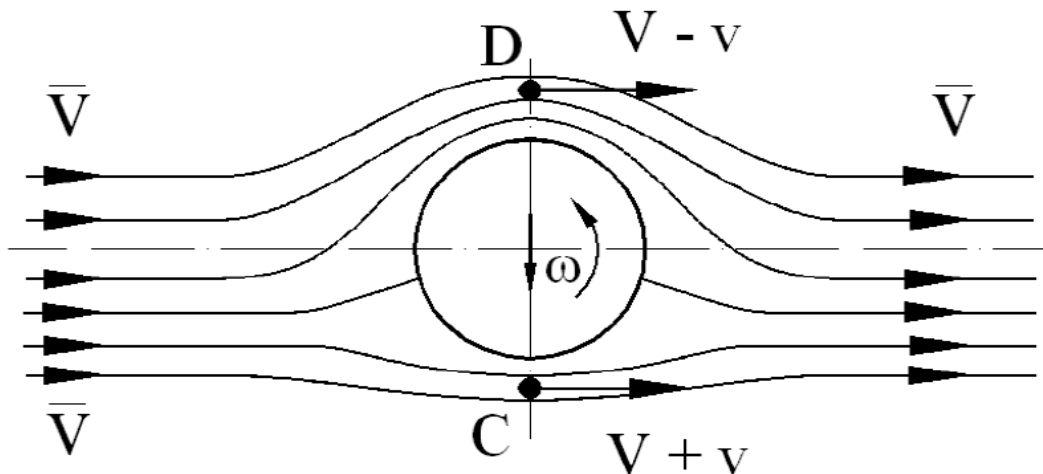


Fig 16:Lift generation on a cylinder due to circulation

The effective force acting on the cylinder with circulation may be shown to be given by the Kutta Jukovski equation.

7.2. Lifting Line Theory

The lifting line model is perhaps the simplest mathematical model of propeller action in that it assumes the aero foil blade sections to be replaced by a single line vortex whose strength varies from section to section. The line, which is a continuous in the radial direction about which vortices act, is termed the lifting line, and is normally considered to pass through the aerodynamic centers of the section.

Since the flow is disturbed due to presence of unsymmetrical blade sections a circulation of streamline around the section is generated as shown in figure 17. The lift generated by propeller blade can be mathematically expressed in strength of circulation of vortices around the lifting line.

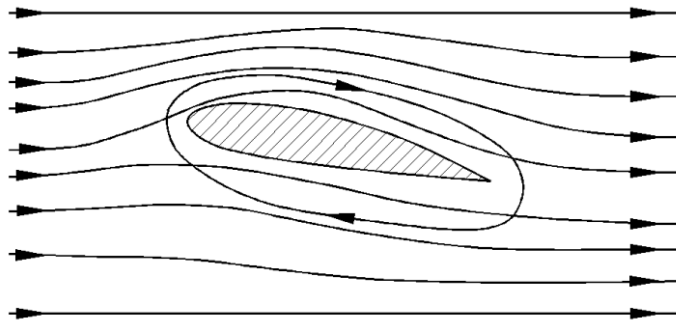


Fig 17:Streamlines around the Blade section

Free vortices are shed from bound vortices which vary in radial direction along this lifting line downstream. The strength of the circulation are given by

$$\Gamma_F = \left(\frac{d\Gamma_b}{dr} \right) \Delta r \tag{17}$$

Where Γ_b is the bound vortex strength and r is the radial position on the propeller.

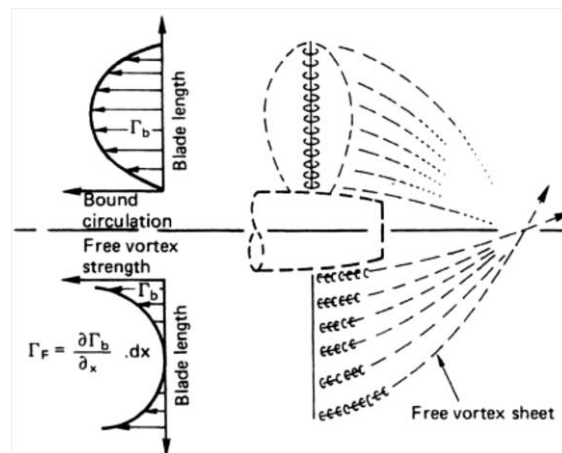


Fig 18: Free Vortices Shedding Varied in radial direction
Taken from Carlton, Marine Propeller and propulsion, chapter 8

7.3. Lifting Line Theory in Propeller Design

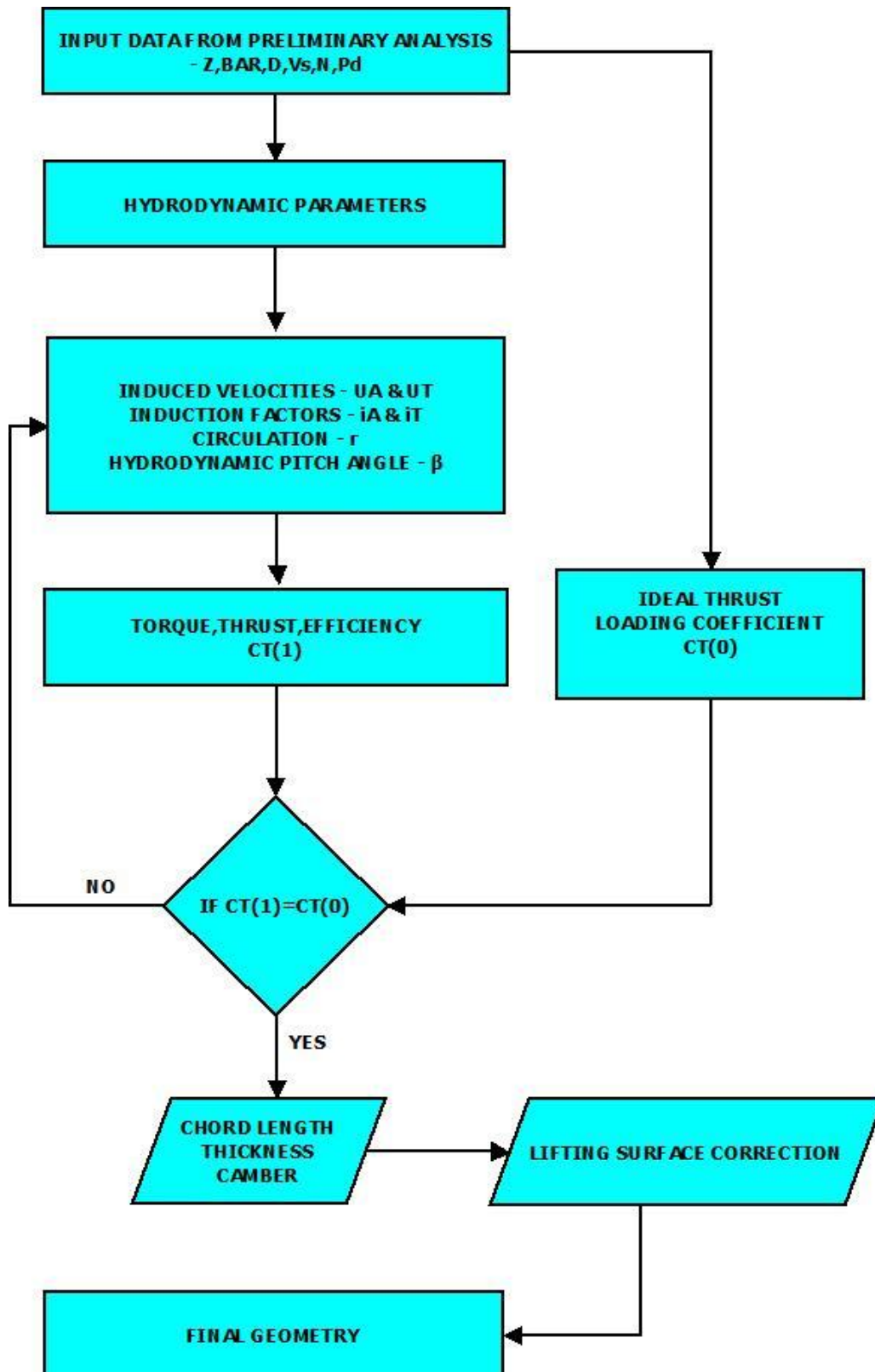


Fig 19: Schematic representation of lifting line theory

Propeller design using lifting line theory can be divided in two stages:

Stage 1 – Hydrodynamic design stage where the circulation, induced velocities (U_A & U_T), resultant velocity and the Hydrodynamic pitch at various radiuses are calculated without knowing propeller geometry through iterative procedure.

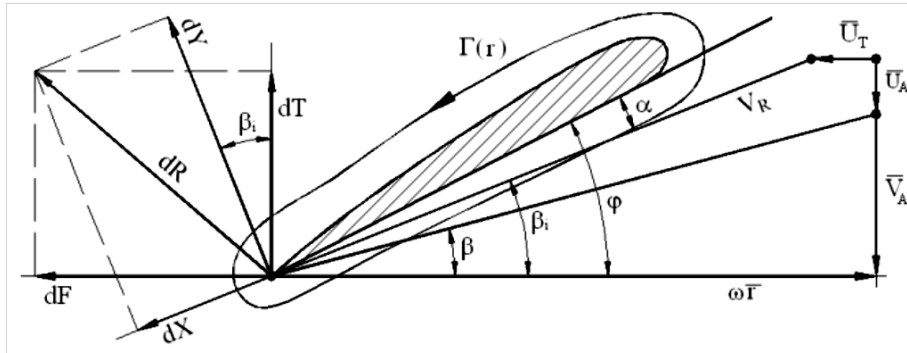


Fig 20: Velocity diagram for a blade section

Where α is the angle of attack, β the advanced angle, β_i hydrodynamic pitch angle, δ the final pitch angle.

From figure 3, relations between induced velocities are determined as follows:

$$v = \sqrt{(V_A + U_A)^2 + (wr - U_t)^2} \quad (18)$$

$$\frac{U_A}{V_A} + \text{tg}(\beta_i) \frac{U_t}{V_A} = \frac{\text{tg}(\beta_i)}{\text{tg}(\beta)} - 1 \quad (19)$$

Velocity induced to flow downstream by the vortex system generated by the propeller is computed using the law of Biot Savart or by Laplace equation.

These laws to determine induced velocities are related to simple aero foil. So in order to modify for practical application in the field of ship propellers, Lerbs and Goldstein have calculated the “induction factors” which are function by which the complicated system of trailing vortices behind a rotating propeller is related to that of a simple aero foil.

$$U_A(r) = \frac{1}{2\pi D} \int_{r_b}^R i_a \frac{d\Gamma}{dr_0} \frac{dr_0}{r - r_0} \quad (20)$$

$$U_T(r) = \frac{1}{2\pi D} \int_{r_b}^R i_T \frac{d\Gamma}{dr_0} \frac{dr_0}{r - r_0} \quad (21)$$

Where, i_a and i_T are the Lerbs induction factors

The thrust developed by the blade element and the torque are computed as function of the circulation $\Gamma(r)$.

From fig 3:

$$dT = dY \cos \beta_i - dX \sin \beta_i = dY \cos \beta_i (1 - \mathcal{E} \cdot \tan \beta_i) \quad (22)$$

$$dF = dY \sin \beta_i + dX \cos \beta_i = dY \sin \beta_i (1 + \mathcal{E} \cdot \cot \beta_i) \quad (23)$$

$$dQ = dF \cdot r = r \cdot dY \sin \beta_i (1 + \mathcal{E} \cdot \cot \beta_i) \quad (24)$$

Where $\mathcal{E} = \frac{X}{Y}$, the efficiency of section as lifting device

Applying Kutta Jukovski equation:

$$dY = \rho \cdot \Gamma(r) dr \cdot V_r \quad (25)$$

We get new equation for elemental thrust and torque respectively at each radius as:

$$dT = \rho \cdot \Gamma(r) \cdot (\omega r - u_T) \cdot (1 - \mathcal{E} \cdot \tan \beta_i) dr \quad (26)$$

$$dQ = r \cdot \rho \cdot \Gamma(r) \cdot (V_A + u_A) \cdot (1 + \mathcal{E} \cdot \cot \beta_i) dr \quad (27)$$

The efficiency of blade element:

$$\eta = \frac{\text{Thrust Generated}}{\text{Torque Applied}}$$

$$\eta = \frac{dT \cdot V_A}{dQ \cdot \omega}$$

Now substituting dT and dQ,

$$\eta = \frac{\tan \beta_i \cdot (1 - \mathcal{E} \cdot \tan \beta_i)}{\tan \beta_i \cdot (1 + \mathcal{E} \cdot \cot \beta_i)} \quad (28)$$

For the thrust:

$$T = \rho z \int_{rb}^R \Gamma(r) (\omega r - U_T) (1 - \mathcal{E} \tan(\beta_i)) dr \quad (29)$$

For the torque:

$$Q = \rho z \int_{rb}^R \Gamma(r) (V_A + U_A) \left(1 + \frac{\mathcal{E}}{\tan(\beta_i)}\right) r dr \quad (30)$$

Solving for the vortex strength distribution, convergence is obtained when the trust coefficient computed equalizes the ideal thrust coefficient value.

Ideal thrust coefficient:

$$C_{Ti} = 4z \int_{rb}^1 G(1 - w(r))^2 \left(\frac{1}{\text{tg}(\beta)} - \frac{U_T}{V_A} \right) dr = \frac{8T_i}{\pi\rho V^2 D^2} \quad (31)$$

Stage 2 - On the basis of above hydrodynamic calculations the optimum blade geometry is generated considering cavitation suppression and strength criteria.

7.4. Lifting Line Theory computation

Final geometry of propeller has been developed using in-house code in Pascal scripting developed by department of Naval Architecture, University of Galati.

Following data are available as input for lifting line method from preliminary analysis stage:

- a) The resistance of hull
- b) The delivery power available for propeller from main engine
- c) Operating conditions like ship speed, propeller revolution rate etc.
- d) Hull-propeller interaction coefficients: w , t , η_r
- e) Propeller characteristics – Diameter, No of blades, Expanded blade area ratio

Table 15: Data input for lifting line method

Resistance(KN)	722
Ship Velocity(Kn)	20.1
Delivered Power(KW)	10390
Propeller RPM	150
Propeller Diameter(m)	5.31
No.of Blades	5
Blade Area Ratio	0.8
Wake	0.27
t	0.2
η_r	1.02

7.4.1. Mean circumferential wake

The mean circumferential data has been provided by ICEPRONAV Engineering SRL which was obtained during model testing carried out.

Table 16: Mean wake value at different radii from experimental test

r/R	Wake mean value
0.2	0.854
0.3	0.768
0.4	0.670
0.5	0.559
0.7	0.352
0.9	0.174
1.0	0.131

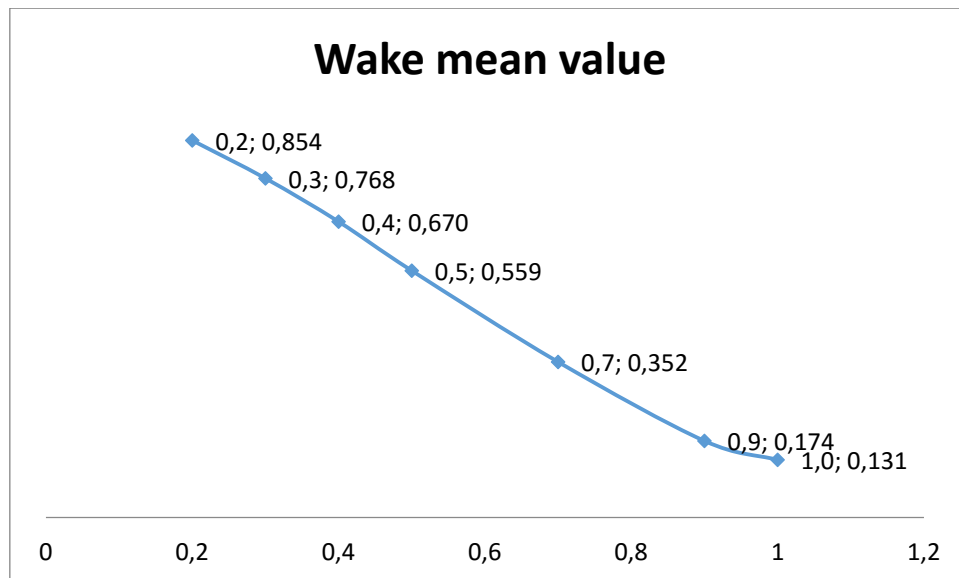


Fig 21: Circumferential wake distribution along blade sections at different radii

7.4.2. Velocities at blade sections

As per the lifting line theory axial and tangential velocities for the converged solution are shown in below table.

Table 17: Axial, Tangential and resultant velocities along the propeller sections at each radii

r/R	Ua/Vr	Ut/Vr	Vr
0.2	0.815	0.980	6.6
0.3	0.628	0.532	12.2
0.4	0.568	0.367	16.4
0.5	0.483	0.254	20.7
0.6	0.398	0.176	24.9
0.7	0.320	0.123	29.1
0.8	0.251	0.085	33.2
0.9	0.197	0.059	37.3
1	0.240	0.065	41.1

The propeller geometry defined by chord length, pitch ratio, thickness and camber has been obtained after computation is given in table:

Table 18: Geometry of blade sections at each radii

r/R	Chord Length(mm)	Thickness(mm)	Camber(mm)	Pitch(mm)
0.2	1454.6	255.5	0	3622.1
0.3	1609.9	218.9	82.3	4174.6
0.4	1749.3	185	54.3	4328.8
0.5	1866.7	152.9	43	4373
0.6	1952.1	123.5	34.4	4403.7
0.7	1987.1	95.8	28.8	4426.1
0.8	1933.8	69.4	24.8	4451.7
0.9	1685.5	44.7	22.2	4447
1	0	2.3	10.6	4443.7

Table 19: Propeller characteristics based on detail design

Velocity(Kn)	20.0005
Thrust(KN)	904.1
Torque(KNm)	693.1
K_t	0.19
K_q	0.027
η	0.6
Adv Coeff	0.5452
P/D	0.824

8. PROPELLER GEOMETRY

8.1. NACA 66(mod-0.8) Profile

The geometry of a marine propeller is generally characterized by Profile Shape, number of Blade, Diameter (D), Pitch (P), expanded blade area ratio (BAR), Skew and Rake. While considering the profile shape most commonly used series defining section profile is NACA.

NACA are series of aero foil sections developed by National Advisory Committee for Aeronautics (NACA) through series of experiments based on aero foil geometry in a rational and systematic way [16]. Each section is defined by a definite set of characteristics like camber and thickness distribution along chord length capable of developing specific velocity or pressure profile along its suction or pressure side to generate lift force.

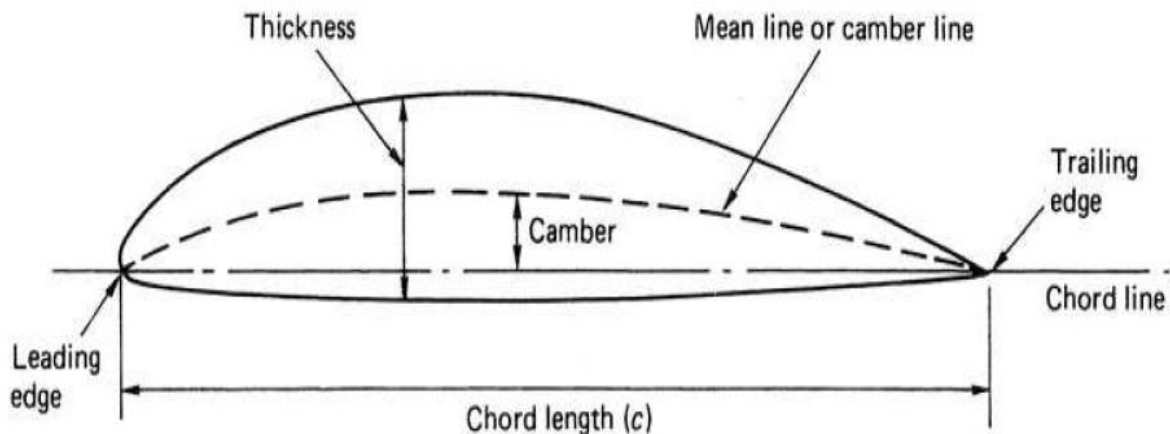


Fig 22: Typical NACA profile
Taken from Carlton, Marine Propeller and propulsion, chapter 3

The above figure shows the general definition of the aero foil. The mean line or camber line is the locus of the mid-points between the upper and lower surfaces when measured perpendicular to the camber line. The extremities of the camber line are termed the leading and trailing edges of the aero foil and the straight line joining these two points is termed the chord line. The distance between the leading and trailing edges when measured along the chord line is termed the chord length (c) of the section. The camber of the section is the maximum distance between the mean camber line and the chord line, measured perpendicular to the chord line. The aero foil thickness is the distance between the upper and lower surfaces

of the section, usually measured perpendicularly to the chord line although strictly this should be to the camber line.

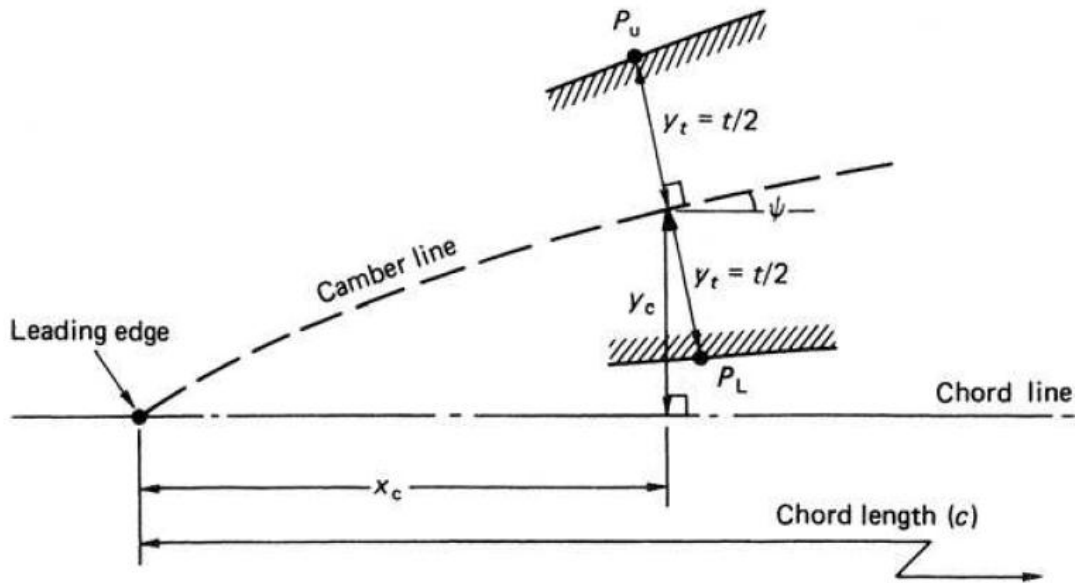


Fig 23:Representation of two dimensional point on NACA profile
Taken from Carlton, Marine Propeller and propulsion, chapter 3

Considering two points along the blade section $P_u(X_u, Y_u)$ on the upper side and $P_l(X_l, Y_l)$ on the lower side with reference to a point on camber line $P_c(X_c, Y_c)$ as shown in the above figure where x-ordinates are the distance from the leading edge.

In 2 dimensional blade section definition the co-ordinates X_u , X_l , Y_u and Y_l can be defined with respect to X_c , Y_c , Y_t (local section semi-thickness) and Θ (the slope of the camber line at the non-dimensional chordal position X_c) as follows :

$$X_u = X_c - Y_t \sin \theta$$

$$X_l = X_c + Y_t \sin \theta$$

$$Y_u = Y_c + Y_t \cos \theta$$

$$Y_l = Y_c - Y_t \cos \theta$$

Developing 3-D geometry of propeller from 2-D we have to consider pitch, rake and skew angles since the propeller sections are lying on a helicoidally surface and corresponding pitch angles which varies at each section.

Considering a point $P(X_p, Y_p, Z_p)$ along upper (u) or lower (l) surface of propeller will be defined w.r.t rake angle (i_G), skew angle (θ_s), pitch angle (θ_{nt}) and radius(r) as follows:

$$X_p = -[i_G + r \theta_s \tan(\theta_{nt})] + (0.5c - X_c) \sin(\theta_{nt}) + Y_{u,l} \cos(\theta_{nt}) \quad (32)$$

$$Y_p = r \sin \left[\theta_s - \frac{180[(0.5c - X_c) \cos(\theta_{nt}) + Y_{u,l} \sin(\theta_{nt})]}{\pi r} \right] \quad (33)$$

$$Z_p = r \cos \left[\theta_s - \frac{180[(0.5c - X_c) \cos(\theta_{nt}) + Y_{u,l} \sin(\theta_{nt})]}{\pi r} \right] \quad (34)$$

8.2. Geometry Generation

The geometry generation has been carried out using NACA 66 (mod) aero foil section [7] with a certain combination of camber and thickness distribution for chord length, maximum thickness and camber obtained from the lifting line theory at each radius.

Author has used NACA 66 (mod) airfoil section as it is the most commonly used sections for marine propeller blades. A code in C++ programming language has been developed to generate points [16] of all blade sections (26 points along each radius) which are attached to appendix.

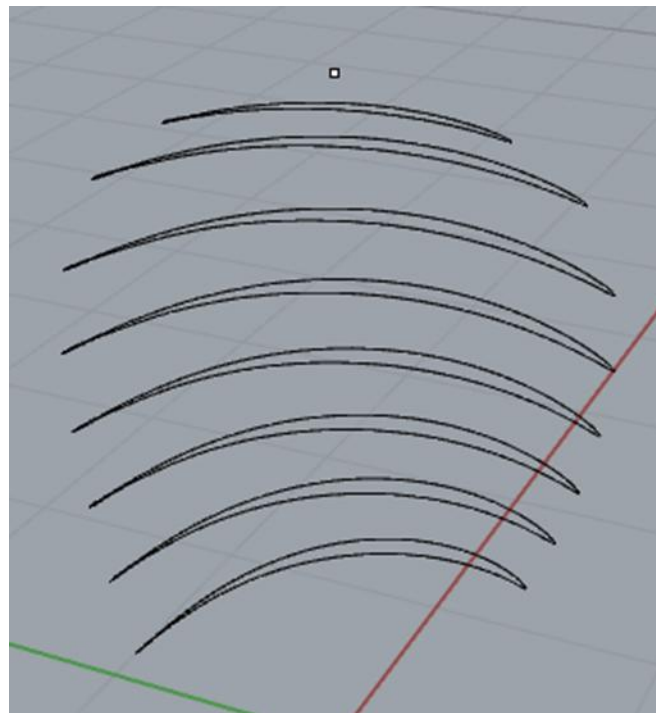


Fig 24: Propeller blade sections generated using Rhino software

9. CFD ANALYSIS

9.1. Numerical Analysis using SHIPFLOW software

CFD analysis of propeller is used to study the hydrodynamic performance of the propeller understand local flow details including both steady as well as unsteady flow. By performing numerical simulation designer can understand the propeller characteristics and hence improve the design or select a most promising candidate design for model testing.

Numerical analysis using SHIPFLOW software can be done in three different stages:

- 1) Resistance Computation
- 2) Open water test to determine propeller characteristics in steady flow
- 3) Self-propulsion to analyze propeller performance in unsteady flow.

9.2. Numerical Solvers of SHIPFLOW software

The main two type of flow solvers in SHIPFLOW are XCHAP is a RANS solver for steady incompressible flow and XPAN which is the potential flow solver.

9.2.1. XPAN module – Potential Flow solver

The potential flow solver determines the potential flow around hull based on non-linear Rankine source panel method [10] using higher order panels with singularity distributions and non-linear free surface boundary conditions.

9.2.2. XCHAP module – RANSE solver

XCHAP in ShipFlow is a finite volume RANS solver which solves the steady incompressible Reynolds Average Navier-Stokes equations using ADI (Alternate direction implicity) discretization method [6].

The fundamental laws governing viscous fluid flow describing conservation of fluid mass and momentum are the equation of continuity and the Navier-Stokes equation respectively.

$$\rho \frac{\partial V}{\partial t} + \rho V \cdot \text{grad}V = \rho g - \text{grad}P + \mu \Delta V + \text{grad}\left(\frac{\mu}{3} \text{div}V\right) \quad (35)$$

The NS equation consists of non-stationary acceleration, inertia, gravity force, pressure force and viscous force terms.

At present there isn't any analytical solution derived for NS equation and it is impossible to solve directly for flow around complex structures like Ship even with super computer computation capability. So in order to avoid complication and obtain a solution with lesser computational resources NS equation is averaged over a period of time and a new variable known as Reynolds stresses defined by turbulence is introduced. Now the velocity and pressure terms in NS equation becomes mean velocity and mean pressure terms. Reynolds stress brings in additional six unknown terms and more equation taking moment of NS is required for solving unknowns.

Solving the RANS equations will give the time average velocity and pressure, but since the time fluctuating velocity and pressure in general are much smaller in amplitude, knowing the average will usually be enough.

9.2.3. Theory behind ShipFlow computation for propeller analysis[4]

The geometry of propeller specified by chord length, thickness, camber and pitch are been defined by the lifting line theory solved during detail design stage.

In XCHAP solver the effect of the propeller is taken into account by a force field computed by the lifting line method depending on circulation strength induced on to the flow due to presence of the propeller.

The propeller is embedded in a cylindrical grid and the interaction with the surrounding grids for the hull is managed by the overlapping grid capability of XCHAP solver. When the flow passes through the propeller it's linear and angular momentum increases as if it had passed a propeller of infinite number of blades. This results in an efficient method to predict the propeller hull interactions i.e. wake and thrust deduction factors in terms of computational time and accuracy similar to a self-propulsion test.

In SHIPFLOW the body forces can be computed with a built in lifting line propeller analysis program. The computation of axial and tangential propeller induced velocities is done using Lerb & Goldstein method similar to the procedure explained in detail design stage. The axial and tangential force components acting on a blade section are related to the local thrust and torque depends upon the circulation which varies in both the radial and circumferential directions of the propeller disk.

Using the Kutta - Jukovski theorem the forces per volume unit can be determined with respect to discretized cell width 'dx 'as:

$$F_x = \frac{z.r}{dx} \left(\frac{\pi}{J} + \frac{U_{TH}-U_T}{v.r} \right) \quad (36)$$

$$F_T = \frac{z.r}{dx.r.v} (V_A + U_A) \quad (37)$$

The lift coefficient of a blade section is given as:

$$C_L = C_{L0} + \frac{\partial C_L}{\partial \alpha} \cdot \alpha \quad (38)$$

Where the slope of lift coefficient with respect to angle of attack is approximated as:

$$\frac{\partial C_L}{\partial \alpha} = 2\pi \cdot c_f \quad (39)$$

C_{L0} is calculated from the two dimensional blade element theory[9] and corrected using lifting surface correction. By varying the angle ' α ' which is the difference between geometric and hydrodynamic pitch the value of circulation strength and body forces can be determined when the equation 38 is satisfied.

The computation of the body forces are embedded in an iterative procedure where first the current approximation of the velocity field is extracted at a representative propeller plane. The effective wake is thereafter obtained by subtracting the induced propeller wake. This is the responsibility of the propeller code and is computed by the circulation from the previous iteration in the lifting line method. The new circulation, forces and torques are computed in the effective wake. Thereafter the forces are distributed over the volume cells in the cylindrical grid. The body forces are added to the right hand side of the flow equations, where they are solved in the cylindrical component grid containing propeller disk. The body forces are updated every tenth iteration in XCHAP. At convergence the total wake computed by XCHAP and the lifting line method should match in the selected propeller plane. A CFD analysis has been carried out as per this method for determination of open water test and self-propulsion characteristics of propeller at full scale.

9.2.4. Computation resources

The computer configuration used for all numerical simulations carried out in this thesis was using 3 Ghz,4 GB ram and processor i5.

9.3. Resistance Calculation

Resistance calculation using CFD technique can be done using different methods namely RANSE or potential flow methods. By using RANSE method, the total resistance of the vessel including the viscous resistance can be determined solving Reynolds averaged Navier-Stokes equations. Whereas potential flow solvers is a simplified form of NS equation considering the fluid to be non-viscous but can only compute the wave resistance while the viscous pressure and frictional resistance can be found by ITTC 1978 procedure or using boundary layer method. RANSE solvers have the significant advantages compared to potential flow solver but they need a lot of computation time and resources. Due to these reasons resistance computation has been carried out using potential flow solver of shipflow – XSPAN based on a surface singularity panel method to determine wave making resistance and frictional resistance using ITTC.

9.3.1. Pre-processing

The pre-processing has been carried out using XSMESH module of Shipflow which generates panels. There are different automatic mesh modes depending upon the mesh density they are classified as very coarse, coarse, medium and fine being the most refined form.

9.3.2. Grid Convergence Study

Grid convergence has been carried out for different mesh sizes at design speed of 20 Knots.

Table 20: Wave resistance coefficient for different automatic mesh modes

Mesh Modes	No. of Panes	No. of Nodes	Cw
Coarse	2622	2853	0.0014
Medium	6666	7030	0.00081
Fine	10396	10852	0.00078

Here as shown in the graph the difference in wave resistance coefficient between fine and medium mesh modes is very small i.e. convergence is obtained for medium. So for easiness and faster computation grid generation for body and free surface has been carried out with automatic mesh mode using medium mesh. (Ship Flow code and result attached as annexure). The free surface has been limited to 2.5 times the length between perpendiculars (LBP) along x-direction where the upstream is about 0.5 times LBP and downstream is as long as LBP.

While the free surface in y-direction is taken as 0.7 times in port & starboard side.

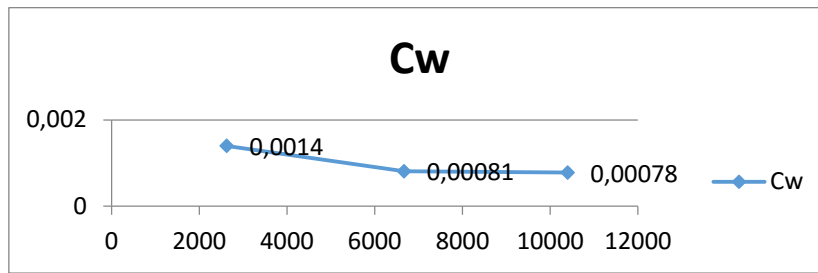


Fig 25: Values of Cw plotted for different panelization mode

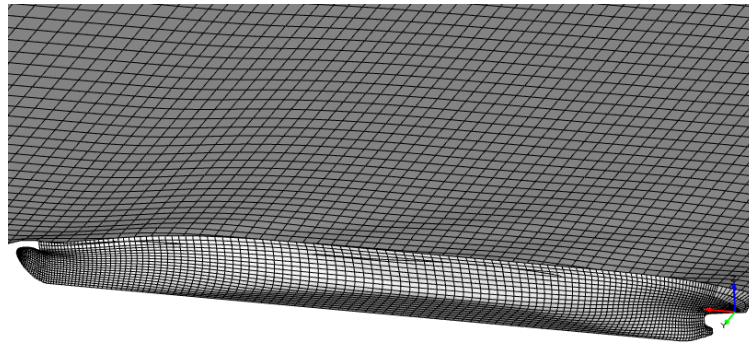


Fig 26: The mesh of the hull below waterline and free surface obtained from CAESES

9.3.3. Post Processing

Post processing has been carried out after computation using CAESES software.

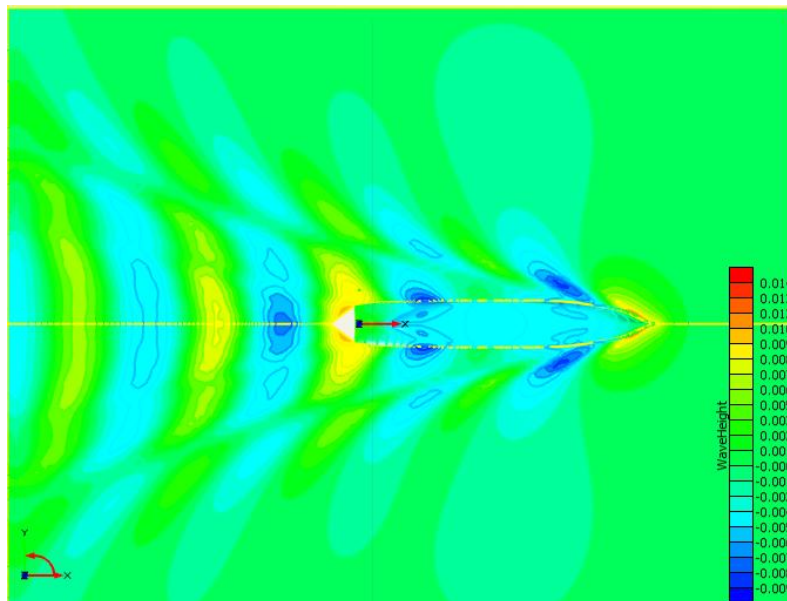


Fig 27: Showing different set of wave system generated due to motion of ship.

From the figure 27 we can identify that there are different set of wave system generated due to the motion of ship. Wave height given in non-dimensional form with respect to Length between perpendiculars. Important system of waves generated are explained briefly below :

- Bow wave is generated at the bow due to stagnation point at bow front where pressure increases resulting in formation of a wave crest.
- Wave generated at the waterline where the stem of ship intersect (Forward perpendicular of ship) due to increase in pressure due to stagnation resulting in a wave crest. Due to interaction between this wave and the bow wave there will be decrease of whole forward wave system which results in reduction of wave making resistance.
- Stern wave generated at stern part of ship due to stagnation resulting in a wave crest due to pressure increase.
- There are other wave systems generated due to curvature of ship as it is seen in figure the about 0.3 times LBP distance from F.P and 0.8 times LBP from F.P where there is generation of wave trough due to pressure drop as flow velocity increases at curvatures in accordance with Bernoulli's principle.

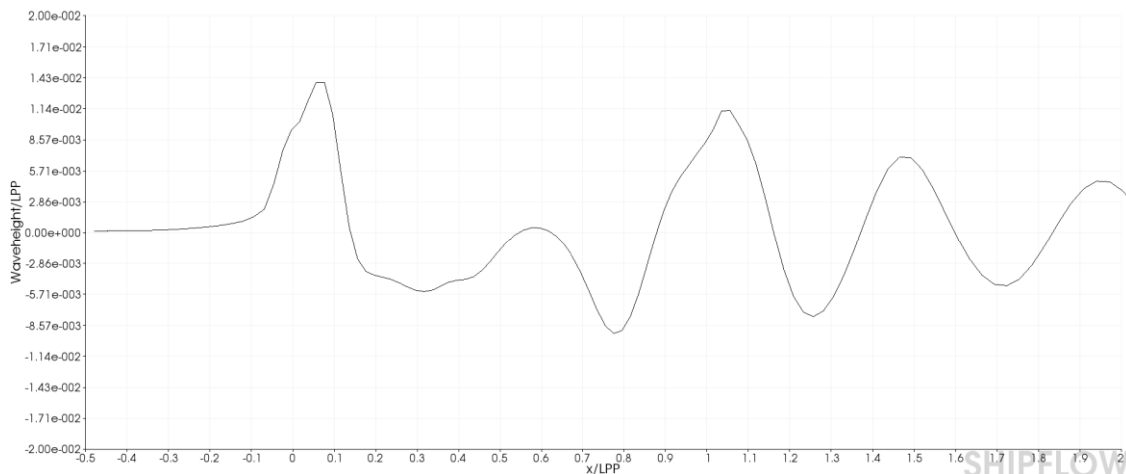


Fig 28: Wave height along the hull from free surface

Table 21: Total Resistance of the ship obtained from Ship Flow

Vel(Kn)	Fn	Rn	CW(XPAN)	CF(ITTC)	1+k(form)
16	0.218	1010780857	0.00005	0.00152	1.12
17	0.231	1073954660	0.00008	0.00151	1.12
18	0.245	1137128464	0.00023	0.00151	1.12
19	0.258	1200302267	0.00046	0.00150	1.12
20	0.272	1263476071	0.00081	0.00149	1.12
21	0.286	1326649875	0.0014	0.00148	1.12
22	0.299	1389823678	0.0019	0.00147	1.12

CA	CT	S(XPAN)	S(m2)	RT(KN)	PE(KW)
0.0004	0.002158	0.2021	4302.0643	322.0	2652.68105
0.0004	0.002173	0.2021	4302.0643	366.4	3204.55748
0.0004	0.002319	0.2021	4302.0643	438.0	4058.67634
0.0004	0.002544	0.2021	4302.0643	534.1	5237.61403
0.0004	0.002966	0.2021	4302.0643	671.1	7121.28239
0.0004	0.00354	0.2021	4302.0643	889.1	9839.96778
0.0004	0.004038	0.2021	4302.0643	1114.3	12904.2811

The form factor k has been obtained using Prohaska's method [11] by simulating resistance test at very low velocities where wave making resistance can be neglected.

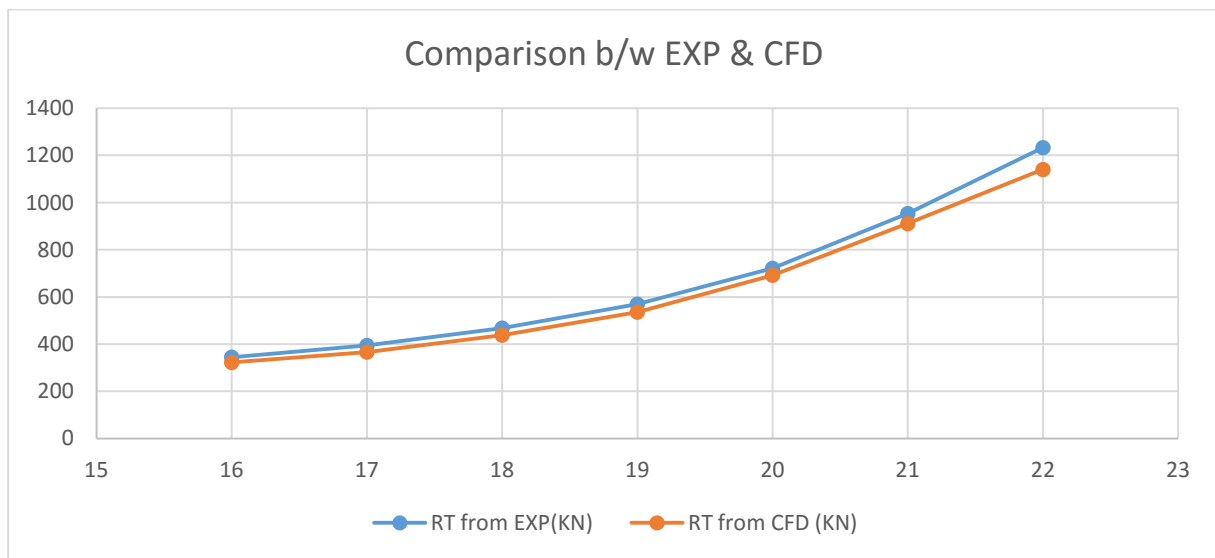


Fig 29: Comparison of resistance for range of velocity obtained from different methods

The figure shows the resistance data obtained from numerical method is in good agreement with experimental results. This resistance data will be used during self-propulsion simulation.

9.4. Open Water Test

The open water characteristics study for Wageningen B propeller and NACA 66 have been carried out using RANSE solver and lifting line command. The geometry of propeller is provided with Propeller command under XFLOW structure of ShipFlow software which is defined with respect to its chord length, camber, pitch and thickness of sections at every non-dimensionalised radii(r/R) from 0.16,0.2,0.3....0.9,0.95,1.(Set up file for ShipFlow computation has been attached to annexure).

Propeller geometry for Wageningen B has been defined as obtained during preliminary analysis while for NACA 66 profile it is from detail design stage.

This study is carried out to determine thrust coefficient, torque coefficient and efficiency of propeller in steady flow condition i.e. is without the hull interactions for the propeller. The computation is carried out as due to interactive coupling between the RANS solver and lifting line method through which body forces accelerating the flow can determined. The result depends upon the geometrical parameters which directly influence the resultant and induced velocities.

The POW module of ShipFlow runs the simulation for the different advance ratios and creates a table with the resulting thrust, torque coefficients and open water efficiency.

9.4.1. Pre-Processing

This command has been used to create a rectilinear grid for XCHAP that can be used as a tunnel for channeling the flow into the propeller which will be placed inside.

The dimensions of the cuboid box have been provided with respect to the size of the propeller (length of box in y and z direction is about 20 times that of propeller diameter) as follows:

Table 22: Dimension of the box tunnel for Propeller

Length	96	m
Breadth	106	m
Height	106	m

Total number of grid in x, y, z direction is (121, 51, and 51) respectively with stretching function to resolve the relatively small cylindrical propeller grid which is positioned in the center in such a way to capture the minute details of the flow.

The turbulence model used is default one which is EASM (Explicit Algebraic stress model).

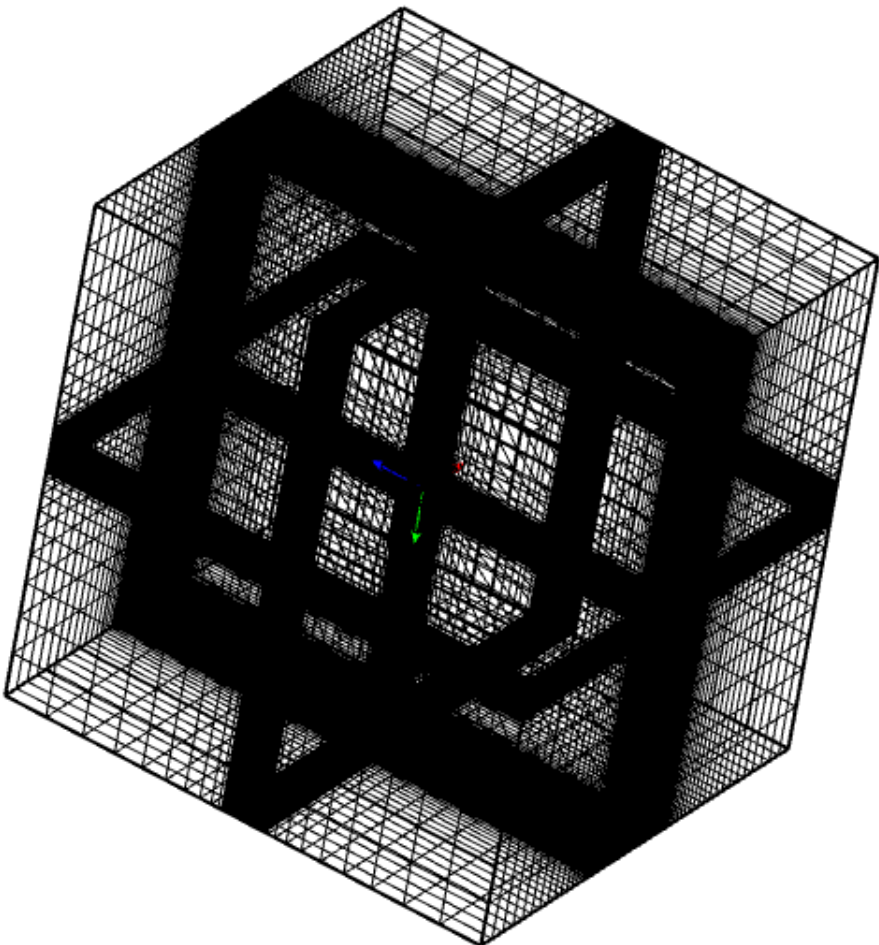


Fig 30: Grid generated for BOX with stretching at center enclosing Propeller Disk

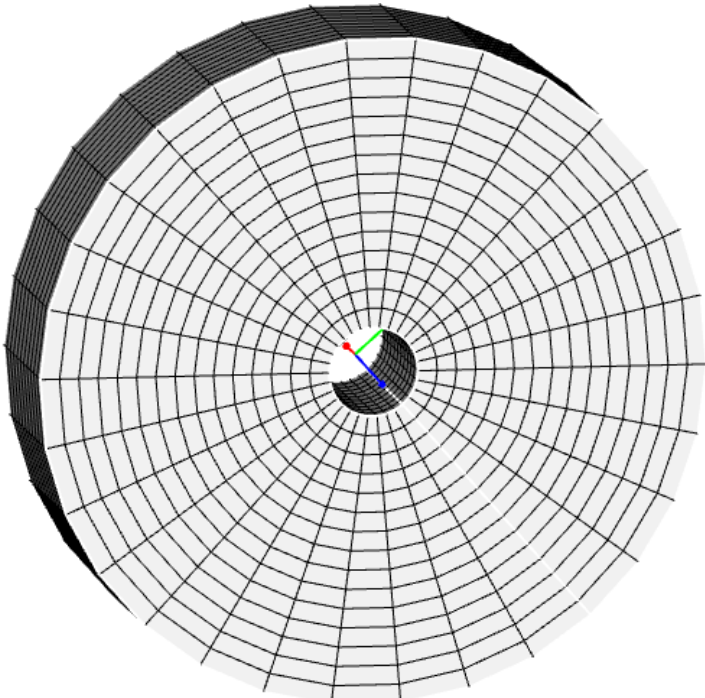


Fig 31: Cylindrical grid generated for Propeller Disk

9.4.1.1. Boundary conditions

Boundary conditions were set as per the ShipFlow manual [10]. Out of the six boundaries of the box two parallel to the propeller plane is defined as inflow and outflow as shown in figure. The boundary starboard side of the propeller looking from the aft side has been set to no slip condition, while remaining three sides are in slip condition. In order for the solver to be stable not more than one boundary condition should be set to no-slip and the stretching has been done towards the no-slip boundary condition. Most of result of boundary conditions was set as default settings in ShipFlow for example the default turbulence used is Explicit Algebraic stress model(EASM)

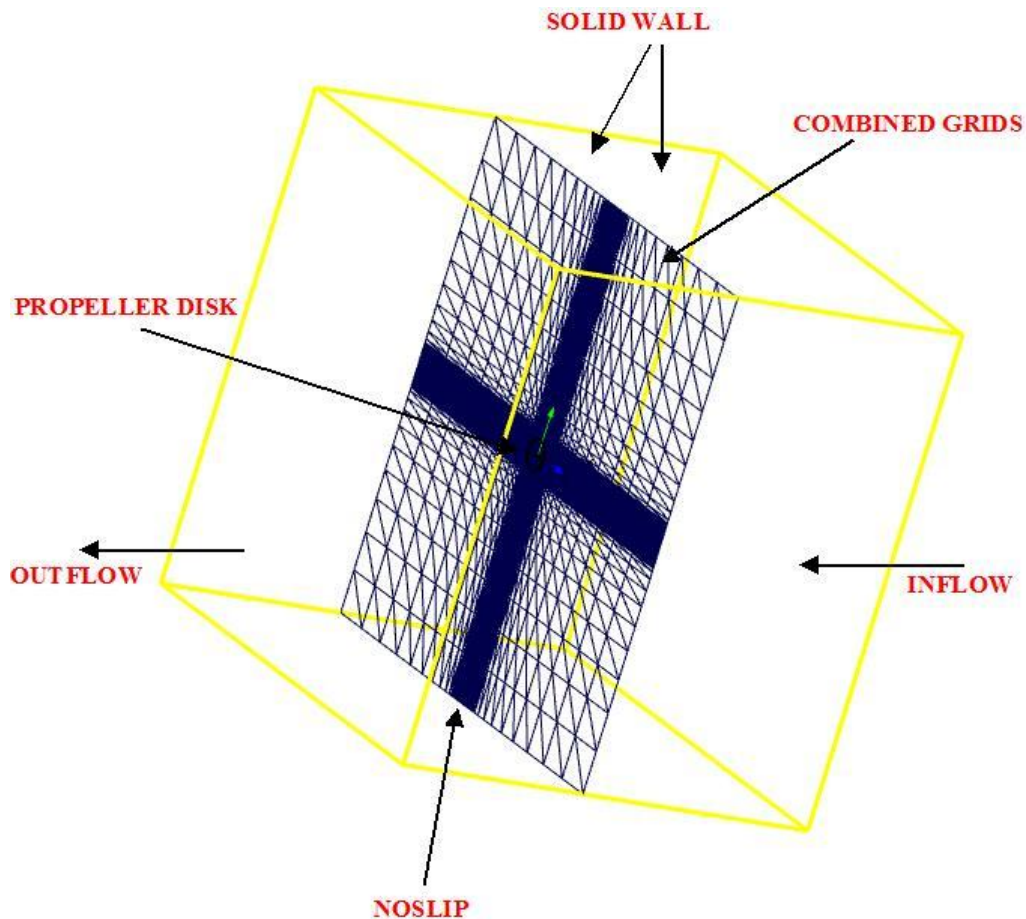


Fig 32: Boundary conditions for Open Water Computation

9.4.2. Computation

Thrust coefficient, torque coefficient and efficiency were computed for each value of advance coefficient (0.1 to 1.0) and were saved in an output file. For each advance coefficient the iteration was limited to 50.

9.4.3. Post Processing

9.4.3.1. Open water characteristics for WAGENINGEN B

The open water test for Wageningen B was carried out in order to compare the propeller characteristics obtained between the experimental and numerical to confirm the result obtained is in acceptable range as these data will be used as input for detail design.

Table 23: K_T, K_Q & η_o (Numerical & Statistical) values for pitch ratio = 0.9 for different values of J

J	Numerical			Experimental		
	K_T	$10*K_Q$	η_o	K_T	$10*K_Q$	η_o
0.1	0.372	0.484	0.122	0.3736	0.467	0.1273
0.2	0.337	0.451	0.238	0.3373	0.4314	0.2489
0.3	0.301	0.415	0.346	0.2987	0.3919	0.3639
0.4	0.260	0.372	0.446	0.2577	0.3485	0.4708
0.5	0.215	0.320	0.534	0.2144	0.3014	0.5661
0.6	0.165	0.260	0.605	0.1688	0.2504	0.6437
0.7	0.110	0.191	0.641	0.1208	0.1956	0.6878
0.8	0.051	0.113	0.578	0.0705	0.1371	0.6547
0.9	0	0.03	0	0	0.07	0

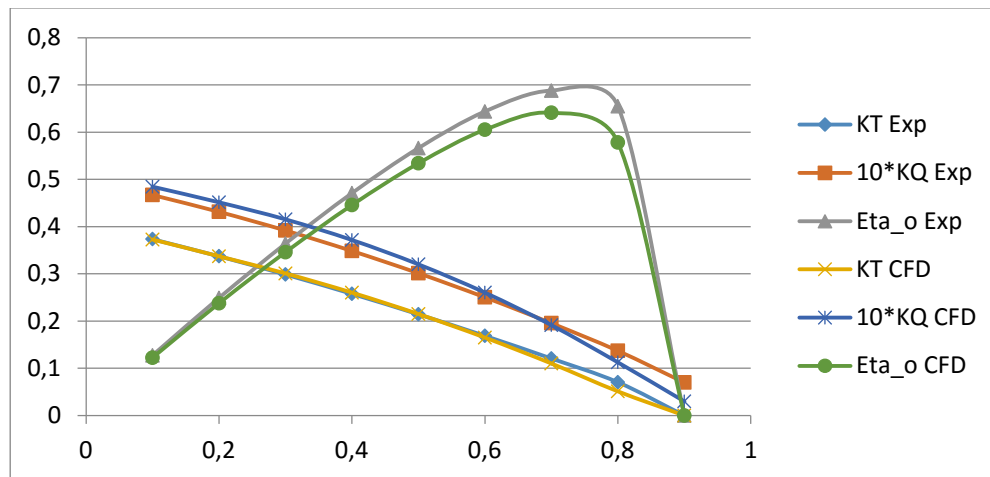


Fig 33: Comparison between K_T, K_Q, η_o obtained from different methods for Wageningen B propeller

From the figure it can be seen that range of values for K_T, K_Q, η_o obtained through numerical and experimental analysis follows same pattern and difference obtained are in the range of 2-3%. Since the numerical analysis are in good agreement with experimental it can be assumed that the pre-processing setup (tunnel & propeller grid) used for open water test is accurate. So the same set up is used to analyze NACA propeller as explained in next section.

9.4.3.2. Open water characteristics for NACA 66 propeller

Propeller characteristics of wake adapted propeller (NACA 66 sections) from open water simulation as given in Table 24 will be used as input value for the self-propulsion simulation.

Table 24: K_T , K_Q , η_o obtained for various advance ratio for final propeller (NACA 66)

J	K_T	$10*K_Q$	η_o
0.1	0.417932	0.508486	0.130812
0.2	0.367202	0.468525	0.249472
0.3	0.326428	0.43062	0.361938
0.4	0.282695	0.387715	0.464179
0.5	0.233572	0.337121	0.551347
0.59	0.184699	0.284442	0.609738
0.6	0.179037	0.278111	0.614746
0.7	0.119803	0.210055	0.635408
0.8	0.0572868	0.131502	0.554667
0.9	0	0.0243621	0

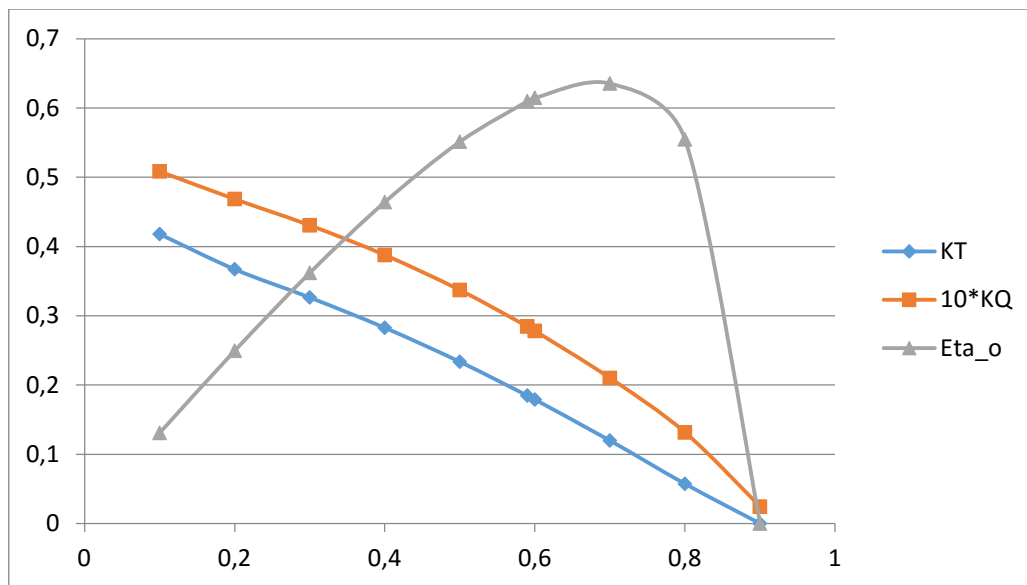


Fig 34: K_T , K_Q , η_o plotted against advance coefficient J for NACA 66 propeller

9.5. Self-Propulsion

The self-propulsion simulations were carried out to study the performance of propeller in unsteady flow condition. The flow reaching the propeller plane is already modified due to the presence of hull.

There are two different approaches namely Zonal and Global approach at present to study propeller characteristics in unsteady flow condition using ShipFlow. Zonal Approach is the basic and most efficient method where the hull is divided into different zones and computation is carried out in a sequence. The free surface and the dynamic trim are first computed by XPAN, thereafter the boundary layer on the fore body by XBOUND and finally the flow around the stern and in the wake by XCHAP. Whereas in global approach, simulation perform numerical analysis for entire fluid domain using RANSE solver XCHAP. The advantage of using Global analysis is it is more accurate compared to Zonal approach. So for this work computation has been carried out only using Global approach.

The self-propulsion test was performed at the design speed of 20 knots.

9.5.1. Pre-Processing

Pre-Processing was carried out using CAESES software to define boundary conditions, discretization. Default settings were used to set turbulence model.

9.5.1.1. Boundary Conditions

The boundary conditions used in XCHAP are inlet, outlet, slip, no-slip and interior. At the inlet velocity and turbulence quantities are defined while the pressure gradient normal to the inlet plane is set to zero.

Whereas at the outlet plane the normal velocity and turbulence gradient is considered to and the pressure quantity is set to zero.

The slip condition is normally used for simulating symmetry conditions at flat boundaries. In this case the normal velocity component and all the normal gradient of all the other quantities are zero. The slip boundary condition is applied for solid walls thus the velocity, the turbulent kinetic energy and the normal pressure gradient are set to zero.

9.5.1.2. Turbulence Model

The turbulence model used in this simulation is default one which is Explicit Algebraic stress model. This model is a good compromise between performance and the ability to predict the important vortex flow in the stern wake and is therefore the standard model in the program. No wall functions are used and the equations are integrated down to the wall.

9.5.1.3. Discretization

Structured grids are used for defining the fluid domain and boundary of hull in XCHAP. Since in our case to perform self-propulsion of hull with propeller which a very complex geometry we use overlapping grids are used for more complex geometries. XCHAP has an automatic algorithm for the cell classification. All cells in the overlapping grid needs to be classified as fluid, outside or interpolation.

The hull grid along with fluid domain was discretized which consisted of 2.43 million cells covering both sides of the model. Including the additional overlapping grid components, the propeller grid and a local refinement grid in the stern the total number of cells were 2.62 million.

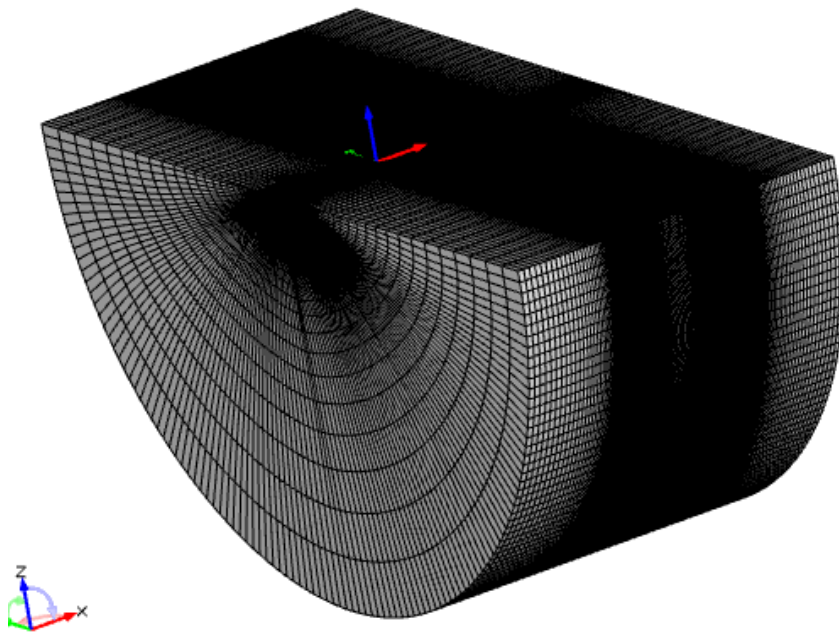


Fig 35: The entire grid setup for fluid domain for XCHAP

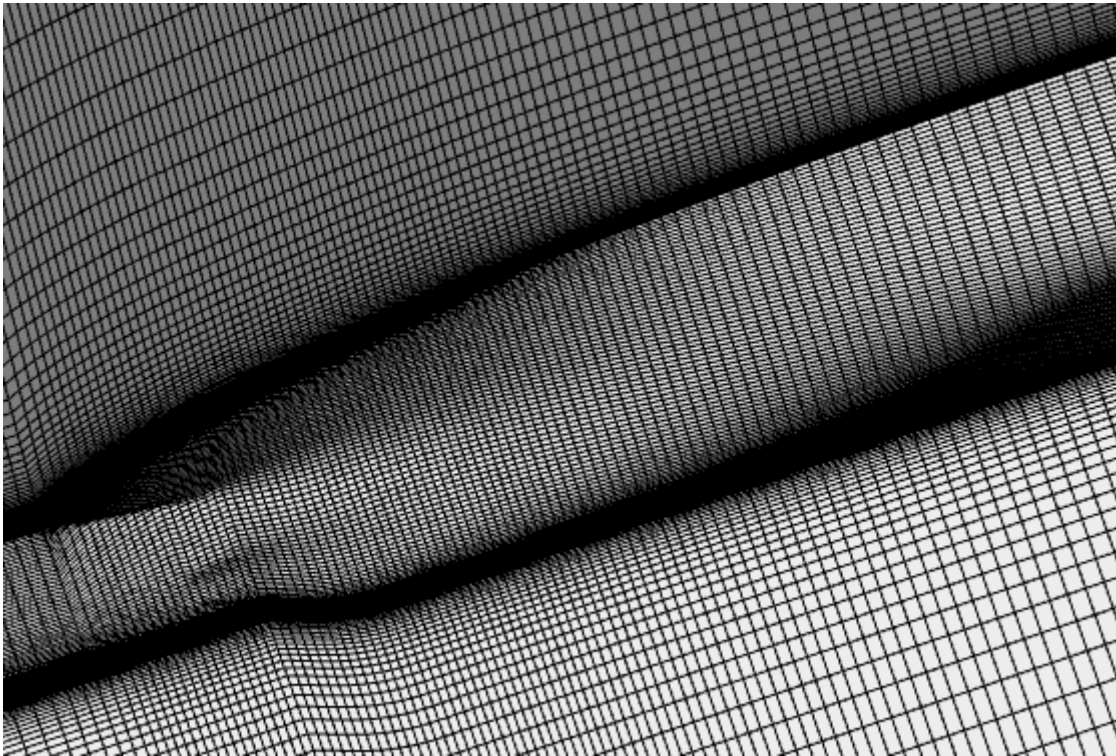


Fig 36: Refinement at stern region

During discretization for RANSE computation cell refinement has been done at the stern region as shown in above figure to capture minute details of flow characteristics.

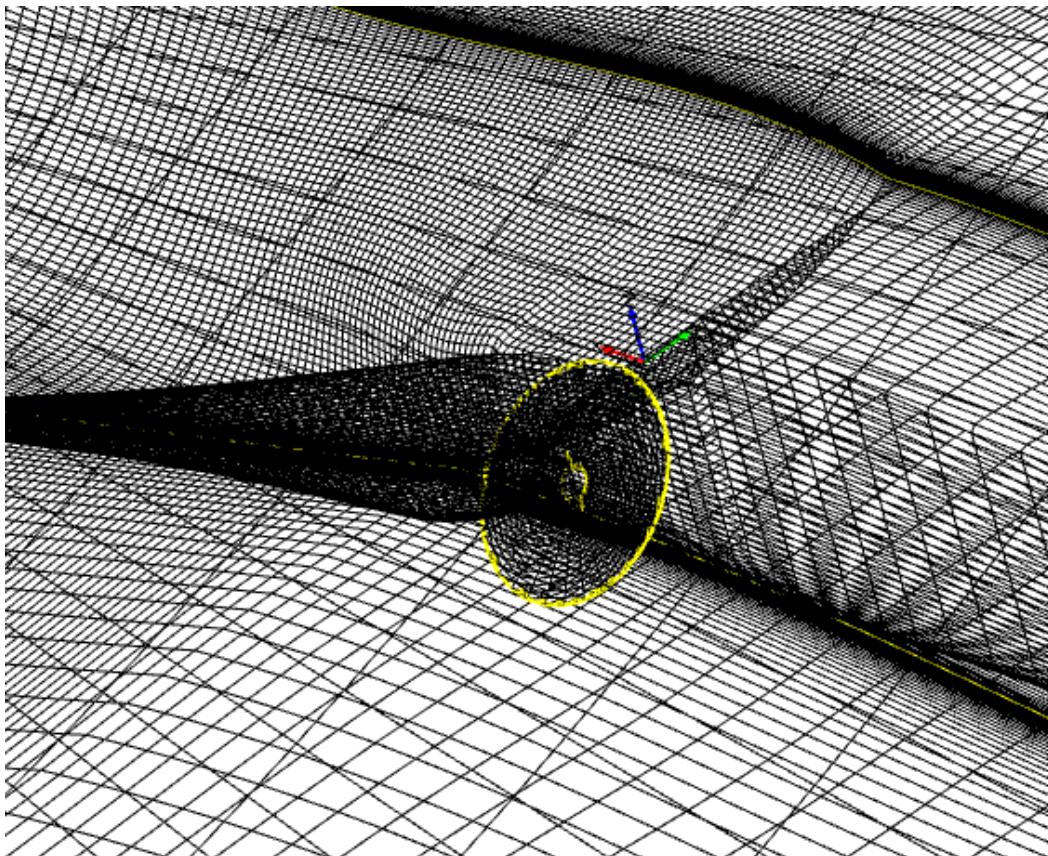


Fig 37: Overlapping grid structure

9.5.2. Computation

The solution was converged after 6500 iteration with each iteration lasting 15 minutes using computer configuration of 3 Ghz,4 GB ram and processor i5.

9.5.3. Post-Processing

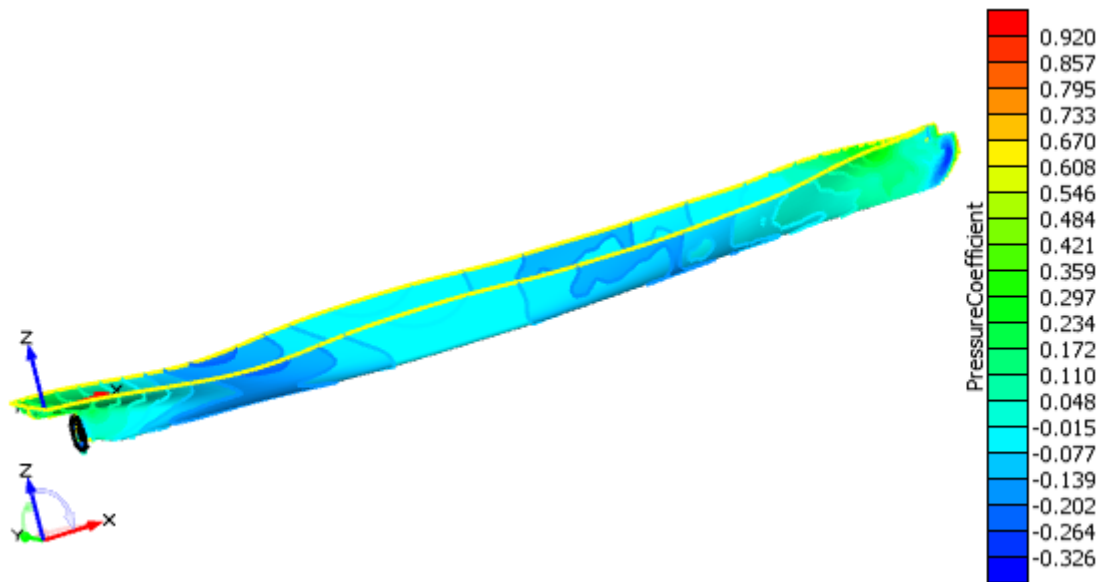


Fig 38: The pressure coefficient distribution around hull using Global approach

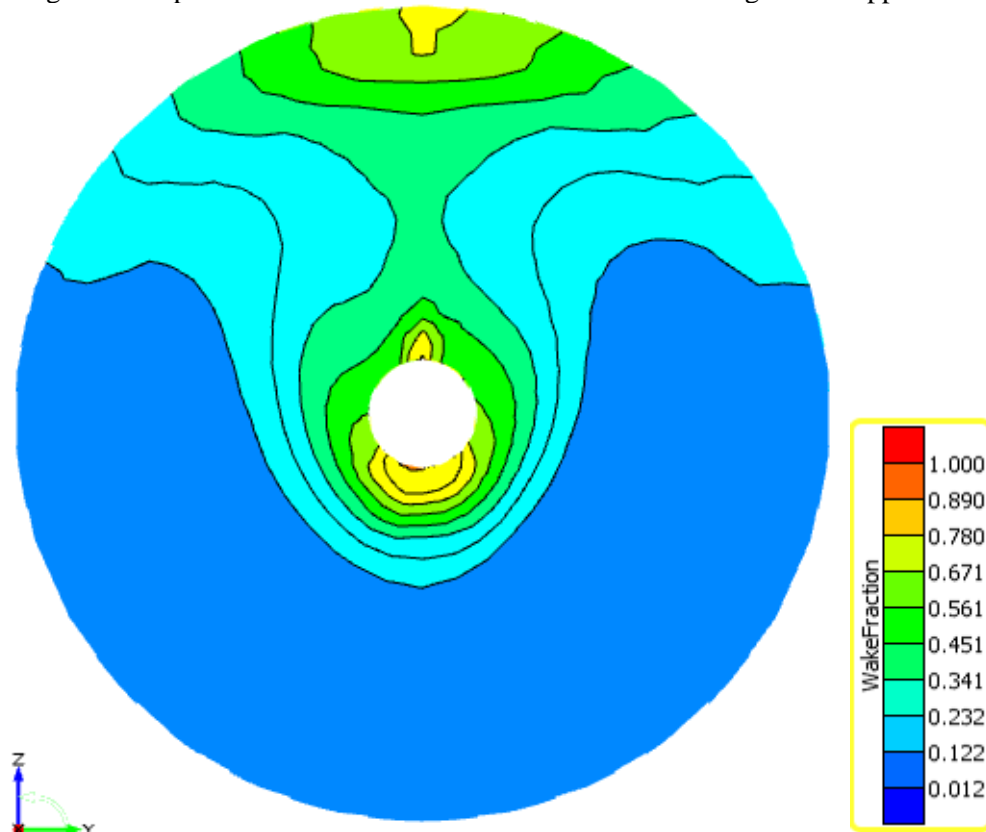


Fig 39: The effective wake distribution along the propeller plane

The figure 44 shows the effective wake distribution along the propeller plane. It is clear that the wake fraction is higher on top region of propeller plane meaning the velocity of advance is higher resulting in reduction of pressure. Pressure drop in top region of propeller indicates that this region is more prone to cavitation.

Table 25: Comparison of various propeller characteristics and propeller-hull interaction factors obtained from numerical analysis and experimental

Parameters	Numerical	Experimental	Difference in %
Effective Mean Wake, w	0.277	0.273	1.44
Thrust Deduction Factor, t	0.18	0.1766	1.88
Advance Coefficient, J	0.60	0.58	-
Resistance(KN)	649	722	10.11
Thrust Coefficient, K_T	0.178	0.177	0.5
Torque Coefficient, K_Q	0.0242	0.026	7.4
Propeller Speed (RPM)	141	144.16	2.24
Thrust generated (KN)	795	876.5	9.3
Torque generated (KNm)	561	702	20
Delivered Power (KW)	8234	10243.7	19.6
Hull efficiency, η_H	1.183	1.1326	4.2
Relative rotative efficiency, η_R	1.018	1.0225	4.2
Propeller Efficiency, η_D	0.71	0.73	2.8

The speed of the propeller was automatically adjusted during the self-propulsion simulation such that the propeller thrust balanced the resistance of the hull from the resistance simulation. The propeller rpm obtained was around 2.2% lower in the computations compared to experimental while the delivered power obtained using CFD was 20 % lower value compared experimental. This is due to reason that the resistance calculated using CFD is about 10% lower compared to experimental so the torque required to generate sufficient thrust to propel ship in numerical analysis is lower.

On comparing the hull-propeller interaction factors like wake fraction, thrust deduction factor and efficiencies computed using both methods are in good agreement as seen in the table 25.

Regarding propeller characteristics a very good agreement has been attained for thrust coefficient for both numerical and experimental while for torque coefficient differed by 7.4 %.

While thrust and torque coefficients determined during detail design stage and numerical analysis were different by 6.32% and 10.37% respectively.

10. PROPELLER STRENGTH CALCULATION

Propeller strength calculation has been carried out as per classification society rule requirement [17]. As per the rule requirement the maximum thickness of blade at radii 0.25 and 0.6 has to be greater or at least same as thickness equation given below. (Calculation has been included in appendix)

Strength Calculation as per Germinister Lloyd rule for 0.25 R:

$$t > k \cdot K_0 \cdot K_1 \cdot C_G \cdot C_{dyn}$$

$$k \cdot K_0 \cdot K_1 \cdot C_G \cdot C_{dyn} = 80 * 1.009 * 1.12 * 1.77 * 1 = 160.01 \text{ mm}$$

As per the result from lifting line theory thickness at 0.25R is

$$t_{0.25R} = 235 \text{ mm}$$

So strength criteria is satisfied for blade section at 0.25 R

Strength Calculation as per Germinister Lloyd rule for 0.6 R:

$$t > k \cdot K_0 \cdot K_1 \cdot C_G \cdot C_{dyn}$$

$$k \cdot K_0 \cdot K_1 \cdot C_G \cdot C_{dyn} = 44 * 1.009 * 1.9 * 1.77 * 1 = 94.3 \text{ mm}$$

As per the result from lifting line theory thickness at 0.6R is

$$t_{0.6R} = 123.5 \text{ mm}$$

So strength criteria is satisfied for blade section at 0.6 R.

11. SHAFTLINE SYSTEM

11.1. Introduction

At this stage once the propeller design and the main engine are finalized, the next step is to design shaft line connecting propeller to main engine.

A shaft usually of circular cross section is used to transmit power or rotatory motion from main engine to propeller. The length of shaft line depends upon location of main engine. Shaft line system of container ship usually consists of propeller shaft, intermediate shaft couplings and bearings.

Calculations of dimension of shaft line has been carried out as per classification rule requirement [17].Detail calculations is included in appendix.

11.2. Purpose of Shaft line

General purpose of propulsion shafting includes:

- a) Transmission of torque from engine to the propeller
- b) In return transmit thrust generated by the propeller to hull
- c) Support the load of propeller and overcome fluctuating operational loads
- d) Ensure reliable operation throughout the operating RPM range of propeller.

11.3. Material Selection

Main criteria for selection of shaft material is based the strength which will ensure system reliability in all operating conditions. Forged steel is most commonly used material for conventional vessels like our container ship due to low initial cost, less maintenance during service, high availability and good performance.

11.4.Components of Shaft line system

The main dimension of components of shaft line like propeller shaft ,intermediate shaft and the coupling bolts are calculated using classification societies rules.(Design calculation is included in appendix).

Other main components of shaft system are shaft bearings which are used to support shaft and components weight. As a general case with propeller and intermediate shaft there will be three bearings, the forward and aftermost stern tube bearings and the main thrust bearing.

The function of forward bearing is to withstand propeller weight and the main thrust bearing will transmit the thrust generated by the propeller to the ship hull through a foundation.

11.5.Installation

Installation of shafts and bearings are decided considering engine room location, under deck support structures and bearing unit loads. Shaft coupling will be performed via forged flange coupling with headed bolts. The aft end of the propeller shaft will be prepared for fitting the keyless propeller and hydraulic nut and a shaft grounding device.

12. CONCLUSION

The work presents aspects regarding systematic design of a propulsion system including main engine, transmission and most importantly an efficient propeller, for a 1200 TEU container ship.

One of the main objectives was to design an optimised propeller and to verify that it is the best available solution. All important stages of propeller design including preliminary design using statistical method (Wageningen B propellers), detail design (Wake adapted propeller) and finally numerical analysis of final propeller were performed. In house codes based on B Wageningen series and lifting line theory for wake adapted propellers have been developed to simplify the process.

Cavitation check for propeller in preliminary stage resulted in a 2.85% back cavitation which is acceptable for ocean going container ship.

The geometry for final propeller has been developed using NACA 66(mod-0.8) since it is the most common blade profile used in marine industry. And Strength has been verified at 0.25R and 0.6R blade sections using classification rules.

Further numerical analysis using SHIPFLOW software have been performed on final propeller to analyse the hydrodynamic performances of it, both in open water as well as behind hull condition(unsteady flow).

Numerical simulation in this work include resistance computation (required to study propeller-hull interaction), open water test of propeller and self-propulsion to understand its performance in steady flow and unsteady flow respectively. And comparison of numerical analysis and experimental test results performed at basin in ICEPRONAV is also performed to understand the effectiveness of CFD software in propeller analysis.

Conclusion from comparison between numerical and experimental results:

- a) Numerical method have predicted efficiently the hull-propeller interaction factors like wake fraction, thrust deduction factor etc. and achieved a good agreement with result from experimental self-propulsion test.
- b) The open water simulation is also in good agreement with experiments.
- c) Regarding propeller characteristics a very good reasonable accuracy has been attained for thrust coefficient between numerical and experimental analysis while for torque a larger deviation was observed.
- d) The propeller rpm and delivered power obtained using CFD were lower compared experimental. This can be explained as the resistance calculated using CFD is lower

compared to experimental (usually the discrepancy existing between experimental and numerical analysis of resistance is 10-15%) so the torque required to generate sufficient thrust to propel ship during self-propulsion analysis was also lower.

So from the above observations CFD analysis can be used to study the hydrodynamic performance of the propeller, understand local flow details including both steady as well as unsteady conditions and to select a most promising candidate design for model testing.

The wake adapted NACA propeller has been concluded as best available solution for containership with respect to its hydrodynamic performance. As final step in design of propulsion system corresponding to this propeller a transmission system has been designed as per classification society requirement.

Recommendations:

- 1) FEM analysis for detail verification of strength
- 2) Detail cavitation analysis of propeller blade sections using experimental or numerical tests.

ACKNOWLEDGEMENT

I am deeply indebted to **Asst.Prof.Mihaela Amoraritei** , my Advisor and teacher for her valuable guidance and assistance for the successful completion of my final semester thesis. I am also thankful to **Mr.Ion Mustață**,Manager,**Mr.Dragoș Totolici**,senior technical engineer and other members of Initial Design department at Icepronav Engineering S.R.L for their continous support during the intership period.

I am grateful to all my class mates especially to **Miss. Tin Yadanar Tun** and **Mr. Binoy Pilakkat**, with out whose help and assistance; my thesis would not have been completed.

Above all, I do strongly believe that **God Almighty**'s blessings are the prime motivation for the successful completion of my thesis.

This thesis was developed in the frame of the European Master Course in “Integrated Advanced Ship Design” named “EMSHIP” for “European Education in Advanced Ship Design”, Ref.: 159652-1-2009-1-BE-ERA MUNDUS-EMMC.

NOUFAL.P.NAJEEB

REFERENCES

- [1] Volker Bertram., 2000. *Practical Ship Hydrodynamics*. 1st ed. Great Britain: Butterworth & Heinemann.
- [2] Holtrop, J., Mennen, G.G.J., 1982. An approximate power prediction method. *International Shipbuilding Progress*, 29 (335), 166-170.
- [3] ITTC - Recommended Procedures, 1999. Performance, Propulsion 1978 ITTC Performance Prediction Method. 7.5 – 02 03 – 01.4.
- [4] Broberg, L. and Orych, M., 2012. An efficient numerical technique to simulate the propeller hull Interaction. *International Journal of Innovative Research & Development*, 1(10), 494 – 508.
- [5] Tocu, A.M. and Amoraritei, M., 2008. Numerical study of the flow field around a ship hull including propeller effects. *Journal of Marine Research*, 5(3), 68 – 78.
- [6] Flowtech International AB, Shipflow 6.0 Xchap theoretical manual. Gothenburg, Sweden, 2007
- [7] Carlton, J., 2007. *Marine propeller and propulsion*. 2nd ed. Great Britain: Butterworth & Heinemann.
- [8] Knutsson, D., Orych, M. and Larsson, L., 2011. Large area propellers. *Second International Symposium on Marine Propulsors, Hamburg, Germany*.
- [9] V Lewis, E.V., 1988. *Principles of Naval Architecture, Vol 2. Resistance, Propulsion and Vibration*. 2nd ed. New Jersey: Society of Naval Architects and Marine Engineers.
- [10] Flowtech International AB, Shipflow 6.0 user manual. Gothenburg, Sweden, 2015.
- [11] Flowtech International AB, Shipflow 6.0 Tutorial – Basics. Gothenburg, Sweden, 2015.
- [12] Oosterveld, and Oossanen, M.W.C., 1975. Further Computer-Analyzed Data of Wageningen B Screw Series. *International Shipbuilding Progress*, 22, 251-261.
- [13] Noufal,P.N. and Amoraritei,M., 2016. Design of a wake-adapted propeller for a Containership. *The annals of “dunarea de jos” university of galati, fascicle xi – shipbuilding*
- [14] Coney, W.B., 1989. *A Method for the Design of a Class of Optimum Marine Propulsors*. Thesis(PhD), MIT.
- [15] Chung, H.L., 2007. *An enhanced propeller design program based on propeller vortex lattice lifting line theory*. Thesis(Masters), MIT.
- [16] Abbott, I.H. and Von Doenhoff, A.E., 1959. *Theory of Wing Sections Dover*. 1st ed. New York: Dover Publication Inc.
- [17] Germinister Lloyd, 2015, *Rules for classification and construction (Machinery)*.

APPENDIX

A1) Output of resistance calculation carried out using Maxsurf Resistance Module

	Item	Value	Units	Holtrop
1	LWL	150.501	m	150.501
2	Beam	23.249	m	23.249
3	Draft	7.306	m	7.306
4	Displaced volume	16057.452	m ³	16057.45
5	Wetted area	4175.184	m ²	4175.184
6	Prismatic coeff. (Cp)	0.635		0.635
7	Waterpl. area coeff. (Cwp)	0.776		0.776
8	1/2 angle of entrance	18.5	deg.	18.5
9	LCG from midships(+ve for'	71.573	m	71.573
10	Transom area	0	m ²	0
11	Transom wl beam	0	m	--
12	Transom draft	0	m	--
13	Max sectional area	167.904	m ²	--
14	Bulb transverse area	0.286	m ²	0.286
15	Bulb height from keel	7.252	m	7.252
16	Draft at FP	7.3	m	7.3
17	Deadrise at 50% LWL	0	deg.	--

	Speed (kn)	Froude No. LWL	Froude No. Vol.	Holtrop Resist. (kN)
1	16.000	0.214	0.523	369.0
2	16.150	0.216	0.528	378.7
3	16.300	0.218	0.533	388.6
4	16.450	0.220	0.538	398.8
5	16.600	0.222	0.543	409.2
6	16.750	0.224	0.548	419.8
7	16.900	0.226	0.553	430.7
8	17.050	0.228	0.558	441.8
9	17.200	0.230	0.563	453.1
10	17.350	0.232	0.567	464.7
11	17.500	0.234	0.572	476.6
12	17.650	0.236	0.577	488.7
13	17.800	0.238	0.582	501.2
14	17.950	0.240	0.587	514.0
15	18.100	0.242	0.592	527.2
16	18.250	0.244	0.597	540.9
17	18.400	0.246	0.602	555.0
18	18.550	0.248	0.607	569.6
19	18.700	0.250	0.612	584.8
20	18.850	0.252	0.617	600.5
21	19.000	0.254	0.621	616.9
22	19.150	0.256	0.626	633.9
23	19.300	0.258	0.631	651.5
24	19.450	0.260	0.636	669.8
25	19.600	0.262	0.641	688.8
26	19.750	0.264	0.646	708.4
27	19.900	0.266	0.651	728.6
28	20.050	0.268	0.656	749.4
29	20.200	0.270	0.661	770.7

A2) Complete C++ code (with header files) for finding the optimum RPM for given Blade area ratio and no. of blades developed using an open source software & compiler - QT

```

#include "mainwindow.h"
#include "ui_mainwindow.h"
#include <iostream>
#include <vector>
#include <string>
#include <fstream>
#include <cmath>
#include <Eigen/QR>
#include <stdio.h>
#include <unsupported/Eigen/Polynomials>
#include <QMessageBox>
#include <QFile>
#include <QTextStream>
#include <QVector>
MainWindow::MainWindow(QWidget *parent) :
    QMainWindow(parent),
    ui(new Ui::MainWindow)
{
    ui->setupUi(this);
}
MainWindow::~MainWindow()
{
    delete ui;
}
using namespace std;
void polyfit(const std::vector<double> &xv, const std::vector<double> &yv,
std::vector<double> &coeff, int order)
{
    Eigen::MatrixXd A(xv.size(), order+1);
    Eigen::VectorXd yv_mapped = Eigen::VectorXd::Map(&yv.front(),
yv.size());
    Eigen::VectorXd result;
    assert(xv.size() == yv.size());
    assert(xv.size() >= order+1);
    // create matrix
    for (size_t i = 0; i < xv.size(); i++)
        for (size_t j = 0; j < order+1; j++)
            A(i, j) = pow(xv.at(i), j);
    // solve for linear least squares fit
    result = A.householderQr().solve(yv_mapped);
    coeff.resize(order+1);
    for (size_t i = 0; i < order+1; i++)
        coeff[i] = result[i];
}
void MainWindow::on_pushButton_clicked()
{
    double
E, prop, Rt, BAR, EM, SM, Z, w, t, Vs, D, Density, Viscosity, MCR, Etash, Etagb, T, n, Vr, CL,
Ktj, Rn, Va, inter, PE, PT, n1, Vr1, CL1, Rn1;
    float Patm, Pv, g, AD;
    BAR=ui->lineEdit->text().toDouble();
    Z=ui->lineEdit_2->text().toDouble();
    Rt=ui->lineEdit_3->text().toDouble();
    w=ui->lineEdit_4->text().toDouble();
    t=ui->lineEdit_5->text().toDouble();
    D=ui->lineEdit_6->text().toDouble();

```

```

Vs=ui->lineEdit_7->text().toDouble();
Density=ui->lineEdit_8->text().toDouble();
Viscosity=ui->lineEdit_9->text().toDouble();
EM=ui->lineEdit_10->text().toDouble();
SM=ui->lineEdit_11->text().toDouble();
Etash=ui->lineEdit_12->text().toDouble();
Etagb=ui->lineEdit_13->text().toDouble();
prop=ui->lineEdit_14->text().toDouble();// Height of the shaftline from
the baseline
const double pi=22/7;
MCR=(100-SM)*(100-EM)/10000;
//Propeller MainWindow begins
T=Rt/(prop*(1-t));
PE=Rt*Vs*0.51444444;
PT=PE*(1-t)/(1-w);
Va=(1-w)*Vs*0.51444444;
Ktj=T/(Density*pow(D,2)*pow(Va,2));
//Finding Polynomial coefficients of Ktj2 curve
std::vector<double> J(15),Ktj2(15),Ktinter(15),coeff1,coeff2;
QVector<double>Ktj2plot(15);
J={0.1,0.2,0.3,0.4,0.5,0.6,0.7,0.8,0.9,1.0,1.1,1.2,1.3,1.4,1.5};
for (int i=0;i<15;i++){
    Ktj2[i]=Ktj*pow(J[i],2);
    Ktj2plot[i]=Ktj2[i];
}
polyfit(J,Ktj2,coeff1,3);
//Entering C,J,PR,BAR,Z data to calculate Kt by Oosterveld equation for
WageningenB propellers
double Ct[]={0.00880496,-0.204554,0.166351,0.158114,-0.147581,-
0.481497,0.415437,0.0144043,-0.0530054,0.0143481,0.0606826,-
0.0125894,0.0109689,-0.133698,0.00638407,-0.00132718,0.168496,-
0.0507214,0.0854559,-0.0504475,0.010465,-0.00648272,-0.00841728,0.0168424,-
0.00102296,-0.0317791,0.018604,-0.00410798,-0.000606848,-
0.0049819,0.0025983,-0.000560528,-0.00163652,-
0.000328787,0.000116502,0.000690904,0.00421749,0.0000565229,-0.00146564};
int JCt[]=
{0,1,0,0,2,1,0,0,2,0,1,0,1,0,0,2,3,0,2,3,1,2,0,1,3,0,1,0,0,1,2,3,1,1,2,0,0,
3,0};
int PRcT[]=
{0,0,1,2,0,1,2,0,0,1,1,0,0,3,6,6,0,0,0,0,6,6,3,3,3,3,0,2,0,0,0,0,2,6,6,0,3,
6,3};
int BARcT[]=
{0,0,0,0,1,1,1,0,0,0,0,1,1,0,0,0,1,2,2,2,2,2,0,0,0,1,2,2,0,0,0,0,0,0,0,1,1,
1,2};
int ZcT[]=
{0,0,0,0,0,0,0,1,1,1,1,1,1,0,0,0,0,0,0,0,0,0,0,0,1,1,1,1,1,1,2,2,2,2,2,2,2,2,
2,2};
//Entering C,J,PR,BAR,Z data to calculate Kq by Oosterveld equation for
WageningenB propellers
double Cq[]={0.00379368,0.00886523,-0.032241,0.00344778,-0.0408811,-
0.108009,-0.0885381,0.188561,-0.00370871,0.00513696,0.0209449,0.00474319,-
0.00723408,0.00438388,-
0.0269403,0.0558082,0.0161886,0.00318086,0.015896,0.0471729,0.0196283,-
0.0502782,-0.030055,0.0417122,-0.0397722,-0.00350024,-
0.0106854,0.00110903,-0.000313912,0.0035985,-0.00142121,-
0.00383637,0.0126803,-0.00318278,0.00334268,-0.00183491,0.000112451,-
0.0000297228,0.000269551,0.00083265,0.00155334,0.000302683,-0.0001843,-
0.000425399,0.0000869243,-0.0004659,0.0000554194};
int JCq[]=
{0,2,1,0,0,1,2,0,1,0,1,2,2,1,0,3,0,1,0,1,3,0,3,2,0,0,3,3,0,3,0,1,0,2,0,1,3,
3,1,2,0,0,0,0,3,0,1};

```

```

int PRCq[]=
{0,0,1,2,1,1,1,2,0,1,1,1,0,1,2,0,3,3,0,0,0,1,1,2,3,6,0,3,6,0,6,0,2,3,6,1,2,
6,0,0,2,6,0,3,3,6,6};
int BARCq[]=
{0,0,0,0,1,1,1,1,0,0,0,0,1,1,1,1,1,1,2,2,2,2,2,2,2,2,0,0,0,1,1,2,2,2,2,0,0,
0,1,1,1,1,2,2,2,2,2};
int ZCq[]=
{0,0,0,0,0,0,0,0,1,1,1,1,1,1,0,0,0,0,0,0,0,0,0,0,0,0,0,0,1,1,1,1,1,1,1,1,1,2,2,
2,2,2,2,2,2,2,2,2,2};
//Defining J,PR,BAR and Z range values
float PR[]={0.5,0.6,0.7,0.8,0.9,1.0,1.1,1.2,1.3,1.4};
double
KT,Ktcorrect,KQ,Kqcorrect,KQ1[10],Kqnew[10],KT2,Ktcorr,Ktnew[10],Eff[10];
QVector<double>
x(15),x1(15),x2(15),x3(15),x4(15),x5(15),x6(15),x7(15),x8(15),x9(15);
QVector<double>L(15);
L={0.1,0.2,0.3,0.4,0.5,0.6,0.7,0.8,0.9,1.0,1.1,1.2,1.3,1.4,1.5};
double Ktplot[15][10]={0},KT1[15], solution[4],
eff,PRcorr,Ktfinal,Kqfinal,Jcorr,rot,QPC,PB,Thrust,PD,EtaH,EtaB,EtaR,rpm;
//Getting Efficiency
for (int k = 0;k<10;k++)// for Pitch ratio
{
Eff[k]=0;
for (int j = 0;j<15;j++) // for J
{
Ktinter[j]=0;
KT= 0,KT1[j]=0,Ktcorrect=0,n=0,Vr=0,CL=0,Rn=0;
for (int i = 0;i<39;+i){
KT =
Ct[i]*(pow(J[j],JCt[i]))*(pow(PR[k],PRCt[i]))*(pow(BAR,BARCt[i]))*(pow(Z,ZC
t[i]));

KT1[j] = KT1[j]+KT;
}
n = Va/(J[j]*D);
Vr = sqrt(pow((((0.7*(22/7))*n)*D),2)+pow(Va,2));
CL = ((2.073*BAR)*D)/Z;
Rn = (Vr/Viscosity)*CL;
Ktcorrect = 0.000353485-(0.00333758*BAR*pow(J[j],2))-
(0.00478125*BAR*PR[k]*J[j])+ (0.000257792*pow((log10(Rn)-
0.301),2)*BAR*pow(J[j],2))+ (0.0000643192*(log10(Rn)-
0.301)*pow(PR[k],6)*pow(J[j],2))- (0.000110636*pow((log10(Rn)-
0.301),2)*pow(PR[k],6)*pow(J[j],2))- (0.0000276305*pow((log10(Rn)-
0.301),2)*Z*BAR*pow(J[j],2))+ (0.0000954*(log10(Rn)-
0.301)*Z*BAR*PR[k]*J[j])+ (0.0000032049*(log10(Rn)-
0.301)*pow(Z,2)*BAR*pow(PR[k],3)*J[j]);
Ktinter[j]=KT1[j]+Ktcorrect;
Ktplot[j][k]=KT1[j]+Ktcorrect;
//printf("Ktinter%f\t",Ktinter[j]);
}
polyfit(J,Ktinter,coeff2,3);
for(int i=0;i<4;i++){
solution[i]=coeff2[i]-coeff1[i];
}
//finding the roots
Eigen::PolynomialSolver<double, Eigen::Dynamic> solver;
Eigen::VectorXd coeff(4);

coeff[0] = solution[0];
coeff[1] = solution[1];
coeff[2] = solution[2];
coeff[3] = solution[3];

```

```

        solver.compute(coeff);
        const Eigen::PolynomialSolver<double,
Eigen::Dynamic>::RootsType & r = solver.roots();
        for(int i =0;i<r.rows();++i)
        {
            if(real(r[i])>0){
                if (real(r[i])<1.5)
                {
                    inter=real(r[i]);
                }
            }
        }
        //Finding Kt at intersection point of Ktj curve and Ktj2
curve
        KT= 0,KT2=0,Ktcorr=0;
        for (int i = 0;i<39;i++){
            KT =
Ct[i]*(pow(inter,Jct[i]))*(pow(PR[k],PRCt[i]))*(pow(BAR,BARCt[i]))*(pow(Z,Z
Ct[i]));

            KT2= KT2+KT;
        }
        n1 = Va/(inter*D);
        Vr1 = sqrt(pow((((0.7*(22/7))*n1)*D),2)+pow(Va,2));
        CL1 = ((2.073*BAR)*D)/Z;
        Rn1 = (Vr1/Viscosity)*CL1;
        Ktcorr = 0.000353485-(0.00333758*BAR*pow(inter,2))-
(0.00478125*BAR*PR[k]*inter)+(0.000257792*pow((log10(Rn1)-
0.301),2)*BAR*pow(inter,2))+(0.0000643192*(log10(Rn1)-
0.301)*pow(PR[k],6)*pow(inter,2))-(0.0000110636*pow((log10(Rn1)-
0.301),2)*pow(PR[k],6)*pow(inter,2))-(0.0000276305*pow((log10(Rn1)-
0.301),2)*Z*BAR*pow(inter,2))+(0.0000954*(log10(Rn1)-
0.301)*Z*BAR*PR[k]*inter)+(0.0000032049*(log10(Rn1)-
0.301)*pow(Z,2)*BAR*pow(PR[k],3)*inter);
            Ktnew[k]=KT2+Ktcorr;
        }
        //Finding Kq at intersection point of Ktj curve and Ktj2
curve
        KQ=0, KQ1[k]=0,Kqcorrect=0;
        for (int i = 0;i<47;i++){
            KQ =
Cq[i]*(pow(inter,JCq[i]))*(pow(PR[k],PRCq[i]))*(pow(BAR,BARCq[i]))*(pow(Z,Z
Cq[i]));

            KQ1[k] = KQ1[k]+KQ;
        }
        Kqcorrect = -0.000591412+0.00696898*PR[k]-
(0.0000666654*Z*(pow(PR[k],6)))+0.0160818*(pow(BAR,2))-
(0.000938091*(log10(Rn1)-0.301))*PR[k]-(0.00059593*(log10(Rn1)-
0.301))*pow(PR[k],2)+(0.0000782099*(pow((log10(Rn1)-
0.301),2))*pow(PR[k],2)+(0.0000052199*(log10(Rn1)-
0.301))*Z*BAR*(pow(inter,2))-((0.00000088528*(pow((log10(Rn1)-
0.301),2))*Z*BAR*PR[k])*inter+((0.0000230171*(log10(Rn1)-
0.301))*Z*(pow(PR[k],6)))-((0.00000184341*(pow((log10(Rn1)-
0.301),2))*Z*(pow(PR[k],6)))-0.00400252*(log10(Rn1)-
0.301))*pow(BAR,2)+(0.000220915*(pow((log10(Rn1)-
0.301),2))*pow(BAR,2));
            Kqnew[k] = KQ1[k]+Kqcorrect;
            Eff[k] = (inter*Ktnew[k]/(Kqnew[k]*(44/7)));
        }
        //comparision of efficiencies to find the maximum
        if(Eff[k]>eff){
            eff=Eff[k];
            PRcorr=PR[k];
            Ktfinal=Ktnew[k];
            Kqfinal=Kqnew[k];
            Jcorr=inter;
        }
    }
}

```

```

        rot=Va/(inter*D); //Required RPS
        rpm=rot*60;
        Thrust=Ktfinal*Density*pow(rot,2)*pow(D,4);
        PD=2*pi*Kqfinal*Density*pow(rot,3)*pow(D,5);
        EtaH=(1-t)/(1-w);
        EtaR=1.02;
        EtaB=EtaR*eff;
        QPC=EtaH*EtaB;
        PB=Rt*Vs*0.51444444*10000/(QPC*MCR*Etash*Etagb);
//Required Brake power
    }}
    //writing the data to txt file
    ofstream myfile;
    myfile.open("EMPROP PROPELLER MainWindow(Dia).txt");
    myfile<<"
*****          Result of Propeller MainWindow          \n
*****          ";
    myfile<<"\n*****Input Details*****"<<"\nBlade Area Ratio:
"<<BAR<<"\n Number of Blades"<<Z<<"\nNumber of Propellers:
"<<prop<<"\nResistance of Ship: "<<Rt<<"\nDiameter of Propeller:
"<<D<<"\nWake Fraction: "<<w<<"\nThrust Deduction Factor: "<<t<<"\nDensity
of Fluid: "<<Density<<"\nViscosity of Fluid: "<<Viscosity<<"\nService Speed
of Vessel: "<<Vs<<"\nMaximum Continous Rating: "<<MCR<<"\n Shaft
Efficiency: "<<Etash<<"\n GearBox Efficiency: "<<Etagb<<"\n
*****Output Details*****";
        ui->lineEdit_42->setText(QString::number(eff));
        ui->lineEdit_34->setText(QString::number(PRCorr));
        ui->lineEdit_35->setText(QString::number(Ktfinal));
        ui->lineEdit_32->setText(QString::number(Kqfinal));
        ui->lineEdit_41->setText(QString::number(Jcorr));
        ui->lineEdit_33->setText(QString::number(rot));
        ui->lineEdit_40->setText(QString::number(rpm));
        ui->lineEdit_37->setText(QString::number(Thrust));
        ui->lineEdit_36->setText(QString::number(PD));
        ui->lineEdit_38->setText(QString::number(EtaH));
        ui->lineEdit_30->setText(QString::number(EtaB));
        ui->lineEdit_29->setText(QString::number(EtaR));
        ui->lineEdit_39->setText(QString::number(QPC));
        ui->lineEdit_31->setText(QString::number(PB));
// For Plotting
for (int j=0;j<15;j++){
    x[j]=Ktplot[j][0];
    x1[j]=Ktplot[j][1];
    x2[j]=Ktplot[j][2];
    x3[j]=Ktplot[j][3];
    x4[j]=Ktplot[j][4];
    x5[j]=Ktplot[j][5];
    x6[j]=Ktplot[j][6];
    x7[j]=Ktplot[j][7];
    x8[j]=Ktplot[j][8];
    x9[j]=Ktplot[j][9];
}
    MainWindow::makePlot(Ktj2plot,L,x,x1,x2,x3,x4,x5,x6,x7,x8,x9);
//passing the data to makePlot to draw graph
}
void MainWindow::makePlot(QVector<double> &Ktj2plot,QVector<double>
&L,QVector<double> &x,QVector<double> &x1,QVector<double>
&x2,QVector<double> &x3,QVector<double> &x4,QVector<double>
&x5,QVector<double> &x6,QVector<double> &x7,QVector<double>
&x8,QVector<double> &x9)
{

```

```

    ui->customPlot->legend->setVisible(false);
    ui->customPlot->axisRect()->insetLayout()->setInsetAlignment(0,
Qt::AlignRight|Qt::AlignTop);
    ui->customPlot->legend->setFont(QFont("Helvetica",8));
    ui->customPlot->addGraph();
    ui->customPlot->graph(0)->setPen(QPen(Qt::blue));
    ui->customPlot->graph(0)->setName("P/D - 0.5");
    ui->customPlot->graph(0)->setData(L, x);
    ui->customPlot->addGraph();
    ui->customPlot->graph(1)->setPen(QPen(Qt::red));
    ui->customPlot->graph(1)->setName("P/D - 0.6");
    ui->customPlot->graph(1)->setData(L, x1);
    ui->customPlot->addGraph();
    ui->customPlot->graph(2)->setPen(QPen(Qt::yellow));
    ui->customPlot->graph(2)->setName("P/D - 0.7");
    ui->customPlot->graph(2)->setData(L, x2);
    ui->customPlot->addGraph();
    ui->customPlot->graph(3)->setPen(QPen(Qt::green));
    ui->customPlot->graph(3)->setName("P/D - 0.8");
    ui->customPlot->graph(3)->setData(L, x3);
    ui->customPlot->addGraph();
    ui->customPlot->graph(4)->setPen(QPen(Qt::magenta));
    ui->customPlot->graph(4)->setName("P/D - 0.9");
    ui->customPlot->graph(4)->setData(L, x4);
    ui->customPlot->addGraph();
    ui->customPlot->graph(5)->setPen(QPen(Qt::cyan));
    ui->customPlot->graph(5)->setName("P/D - 1.0");
    ui->customPlot->graph(5)->setData(L, x5);
    ui->customPlot->addGraph();
    ui->customPlot->graph(6)->setPen(QPen(Qt::blue));
    ui->customPlot->graph(6)->setName("P/D - 1.1");
    ui->customPlot->graph(6)->setData(L, x6);
    ui->customPlot->addGraph();
    ui->customPlot->graph(7)->setPen(QPen(Qt::red));
    ui->customPlot->graph(7)->setName("P/D - 1.2");
    ui->customPlot->graph(7)->setData(L, x7);
    ui->customPlot->addGraph();
    ui->customPlot->graph(8)->setPen(QPen(Qt::yellow));
    ui->customPlot->graph(8)->setName("P/D - 1.3");
    ui->customPlot->graph(8)->setData(L, x8);
    ui->customPlot->addGraph();
    ui->customPlot->graph(9)->setPen(QPen(Qt::green));
    ui->customPlot->graph(9)->setName("P/D - 1.4");
    ui->customPlot->graph(9)->setData(L, x9);
    ui->customPlot->addGraph();
    ui->customPlot->graph(10)->setPen(QPen(Qt::black));
    ui->customPlot->graph(10)->setName("Ktj2");
    ui->customPlot->graph(10)->setData(L, Ktj2plot);
    // give the axes some labels:
    ui->customPlot->xAxis->setLabel("Advance Coeff J");
    ui->customPlot->yAxis->setLabel("Kt");
// set axes ranges, so we see all data:
ui->customPlot->xAxis->setRange(0, 1.5);
ui->customPlot->yAxis->setRange(0, 1);
ui->customPlot->replot();
ui->customPlot->legend->clearItems();
}

```

A3) Main content of C++ code for finding the optimum Diameter for given Brake Power and RPM of selected engine

```

for (int k = 0;k<10;k++)// for Pitch ratio
{
    Eff[k]=0,D1=0,Vr1=0,CL1=0,Rn1=0;
    for (int j = 0;j<15;j++) // for J
    {
        Kqinter[j]=0;
        KQ= 0,KQ2[j]=0,Kqcorr=0,D=0,Vr=0,CL=0,Rn=0;
        for (int i = 0;i<47;+i){
            KQ =
Cq[i]*(pow(J[j],JCq[i]))*(pow(PR[k],PRCq[i]))*(pow(BAR,BARCq[i]))*(pow(Z,ZC
q[i]));
            KQ2[j] = KQ2[j]+KQ;
        }
        D = Va/(J[j]*n);
        Vr = sqrt(pow(((0.7*(22/7))*n)*D),2)+pow(Va,2));
        CL = ((2.073*BAR)*D)/Z;
        Rn = (Vr/Viscosity)*CL;
        Kqcorr = -0.000591412+0.00696898*PR[k]-
(0.0000666654*Z*(pow(PR[k],6))+0.0160818*(pow(BAR,2))-
(0.000938091*(log10(Rn)-0.301))*PR[k]-(0.00059593*(log10(Rn)-
0.301))*(pow(PR[k],2))+0.0000782099*(pow((log10(Rn)-
0.301),2)))*(pow(PR[k],2))+0.0000052199*(log10(Rn)-
0.301))*Z*BAR*(pow(J[j],2))-((0.00000088528*(pow((log10(Rn)-
0.301),2))*Z*BAR*PR[k])*J[j]+((0.0000230171*(log10(Rn)-
0.301))*Z*(pow(PR[k],6)))-((0.00000184341*(pow((log10(Rn)-
0.301),2))*Z*(pow(PR[k],6)))-(0.00400252*(log10(Rn)-
0.301))*(pow(BAR,2))+0.000220915*(pow((log10(Rn)-0.301),2)))*(pow(BAR,2));
        Kqinter[j]=KQ2[j]+Kqcorr;
        Kqplot[j][k]=KQ2[j]+Kqcorr;
    }
    polyfit(J,Kqinter,coeff2,6);
    //printf("%f + %f*x + %f*x^2 + %f*x^3\n", coeff2[0],
coeff2[1], coeff2[2], coeff2[3]);
    for(int i=0;i<7;i++){
        solution[i]=coeff2[i]-coeff1[i];
    }
    //finding the roots
Eigen::PolynomialSolver<double, Eigen::Dynamic> solver;
Eigen::VectorXd coeff(7);

coeff[0] = solution[0];
coeff[1] = solution[1];
coeff[2] = solution[2];
coeff[3] = solution[3];
coeff[4] = solution[4];
coeff[5] = solution[5];
coeff[6] = solution[6];
solver.compute(coeff);

const Eigen::PolynomialSolver<double,
Eigen::Dynamic>::RootsType & r = solver.roots();
for(int i =0;i<r.rows();+i)
{
    if(real(r[i])>0){
        if (real(r[i])<1.5)
        {
            inter[k]=real(r[i]);
        }
    }
}

```

```

    }}}
    //Finding Kt at intersection point of Ktj curve and Ktj2
curve
    KT= 0,KT2=0,Ktcorr=0;
    for (int i = 0;i<39;i++){
    KT =
Ct[i]*(pow(inter[k],JCt[i]))*(pow(PR[k],PRCt[i]))*(pow(BAR,BARCt[i]))*(pow(
Z,ZCt[i]));
    KT2= KT2+KT;
    }
    D1 = Va/(inter[k]*n);
    Vr1 = sqrt(pow(((0.7*(22/7))*n)*D1),2)+pow(Va,2));
    CL1 = ((2.073*BAR)*D1)/Z;
    Rn1 = (Vr1/Viscosity)*CL1;
    Ktcorr = 0.000353485-(0.00333758*BAR*pow(inter[k],2))-
(0.00478125*BAR*PR[k]*inter[k])+(0.000257792*pow((log10(Rn1)-
0.301),2)*BAR*pow(inter[k],2))+(0.0000643192*(log10(Rn1)-
0.301)*pow(PR[k],6)*pow(inter[k],2))-(0.0000110636*pow((log10(Rn1)-
0.301),2)*pow(PR[k],6)*pow(inter[k],2))-(0.0000276305*pow((log10(Rn1)-
0.301),2)*Z*BAR*pow(inter[k],2))+(0.0000954*(log10(Rn1)-
0.301)*Z*BAR*PR[k]*inter[k])+(0.0000032049*(log10(Rn1)-
0.301)*pow(Z,2)*BAR*pow(PR[k],3)*inter[k]);
    Ktnew[k]=KT2+Ktcorr;
    //Finding Kq at intersection point of Ktj curve and Ktj2
curve
    KQ=0, KQ1[k]=0,Kqcorrect=0;
    for (int i = 0;i<47;i++){
    KQ =
Cq[i]*(pow(inter[k],JCq[i]))*(pow(PR[k],PRCq[i]))*(pow(BAR,BARCq[i]))*(pow(
Z,ZCq[i]));
    KQ1[k] = KQ1[k]+KQ;
    }
    Kqcorrect = -0.000591412+0.00696898*PR[k]-
(0.0000666654*Z*(pow(PR[k],6)))+0.0160818*(pow(BAR,2))-
(0.000938091*(log10(Rn1)-0.301))*PR[k]-(0.00059593*(log10(Rn1)-
0.301))*(pow(PR[k],2))+0.0000782099*(pow((log10(Rn1)-
0.301),2))*(pow(PR[k],2))+0.0000052199*(log10(Rn1)-
0.301))*Z*BAR*(pow(inter[k],2))-((0.00000088528*(pow((log10(Rn1)-
0.301),2))*Z*BAR*PR[k])*inter[k]+((0.0000230171*(log10(Rn1)-
0.301))*Z*(pow(PR[k],6)))-((0.00000184341*(pow((log10(Rn1)-
0.301),2))*Z*(pow(PR[k],6)))-(0.00400252*(log10(Rn1)-
0.301))*(pow(BAR,2))+0.000220915*(pow((log10(Rn1)-
0.301),2))*(pow(BAR,2)));
    Kqnew[k] = KQ1[k]+Kqcorrect;
    Eff[k] = (inter[k]*Ktnew[k]/(Kqnew[k]*(2*pi)));
    Diameter[k]=Va/(inter[k]*n);
    //comparision of efficiencys to find the maximum
    if(Eff[k]>eff && Diameter[k]<DiaMax){
    eff=Eff[k];
    PRcorr=PR[k];
    Ktfinal=Ktnew[k];
    Kqfinal=Kqnew[k];
    Jcorr=inter[k];
    Dia=Va/(inter[k]*n);
    Torque=Kqfinal*Density*pow(n,2)*pow(Dia,5);
    //PD=2*pi*Kqfinal*Density*pow(rot,3)*pow(D,5)*MCR;
    EtaH=(1-t)/(1-w);
    EtaR=1.02;
    EtaB=EtaR*eff;
    QPC=EtaH*EtaB;
    }}

```

A4) C++ code (only main part) for determining the resistance using Holtrop & Mennen

```

{
    double Cb, LWL, LBP, B, Draft, Depth, Vs, AT, Hs, Dair, Density, Viscosity;
    LWL=ui->lineEdit->text().toDouble(); //Length at waterline
    LBP=ui->lineEdit_2->text().toDouble(); //Length between
perpendiculars
    B=ui->lineEdit_3->text().toDouble(); //Breadth at waterline
    Draft=ui->lineEdit_4->text().toDouble(); //Draft of ship
    Depth=ui->lineEdit_5->text().toDouble(); //Depth of Ship
    Vs=ui->lineEdit_6->text().toDouble(); //Service speed
    Density=ui->lineEdit_7->text().toDouble(); //Density of fluid
    Dair=ui->lineEdit_8->text().toDouble(); //Density of air
    AT=ui->lineEdit_10->text().toDouble(); //Area of transom underwater
    Viscosity=ui->lineEdit_11->text().toDouble(); //Viscosity of fluid
    Cb=ui->lineEdit_13->text().toDouble(); //Block Coefficient
    double
Cm, Cp, Cw, lcb1, lcb, Cf1, Rn, Fn, Cs, C13, C12, Vm, LR, K1, Cf, RF, iE, C7, C1, Rapp, Cabt, hB
, C3, C5, C2, C16, C15, d1, RW, PB, Fri, RB, Rtr, Frt, C6, C4, CA, RA, RAA, RT, Rt, AM, ABT, m1, m
4, lamda, Aair, Vol, Disp, Sw;
    Rn=Vs*0.5144*LBP/Viscosity; //Reynolds Number
    Fn=Vs*0.5144/sqrt(9.81*LBP); //Froude Number
    Cm=1-0.062*pow(Fn, 0.792); //Midship Coefficient by Meizoso
    Cp=Cb/Cm; //Prismatic Coefficient
    Cw=0.67*Cb+0.32; //Waterplane area Coefficient
    lcb1=(8.8-38.9*Fn)/100; //lcb as percentage from midship
    lcb=LBP/2+(lcb1*LBP/2); //longitudinal centre of bouyancy
    Vol=LBP*Draft*B*Cb; //Vol Displacement in m3
    Disp=Vol*Density; //Displacement in tonnes
    Sw=1.7*LBP*Draft+(Vol/Draft); //Wetted surface area by mumfords formila
    Cf1=0.075/pow((log10(Rn)-2), 2); //Frictional resistance coefficient by
ITTC 1957
    Cs=-10;
    C13=1+0.003*Cs;
    if(Draft/LBP>0.05)
    {
        C12=pow((Draft/LBP), 0.2228446);
    }
    elseif(Draft/LBP>0.02)
    {
        C12=48.2*pow((Draft/LBP-0.02), 2.078)+0.479948;
    }
    Else{C12=0.479948;}
    Vm=Vs*0.5144;
    LR=(1-Cp+0.06*Cp*lcb1/(4*Cp-1))*LWL;
    K1=C13*(0.93+C12*(pow((B/LR), 0.92497)*pow((0.95-Cp), -0.521448)*pow((1-
Cp+0.0225*lcb1), 0.6906))-1;
    Cf=(1+K1)*Cf1; //Frictional resistance coefficient by ITTC 1978
    RF=Cf*0.5*Density*Sw*pow((Vs*0.5144), 2); //Frictional resistance in KN
    iE=1+89*exp(-(pow((LBP/B), (0.80856)))*pow((1-Cw), (0.30484))*pow((1-Cp-
0.0225*lcb1), (0.6367))*(pow((LR/B), (0.34574)))*(pow((100*Vol/pow(LBP, 3)), (0
.16302)))); //Angle of entrance
    if((B/LBP)>0.25)
        C7=0.5-0.0625*LBP/B;
    else
        if((B/LBP)>0.11)
            C7=B/LBP;
        else
            C7=0.229577*pow((B/LBP), 0.33333);
    C1=2223105*pow(C7, 3.78613)*pow((Draft/B), 1.07961)*pow((90-iE), -1.37565);
    Cabt=(40*Fn-3.5)/100; //Sectional Area coefficient of Bulb

```

```

AM=Cm*B*Draft;

ABT=Cabt*AM; //Transverse sectional area of Bulb
hB=0.6*Draft; //Centroid of the Bulb from centreline
C3=0.56*pow(ABT,1.5)/(B*Draft*(0.31*sqrt(ABT)+Draft-hB));
C5=1-0.8*AT/(B*Draft*Cm);
C2=exp(-1.89*sqrt(C3));
if(Cp<0.8)
    C16=8.07981*Cp-13.8673*pow(Cp,2)+6.984388*pow(Cp,3);
else
    C16=1.73014-0.7067*Cp;
m1=(0.0140407*LBP/Draft)-(1.75254*pow(Vol,0.33334)/LBP)-
(4.79323*B/LBP)-C16;
if((pow(LBP,3)/Vol)<512)
    C15=-1.69385;
else
    if((pow(LBP,3)/Vol)<1726.81)
        C15=-1.69385+(LWL/(pow(Vol,0.33334))-8)/2.36;
    else
        C15=0;
m4=C15*0.4*exp(-0.034*pow(Fn,-3.29));
d1=-0.9;
if((LBP/B)<12)
    lamda=1.446*Cp-0.03*LBP/B;
else
    lamda=1.446*Cp-0.36;
RW=C1*C2*C5*Vol*Density*9.81*exp(m1*pow(Fn,d1)+m4*cos(lamda*pow(Fn,-
2))); //Wave making Resistance in KN
PB=0.56*sqrt(ABT)/(Draft-1.5*hB);
Fri=Vm/sqrt(9.81*(Draft-hB-0.25*sqrt(ABT))+0.15*pow(Vm,2));
RB=0.11*exp(-3*pow(PB,-
2))*pow(Fri,3)*pow(ABT,1.5)*Density*9.81/(1+pow(Fri,2)); //Resistance due
Bulb in KN
if(AT==0)
    Rtr=0;
else
    Frt=Vm/sqrt(2*9.81*AT/(B+B*Cw));
if(Frt<5)
    C6=0.2*(1-0.2*Frt);
else
    C6=0;
Rtr=0.5*Density*pow(Vm,2)*AT*C6; //Resistance due to immersed portion
of Transom
if(Draft/LBP<0.04)
    C4=Draft/LBP;
else
    C4=0.04;
CA=0.006*pow((LBP+100),-0.16)-
0.00205+0.003*sqrt(LBP/7.5)*pow(Cb,4)*C2*(0.04-C4);
RA=0.5*Density*Sw*pow(Vm,2)*CA; //Correlation resistance
Aair=B*(Depth-Draft+Hs); //Transverse sectional area of Ship above LWL
RAA=0.8*0.5*Dair*pow(Vm,2)*Aair; // Air resistance in KN
RT=RF+RW+RB+RAA+RA+Rtr; //Resistance of the vessel(KN)
if(ui->checkBox->isChecked())
    {Rapp=RT*0.08;}
else{ Rapp=0;}
Rt=RT+Rapp; //Final resistance with appendage resistance
}

```

A5) C++ code (only main part) for generating 3-D geometry of Propeller with NACA sections

```

{
double const pi=22/7;
    float roR[]={0.2,0.3,0.4,0.5,0.6,0.7,0.8,0.9,0.95,1};
    double cD[] =
{1.4341,1.5871,1.7246,1.8403,1.9246,1.9591,1.9065,1.6617,1.188,0};
    double
tmax[]={0.2531,0.2169,0.1833,0.1516,0.1224,0.0951,0.0689,0.0445,0.028,0};
    double
pitch_r[]={0.764,0.841,0.857,0.858,0.859,0.859,0.86,0.857,0.856,0.855};
    QVector<double>
x(26),y(26),yy(26),x1(26),y1(26),yy1(26),x2(26),y2(26),yy2(26),x3(26),y3(26)
),yy3(26),x4(26),y4(26),yy4(26),x5(26),y5(26),yy5(26),x6(26),y6(26),yy6(26)
,x7(26),y7(26),yy7(26),x8(26),y8(26),yy8(26),x9(26),y9(26),yy9(26);
    for (int i=0;i<10;i++){
        //c[i]=(cr[i]*D*BAR)/Z;//Finding chord lengths at each section as per
Wageningen B series
        //cD[i]=c[i]*D;
        r[i]=roR[i]*D/2;//radius of propeller section from shaft centreline
        theta_p[i]=atan((pitch_r[i]*D)/(2*3.14*r[i]))*(180/3.14);
        theta_s[i]= 0;
        theta_r[i]= 0;
    }
    ofstream myfile;
    myfile.open("NACA Geometry.txt");
    // Maximum thickness calculation at each section
    double
xoc[]={0,0.005,0.0075,0.0125,0.025,0.05,0.075,0.10,0.15,0.20,0.25,0.30,0.35
,0.40,0.45,0.50,0.55,0.60,0.65,0.70,0.75,0.80,0.85,0.90,0.95,1.00}; // non
dimensionalized distance over the chordlength
    double
ytocs[]={0,0.0665,0.0812,0.1044,0.1466,0.2066,0.2525,0.2907,0.3521,0.4,0.43
63,0.4637,0.4832,0.4952,0.5,0.4962,0.4846,0.4653,0.4383,0.4035,0.3612,0.311
,0.2532,0.1877,0.1143,0.0333}; // thickness as ratio of maximum thickness
of section
    double
ycocs[]={0,0.00281,0.00396,0.00603,0.01055,0.01803,0.02432,0.02981,0.03903,
0.04651,0.05257,0.05742,0.0612,0.06394,0.06571,0.06651,0.06631,0.06508,0.06
274,0.05913,0.05401,0.04673,0.03607,0.02452,0.01226,0}; //camber over the
chord length
    double
dyodxocs[]={0,0.47539,0.44004,0.39531,0.33404,0.27149,0.23378,0.20618,0.165
46,0.13452,0.10873,0.08595,0.06498,0.04507,0.02559,0.00607,-0.01404,-
0.03537,-0.05887,-0.08610,-0.12058,-0.18034,-0.23430,-0.24521,-0.24521,-
0.24521};
    double cm_angle[26]={0};

    for (int j=0;j<26;j++){
        cm_angle[j]=atan(dyodxocs[j]);
        //myfile<<" j "<<j<<" Ycocs "<<ycocs[j]<<" dyodxocs[j]
"<<dyodxocs[j]<<" cm_angle[j] \n"<<cm_angle[j];
    }
    double ycoc[26][10]={0}; double ytoc[26][10]={0}; double
xu[26][10]={0}; double yu[26][10]={0};
    double xl[26][9]={0};double yl[26][9]={0};
    for (int i=0;i<10;i++){
        for (int j=0;j<26;j++){
            ycoc[j][i]=ycocs[j]*cD[i];
            ytoc[j][i]=ytocs[j]*tmax[i];
        }
    }
}

```

```

    xu[j][i]=xoc[j]*cD[i]-ytoc[j][i]*sin(cm_angle[j]);
    yu[j][i]=ycoc[j][i]+ytoc[j][i]*cos(cm_angle[j]);
    xl[j][i]=xoc[j]*cD[i]+ytoc[j][i]*sin(cm_angle[j]);
    yl[j][i]=ycoc[j][i]-ytoc[j][i]*cos(cm_angle[j]);
}
double xpu[26][10]={0};double ypu[26][10]={0};double
zpu[26][10]={0};double xpl[26][10]={0};double ypl[26][10]={0};double
zpl[26][10]={0};

// Generating 3D points
for(int i=0;i<10;i++){
for(int j=0;j<26;j++){
xpu[j][i]=- (ig[i]+is[i]*r[i])+(0.5*cD[i]-
xu[j][i])*sin((pi/180)*theta_p[i])+yu[j][i]*cos((pi/180)*theta_p[i]);
ypu[j][i]=r[i]*sin((pi/180)*(theta_s[i]-(180*((0.5*cD[i]-
xu[j][i])*cos((pi/180)*theta_p[i])-
yu[j][i]*sin((pi/180)*theta_p[i]))/(pi*r[i]))));
zpu[j][i]=r[i]*cos((pi/180)*(theta_s[i]-(180*((0.5*cD[i]-
xu[j][i])*cos((pi/180)*theta_p[i])-
yu[j][i]*sin((pi/180)*theta_p[i]))/(pi*r[i]))));
xpl[j][i]=- (ig[i]+is[i]*r[i])+(0.5*cD[i]-
xl[j][i])*sin((pi/180)*theta_p[i])+yl[j][i]*cos((pi/180)*theta_p[i]);
ypl[j][i]=r[i]*sin((pi/180)*(theta_s[i]-(180*((0.5*cD[i]-
xl[j][i])*cos((pi/180)*theta_p[i])-
yl[j][i]*sin((pi/180)*theta_p[i]))/(pi*r[i]))));
zpl[j][i]=r[i]*cos((pi/180)*(theta_s[i]-(180*((0.5*cD[i]-
xl[j][i])*cos((pi/180)*theta_p[i])-
yl[j][i]*sin((pi/180)*theta_p[i]))/(pi*r[i]))));
}}
//write to file named NacaGeometry.txt
for(int i=1;i<10;i++)
{
if(i<9){
myfile<<"InterpCrv\n";
}
else{myfile<<"Point\n";}
for (int j=0;j<26;j++){
myfile<<xpu[j][i]<<","<<ypu[j][i]<<","<<zpu[j][i]<<"\n";
}
for(int j=25;j>=0;j--){
myfile<<xpl[j][i]<<","<<ypl[j][i]<<","<<zpl[j][i]<<"\n";
}}}

```

A6) Shipflow code for calculating resistance at 20 Knots

```

xflow
  titl(titl="Ice container, T=7.3 m at velocity 20")
  prog(xmesh,xpan,xbou)
  hull(xmmanu,mono,h1gr="hull",ogrp="stern",fbgr="bulb",abgr="boss",fsfl)
  offs(file="Icecontainer_offset_potential_final1.txt",
  xaxd=-1,ysig=1,xori=145.6,zori=7.3,lpp=145.6)
  vshi(fn=[0.272],rn=[1.16e09])
  opti(on)
end

xmesh
BODY (GRNO = 1, HIGHER, FSINCLUDE, ONEINT, STN = 100,POINT = 40,EXPANEL
= 3, VELBC = 0,
XTRA = 0.0, YTRA = 0.0, ZTRA = 0.0, XROT = 0.0, YROT = 0.0, ZROT =
0.0, STR1 = 0, DF1 = 0.0, DL1 = 0.0, STR2 = 5, DF2 = 0.0, DL2 = 0.0, STR3= STR1, DF3 =
DF1, DL3 = DL1, STR4 = STR2, DF4 = DF2, DL4 = DL2)
FREE (GRNO = 5, FIRST, SMOOTH = 10, Y2SIDE = 0.0, Y4SIDE = -1, XUPS = -0.5,
XBOW = 0.0, XSTE = 1.0, XDOW = 2.0,STR1 = 1, DF1 = 0.02, DL1 = 0.0,
NBD2 = 4, IBD2 = [1,2,3,4], STRU = 1, DFU = 0.0, DLU =0.01,
STRM = 5, DFM = 0.01, DLM = 0.01, STRD = 1, DFD = 0.01, DLD = 0.0)
End

xpan
  cont(free,nonl)
  para(nthr=4)
end

xbound
  inic(sgro=1,t11=[1.0e-04],turb)
end

```

A7) Shipflow code for open water characteristics of Wageningen/NACA 66 Propeller series.

```

xflow
  titl ( titl="5 Blade B-90 Wageningen")
  prog ( xchap )
  hulltype ( POW )
  fluid (density = 1025.0, viscosity = 1.18e-6, gravity = 9.80665)
  vshi ( fn= [ 0.272 ], rn= [ 7.9e6 ] )
  /*****elice*****/
//Geometry for Wageningen B propeller
  prop ( id="ID1", xsh=0, zsh=0, dprop=5.3, dhub=0.85,
        nbla=5, jv=0.59, ear=0.8, numb=10,rotmdir=1,
        r_rt=[0.16,0.2,0.3,0.4,0.5,0.6,0.7,0.8,0.9,1],
        p_d =[0.9,0.9,0.9,0.9,0.9,0.9,0.9,0.9,0.9,0.9],
        thic=[0.1806,0.176,0.156,0.136,0.116,0.096,0.076,0.056,0.036,0.016],
        leng=[1.232,1.4094,1.5959,1.7384,1.8249,1.8546,1.8181,1.6706,1.3415,0.00],
        camb=[0,0,0,0,0,0,0,0,0,0])

  /*****elice*****/
//Geometry for NACA 66 propeller
  prop ( id="ID1", xsh=0, zsh=0, dprop=5.3, dhub=0.85,
        nbla=5, jv=0.59, ear=0.8, numb=9,ROTDIR=1,
        r_rt=[0.2,0.3,0.4,0.5,0.6,0.7,0.8,0.9,1],
        p_d =[0.764,0.841,0.857,0.858,0.859,0.859,0.86,0.857,0.855],
        t_d=[0.0476,0.0408,0.0345,0.0285,0.023,0.018,0.013,0.0083,0],
        c_d=[0.27,0.299,0.3247,0.3465,0.3624,0.369,0.359,0.313,0],
        camb=[0,0.0727,0.0494,0.0398,0.0324,0.0277,0.0242,0.0219,0])

  /*****elice*****/

stretching( id="middles", middle, s0=0.15, s1=0.8, ds0=0.35)
stretching( id="middlez", middle, s0=0.20, s1=0.8, ds0=0.15)
box ( low= [-2.0,-2.54,-2.54],high=[2.54, 2.54,.54],dime=[121,51,51],
      str1="middles", str2="middlez",str3="middlez",
      bc11="INFLOW", bc12="OUTFLOW", bc21="SLIP",
      bc22="SLIP",bc31="SLIP", bc32="SLIP")
symm( nosym )
end

xchap
parallel( nthr=4,nproc=1)
control( start,adi, maxiter=300)
lline( id="ID1",cf = 0.004, RELAX=0.15, ON)
POW( J=[0.1 , 0.2 , 0.3 , 0.4 , 0.5, 0.59 , 0.6 , 0.7 , 0.8 , 0.9 , 1],outputfile="ice_pow.dat" , RN
= 4.47e7)
end

```

A8) Shipflow code for Self Propulsion test carried out with NACA 66 Propeller to study characteristics in unsteady flow.

```

xflow
  title ( titl="ICE, Lifting Line Propeller with self-propulsion for NACA" )
  program ( all )
  hulltype ( mono,xmauto, medium, h1gr="hull", ogrp="stern",
            fbgr="bulb", abgr="boss", fsflow,vfsflow)
  offsetfile( file="Icecontainer_offset_ranse_final1.txt", xaxdir=-1.0, ysign=1.0, xori=145.90,
zori=7.3, lpp=145.90 )
  /ipos ( trim = 0.41 )
  Vship ( fn=[0.272], rn=[7.96e6] )
  fluid (density = 1025.0, viscosity = 1.18e-6, gravity = 9.80665)
  prtopt ( strlres )
  symm ( nosy )
  spauto(all)
  prop ( id="ID1", xsh=4.28, zsh=2.8, dprop=5.3, dhub=0.85,
        nbla=5, jv=0.59, ear=0.8, numb=9,ROTDIR=1,
        r_rt=[0.16,0.3,0.4,0.5,0.6,0.7,0.8,0.9,1],
        p_d=[0.682,0.786,0.815,0.8235,0.829,0.833,0.838,0.837,0.836],
        t_d=[0.048,0.041,0.0348,0.0287,0.0232,0.018,0.013,0.0084,0.0004],
        c_d=[0.274,0.303,0.3294,0.3515,0.3676,0.3742,0.364,0.3174,0],
        camb=[0,0.0823,0.0543,0.043,0.0344,0.0288,0.0248,0.0222,0.0106])
  selfprop(on,pow="NACA_pow.dat")
  optim(on)
end

xpan
cont(save)
iteration(maxit=2000)
para( nthr = 4 )
end

xgrid
  size(global,medium)
  offset (h1gr="hull1", ogrp="stern1",fbgr="bulb1", abgr="boss1")
  yplus(ytarget=0.75)
  XDISTR ( NM=68, NA=42, NW=38,NF=60 )
end

xchap
  paral ( nthr=4,nproc=1 )
  cont ( start, adi, maxit=8000)
  lline (id="ID1",cf=0.004,relax=0.15,active,on)
  POW( start,J=[0.1 , 0.2 , 0.3 , 0.4 , 0.5 , 0.59 , 0.6 , 0.7 , 0.8 , 0.9 ,
1],outputfile="NACA_pow.dat" , RN = 4.4e7)
End

```

A9) Propeller Strength Calculation

Strength Calculation as per Germinister Lloyd rule for 0.25 R:

$$t > k \cdot K_0 \cdot K_1 \cdot C_G \cdot C_{dyn}$$

$$k_{0.25R} = 80,$$

$$K_0 = 1 + \frac{e \cdot \cos \alpha}{H} + \frac{n_2}{15000}$$

$$n_2 = 150$$

$$\alpha_{0.25R} = \tan^{-1} \frac{1.27 \cdot H}{D} = 42.34 \text{ degree}$$

$$e = 0$$

$$H_{0.25R} = 3810 \text{ mm}$$

$$K_0 = 1.009$$

$$K_1 = \sqrt{\frac{P_w \cdot 10^5 \cdot (2 \cdot \frac{D}{H_m} \cdot \cos \alpha + \sin \alpha)}{n_2 \cdot B \cdot z \cdot C_w \cdot \cos^2 \epsilon}}$$

$$P_w = 10390 \text{ KW}$$

$$H_m = 4380 \text{ mm}$$

$$C_w = 590$$

Since the material used is cast Nickel Aluminium Bronze

$$\epsilon = 21 \text{ degree}$$

$$B_{0.25R} = 1525 \text{ mm}$$

$$Z=5$$

$$D=5310 \text{ mm}$$

$$K_{1(0.25R)} = \sqrt{\frac{10390 * 10^5 * (2 * \frac{5310}{4380} * 0.74 + 0.673)}{150 * 1525 * 5 * 590 * 0.87}} = 1.12$$

$$C_G = \sqrt{\frac{f_1 \cdot \frac{D}{1000}}{12.2}}$$

$$f_1 = 7.2$$

$$C_G = 1.77$$

$$C_{Dym} = 1.0$$

$$t > k \cdot K_0 \cdot K_1 \cdot C_G \cdot C_{dyn}$$

$$k \cdot K_0 \cdot K_1 \cdot C_G \cdot C_{dyn} = 80 * 1.009 * 1.12 * 1.77 * 1 = 160.01 \text{ mm}$$

Strength Calculation as per Germinister Lloyd rule for 0.6 R:

$$k_{0.6R} = 44$$

$$K_0 = 1 + \frac{e \cdot \cos \alpha}{H} + \frac{n_2}{15000}$$

$$\alpha_{0.6R} = \tan^{-1} \frac{0.53 \cdot H}{D} = 23.7 \text{ degree}$$

$$e = 0$$

$$H_{0.6R} = 4403 \text{ mm}$$

$$K_0 = 1.009$$

$$K_1 = \sqrt{\frac{P_w \cdot 10^5 \cdot (2 \cdot \frac{D}{H_m} \cdot \cos \alpha + \sin \alpha)}{n_2 \cdot B \cdot z \cdot C_w \cdot \cos^2 \varepsilon}}$$

$$P_w = 10390 \text{ KW}$$

$$H_m = 4380 \text{ mm}$$

$$C_w = 590$$

Since the material used is cast Nickel Aluminium Bronze

$$\varepsilon = 21 \text{ degree}$$

$$B_{0.25R} = 1525 \text{ mm}$$

$$B_{0.6R} = 1952 \text{ mm}$$

$$K_{1(0.25R)} = \sqrt{\frac{10390 * 10^5 * (2 * \frac{5310}{4380} * 0.915 + 0.4)}{150 * 1952 * 5 * 590 * 0.87}} = 1.2$$

$$C_G = \sqrt{\frac{f_1 \cdot \frac{D}{1000}}{12.2}}$$

$$f_1 = 7.2$$

$$C_G = 1.77$$

$$C_{Dym} = 1.0$$

$$t > k \cdot K_0 \cdot K_1 \cdot C_G \cdot C_{dyn}$$

$$k \cdot K_0 \cdot K_1 \cdot C_G \cdot C_{dyn} = 44 * 1.009 * 1.9 * 1.77 * 1 = 94.3 \text{ mm}$$

A10) Calculation of Shaft Line

The symbols used in this section are defined as follows:

- P - Shaft power in kW
 R - Corresponding revolutions per minute
 F - Coefficient according to installation type
 k - Coefficient according to type of connection
 σ_u - Specified minimum tensile strength of the material in N/mm²
 n - Number of bolts in the coupling
 D - Pitch circle diameter of bolts in mm

Intermediate Shaft

$$Dia_i = F * K * \sqrt[3]{\frac{P * 560}{R(\sigma_u + 160)}}$$

$$Dia_i = 100 * 1 * \sqrt[3]{\frac{13860 * 560}{150(600 + 160)}}$$

Dia_i= 408 mm

Propeller Shaft

$$Dia_p = F * K * \sqrt[3]{\frac{P * 560}{R(\sigma_u + 160)}}$$

$$Dia_p = 100 * 1.22 * \sqrt[3]{\frac{13860 * 560}{150(600 + 160)}}$$

Dia_p= 497 mm

Coupling Bolt

$$Dia_c = \sqrt{\frac{240 * 10^6 * P}{nD * \sigma_u * R}}$$

$$Dia_c = \sqrt{\frac{240 * 10^6 * 13860}{10 * 590 * 600 * 150}}$$

Dia_c= 79 mm